



HAL
open science

Volcanic successions in Marquesas eruptive centers: A departure from the Hawaiian model

Hervé Guillou, René C. Maury, Gérard Guille, Catherine Chauvel, Philippe Rossi, Carlos Pallares, Christelle Legendre, Sylvain Blais, Céline C. Liorzou, Sébastien Deroussi

► **To cite this version:**

Hervé Guillou, René C. Maury, Gérard Guille, Catherine Chauvel, Philippe Rossi, et al.. Volcanic successions in Marquesas eruptive centers: A departure from the Hawaiian model. *Journal of Volcanology and Geothermal Research*, 2014, 276, pp.173-188. 10.1016/j.jvolgeores.2013.12.003 . insu-00933782

HAL Id: insu-00933782

<https://insu.hal.science/insu-00933782>

Submitted on 25 Feb 2014

HAL is a multi-disciplinary open access archive for the deposit and dissemination of scientific research documents, whether they are published or not. The documents may come from teaching and research institutions in France or abroad, or from public or private research centers.

L'archive ouverte pluridisciplinaire **HAL**, est destinée au dépôt et à la diffusion de documents scientifiques de niveau recherche, publiés ou non, émanant des établissements d'enseignement et de recherche français ou étrangers, des laboratoires publics ou privés.

1 Volcanic successions in Marquesas eruptive centers: A departure 2 from the Hawaiian model

3 Hervé Guillou ^{a*}, René C. Maury ^b, Gérard Guille ^c, Catherine Chauvel ^{d,e}, Philippe Rossi ^f, Carlos
4 Pallares ^{b,g}, Christelle Legendre ^b, Sylvain Blais ^h, Céline Liorzou ^b, Sébastien Deroussi ⁱ

5
6 ^aUMR 8212 LSCE-IPSL/CEA-CNRS-UVSQ, Domaine du CNRS, 12 avenue de la Terrasse, 91198 Gif-
7 sur-Yvette, France

8 ^bUniversité de Brest; Université Européenne de Bretagne, CNRS; UMR 6538 Domaines Océaniques;
9 Institut Universitaire Européen de la Mer, Place N. Copernic, 29280 Plouzané, France.

10 ^cLaboratoire de Géophysique, CEA-DASE, 91680 Bruyères-le-Chatel, France.

11 ^dUniv. Grenoble Alpes, ISTerre, F-38041 Grenoble, France

12 ^eCNRS, ISTerre, F-38041 Grenoble, France

13 ^fBRGM, SGN-CGF, 3 avenue Claude-Guillemin, BP 36009,45060 Orléans cedex 2, France.

14 ^gUniversité de Paris-Sud, Laboratoire IDES, UMR 8148, Orsay, F-91405, France;CNRS,Orsay, F-
15 91405, France.

16 ^hUniversité de Rennes 1; Université Européenne de Bretagne, CNRS; UMR 6518 Géosciences Rennes;
17 Campus de Beaulieu, Avenue du Général Leclerc, 35042 Rennes Cedex, France.

18 ⁱObservatoire Volcanologique et Sismologique de Guadeloupe, IPGP, 97113 Courbeyre, La
19 Guadeloupe, France.

20
21
22
23 * Corresponding author. Tel.: + 33169823556; fax: +33169823568

24 E-mail address: herve.guillou@lsce.ispl.fr

25 26 27 **Abstract**

28
29 The temporal and geochemical evolution of Marquesas hotspot volcanoes have often been interpreted
30 with reference to the Hawaiian model, where a tholeiitic shield-building stage is followed by an alkali basaltic
31 post-shield stage, followed after a 0.4 to 2.5 Myr long quiescence period, by a rejuvenated
32 basanitic/nephelinitic stage. Here we discuss geochemical data on 110 Marquesas lavas also dated using
33 the unspiked ⁴⁰K-⁴⁰Ar method on separated groundmass (including 45 new ages measured on the southern
34 islands of Hiva Oa, Motane, Tahuata and Fatu Hiva). Sample locations were positioned on detailed
35 geological maps to determine their shield or post-shield position with respect to the caldera collapse
36 event(s), without taking into account their geochemical features. A rather regular decrease of the ages
37 towards SE, consistent with the Pacific plate motion, is observed from Eiao (5.52 Ma) to Fatu Hiva (1.11
38 Ma), and rejuvenated basanitic volcanism occurs only in Ua Huka (1.15-0.76 Ma). The occurrence of
39 intermediate and evolved lavas is restricted to the post-caldera stage, with the exception of Eiao island.
40 However, many other features of the Marquesas chain are rather atypical with respect to those of Hawaii.

41 Although Marquesas shields are tholeiitic, several of them (Eiao, Tahuata) contain interbedded alkali
42 basaltic and basanitic flows. Moreover, post-shield volcanoes are either alkali basalts (Ua Huka), tholeiites
43 (Hiva Oa, Tahuata, Fatu Hiva) or both (Nuku Hiva). This feature is consistent with the temporal continuity of
44 the two stages and the usually short length of the post-shield period (<0.2 Myr). In a given island, the trace
45 element and isotopic compositions of shield and post-shield lavas overlap, although both display large
46 variations. The sources of alkali basalts and basanites are more enriched than those of the
47 contemporaneous tholeiites. These specific features support the hypothesis of an extremely heterogeneous
48 Marquesas plume. The “weak” character of this plume led to low partial melting degrees, which in turn
49 resulted in the preservation in the basaltic magmas of geochemical features inherited from small-size source
50 heterogeneities.

51

52 *Keywords:* Shield, Post-shield, Tholeiite, Alkali basalt, Trachyte, ^{40}K - ^{40}Ar age, Hotspot, Marquesas.

53

54

55

56 **1. Introduction**

57

58 The temporal evolution of plume-related oceanic intraplate volcanoes has often been investigated with
59 reference to the classical Hawaiian model, in which four successive growth stages are distinguished (Clague
60 and Dalrymple, 1987; Clague, 1987; Hanano et al., 2010): (1) a small volume (ca. 3%) alkalic pre-shield
61 stage, emplacing mostly submarine alkali basalts and basanites; (2) the main shield-building stage, during
62 which the majority (95-98%) of the volcano is rapidly constructed, culminating in subaerial flows of tholeiitic
63 basalts; (3) the alkalic post-shield phase, during which small volumes (1-2%) of alkali basalts and related
64 intermediate/evolved lavas (hawaiites, mugearites, benmoreites and trachytes) are erupted; and finally (4)
65 the alkalic rejuvenated stage, during which very small volumes (<<1%) of basanites, alkali basalts and
66 nephelinites are emplaced after a quiescence period. In the Hawaiian chain, shield tholeiitic basalts are less
67 enriched in incompatible elements and derive from larger melting rates than the post-shield and rejuvenated
68 alkalic lavas; in addition, the mantle sources of the latter are isotopically depleted with respect to those of
69 the tholeiites (lower $^{87}\text{Sr}/^{86}\text{Sr}$ and $^{206}\text{Pb}/^{204}\text{Pb}$, higher $^{143}\text{Nd}/^{144}\text{Nd}$: Frey et al., 1990, 2005; Shafer et al., 2005;
70 Fekiacova et al., 2007; Garcia et al., 2010; Hanano et al., 2010).

71 For Hawaiian volcanoes, the main criterion used for the distinction between the shield-building and post-
72 shield stages is the change from tholeiites to alkali basalts. Indeed, Clague and Dalrymple (1987) stated
73 (their page 7) that “the shield stage usually includes caldera collapse and eruptions of caldera-filling tholeiitic
74 basalt. During the next stage, the alkalic postshield stage, alkalic basalt also may fill the caldera and form a
75 thin cap of alkalic basalt and associated differentiated lava that covers the main shield”. They also
76 mentioned (their page 8) that “we have omitted the main caldera-collapse stage of Stearns (1966) from the
77 eruption sequence because it can occur either during the shield stage or near the beginning of the alkalic
78 postshield stage. The lava erupted may therefore be tholeiitic or alkali basalt, or of both types”.

79 Large major, trace element and isotopic variations in Marquesas lavas have been known for decades
80 (Vidal et al., 1984, 1987; Duncan et al., 1986). They have been interpreted with reference to the shield/post-
81 shield Hawaiian model by several authors (Duncan et al., 1986; Woodhead, 1992; Desonie et al., 1993;
82 Castillo et al., 2007). However, most of these works were based on the pioneer (and hence limited) sampling
83 of Marquesas Islands made during the 1970's by R.A. Duncan (Duncan and McDougall, 1974; Duncan,
84 1975; McDougall and Duncan, 1980) and R. Brousse (Vidal et al., 1984; Brousse et al., 1990). No geological
85 maps of the islands were available at that time, and therefore the distinction between shield and post-shield
86 lavas was usually made using geochemical criteria. For instance, the observation that the oldest lavas from
87 Nuku Hiva, Ua Pou and Hiva Oa are tholeiitic basalts (Duncan, 1975; Duncan et al., 1986) led Woodhead
88 (1992) to classify hypersthene-normative Marquesas lavas as shield-related and alkali basalts/basanites as
89 post-shield. Later, Castillo et al. (2007) studied samples collected by H. Craig, and used $^{87}\text{Sr}/^{86}\text{Sr}$ (>0.7041)
90 and $^{143}\text{Nd}/^{144}\text{Nd}$ (<0.51285) ratios to characterize post-shield lavas, based on the isotopic data of Woodhead
91 (1992) obtained on R.A. Duncan's samples.

92 A mapping program of the Marquesas archipelago (2001-2009) led us to collect a number of new
93 samples and draw detailed geological maps of the islands. The trace element and Sr, Nd, Pb and Hf isotopic
94 features of these samples (Chauvel et al., 2012) point towards relationships between shield and post-shield
95 lavas more complex than previously thought. Here, we use geological settings combined with unspiked ^{40}K -
96 ^{40}Ar ages measured on groundmass and petrologic/geochemical features of this new sample set to
97 demonstrate that the temporal evolution of the Marquesas volcanoes is rather different from that of Hawaiian
98 volcanoes. We also discuss the constraints that they set on the corresponding plume/hotspot model.

99

100

101 **2. Geological setting and previous work**

102

103 *2.1. The Marquesas archipelago*

104 The ca. 350 km-long Marquesas archipelago, located in northern French Polynesia, includes eight main
105 islands (Fig. 1) that cluster into a northern group (Eiao, Nuku Hiva, Ua Huka and Ua Pou) and a southern
106 group (Hiva Oa, Tahuata, Motane, Fatu Hiva); few islets ("motu"), banks and seamounts also exist (Fig. 1).
107 The age of the islands decreases towards the SE (Duncan and McDougall, 1974; Brousse et al., 1990) from
108 5.5 Ma in Eiao to 0.6-0.35 Ma on the DH12 seamount south of Fatu Hiva (Desonie et al., 1993). However,
109 no active volcanoes are known at the southeastern edge of the chain. ^{40}K - ^{40}Ar ages younger than 1 Ma have
110 been obtained only on DH12 and on the Teepoepo (1.15-0.96 Ma) and Tahoatikikau (0.82-0.76 Ma)
111 strombolian cones on Ua Huka (Legendre et al., 2006; Blais et al., 2008). These cones were emplaced after
112 a 1.3 Myr quiescence period, and are considered as the only example of rejuvenated volcanism in the
113 Marquesas (Legendre et al., 2006; Chauvel et al., 2012). Most authors believe that the Marquesas Fracture
114 Zone (MFZ; Pautot and Dupont, 1974) overlies the present position of the hotspot activity (McNutt et al.,
115 1989; Brousse et al., 1990; Guille et al., 2002). However, the MFZ is aseismic (Jordahl et al., 1995) and no
116 young volcanic rock has been recovered from the adjacent Marquesas Fracture Zone Ridge (MFZR; Fig. 1).
117 The seamount chain parallel to the MFZ ridge ca. 50 km to the north (Fig. 1) has not yet been dredged and it
118 could possibly mark the present location of Marquesas hotspot activity.

119 The Marquesas archipelago is atypical in many respects (Brousse et al., 1990; Guille et al., 2002; Devey
120 and Haase, 2003). It lies on an anomalously shallow (less than 4,000 m deep) 53-49 Ma old oceanic crust
121 generated at the axis of the Pacific-Farallon ridge (Crough and Jarrard, 1981), and its crustal thickness
122 reaches 15-20 km below the central part of the chain (Filmer et al., 1993; Caress et al., 1995). This
123 abnormally thick crust is attributed either to underplating of plume magmas below the Moho (Caress et al.,
124 1995; McNutt and Bonneville, 2000) or to the construction of the archipelago over a small 50-45 Ma old
125 oceanic plateau that formed near the axis of the Pacific-Farallon ridge (Gutscher et al., 1999). In addition,
126 the N30-40°W direction of the archipelago is oblique to that of the current N65°W motion of the Pacific plate
127 (Fig. 1), but parallel to the spreading axis of the Pacific-Farallon ridge prior to the current orientation of
128 accretion along the East Pacific Rise. This feature suggests that zones of weakness in the underlying
129 Pacific-Farallon plate might have controlled the emplacement of the Marquesas magmas (Crough and
130 Jarrard, 1981; McNutt et al., 1989). Age-distance to the MFZR plots using the main N30-40°W trend of the
131 chain and all available ^{40}K - ^{40}Ar ages display considerable scatter (Brousse et al., 1990; Desonie et al., 1993;
132 Guille et al., 2002). Similar plots using the N65°W trend give better fits (Legendre et al., 2006; Chauvel et al.,
133 2012), especially when considering only unspiked ^{40}K - ^{40}Ar ages measured on separated groundmass (Fig.
134 2), which are more accurate and reliable than conventional ^{40}K - ^{40}Ar data on whole rocks. Recently, Chauvel
135 et al. (2012) showed that the chain is made of two adjacent rows of islands with distinct Sr, Nd, Pb isotopic
136 features, delineating two isotopic stripes. At any given $^{143}\text{Nd}/^{144}\text{Nd}$ value, the northeastern row (the “Ua Huka
137 group”) has systematically higher $^{87}\text{Sr}/^{86}\text{Sr}$ and lower $^{206}\text{Pb}/^{204}\text{Pb}$ ratios than the southwestern row (the “Fatu
138 Hiva group”). These rows are thought to originate from the partial melting of two adjacent filaments
139 contained in an elongated ascending plumelet or secondary plume, rooted in a larger dome located at the
140 base of the upper mantle (Davaille et al., 2002; Courtillot et al., 2003; Cadio et al., 2011).

141 The common occurrence of nested volcanoes in the Marquesas was first reported by L.J. Chubb (1930).
142 Half of the islands (Nuku Hiva, Ua Huka, Tahuata, Fatu Hiva) are made up of a large external (outer) shield
143 volcano with a central caldera. A younger and smaller internal (inner) post-shield volcanic edifice has grown
144 inside this caldera. Hiva Oa comprises three adjacent shields: the larger one is unconformably overlain by
145 post-shield flows, which also filled up part of its caldera. Ua Pou is rather unusual, because this island lacks
146 a well-exposed outer shield and is mostly made up of phonolitic flows interbedded with basanitic and
147 tephritic flows (Fig. 3), and crosscut by huge phonolitic spines (Legendre et al., 2005a). The two smallest
148 islands, Eiao and Motane, represent crescent-shaped remnants of the caldera wall and external upper
149 slopes of much larger collapsed shield volcanoes (Brousse et al., 1990; Guille et al., 2002). Therefore, the
150 shield-building or post-shield character of a given Marquesan sample with respect to caldera collapse events
151 (see Stearns, 1966, for the case of Hawaii) can be determined using only its geological position deduced
152 from field relationships and its ^{40}K - ^{40}Ar age, without making any assumption based on its petrologic and
153 geochemical features. We choose this approach because no well-defined temporal change from tholeiitic to
154 alkali volcanism is observed in most Marquesas volcanoes. In the present work, we use a coherent set of
155 110 lava samples to investigate the temporal geochemical evolution of the Marquesas volcanoes, with
156 special attention to the respective features of shield-building, post-shield and rejuvenated (Ua Huka) stages
157 of volcanic activity. All samples were collected during the 2001-2009 mapping program, dated by the

158 unspiked ^{40}K - ^{40}Ar method on groundmass at Gif-sur-Yvette laboratory and analyzed for major and trace
159 elements by ICP-AES at Plouzané (Brest) laboratory.

160

161 *2.2. Summary of the geological and geochemical features of the northern group islands*

162 The four islands from the northern group (Eiao, Nuku Hiva, Ua Huka and Ua Pou) were studied
163 previously using the same methods (Caroff et al., 1995, 1999; Legendre et al., 2005a, 2005b, 2006; Maury
164 et al., 2006, 2009; Blais et al., 2008; Guille et al., 2010). Their volcanic successions are shown schematically
165 in Figure 4. Below we provide a short description of their main features.

166 *2.2.1. Eiao*

167 Eiao (Maury et al., 2009) is the northernmost (Fig. 1) and largest (44 km^2) uninhabited island in French
168 Polynesia. It corresponds to the northwestern crescent-shaped remains of the caldera wall and of the
169 external upper slopes of a 20 km large collapsed volcano. Its coastal cliffs expose a ca 400 m thick pile of
170 tholeiitic basaltic flows interbedded with less common alkali basalts and crosscut by a dense network of
171 radial dykes. Three deep core drillings have sampled the upper 1,200 m thick sequence of the Eiao shield,
172 down to -700 m below sea level (Caroff et al., 1995, 1999). The base of this sequence, dated at 5.52-5.48
173 Ma (Fig. 2), is made up of quartz-normative tholeiitic flows overlain by olivine tholeiitic flows (Fig. 3). These
174 are in turn overlain by a ca 250 m thick sequence of hawaiites and mugearites, with a single intercalated
175 trachytic flow 5.44 Ma old (Fig. 4). The middle (dated at 5.36-5.25 Ma) and upper (4.98-4.95 Ma) parts of the
176 drilled pile are mostly made up of olivine tholeiites intercalated with picobasaltic and alkali basaltic flows
177 (Caroff et al., 1995, 1999; Maury et al., 2009). The old quartz tholeiites are less enriched in incompatible
178 elements than the overlying olivine tholeiites and alkali basalts, and their Sr, Nd, Pb isotopic composition
179 tends towards a HIMU end-member. Hawaiites and mugearites result from open-system fractional
180 crystallization of the latter basaltic magmas, coupled with variable extents of assimilation of materials from
181 the underlying oceanic crust (Caroff et al., 1999).

182 *2.2.2. Nuku Hiva*

183 Nuku Hiva (Legendre et al., 2005b; Maury et al., 2006) is the largest island of the archipelago (339 km^2).
184 It has a semicircular shape, and its northern, western and eastern parts correspond to the northern half of a
185 huge shield, the Tekao volcano (Fig. 4). It is exclusively made up of olivine tholeiites (Fig. 2) derived from a
186 mantle source containing a depleted MORB mantle (DMM) component. Its upper flows were emplaced
187 between 4.01 and 3.83 Ma according to unspiked ^{40}K - ^{40}Ar data (Fig. 3), although altered flows from the
188 lower part of the exposed pile yielded ^{40}Ar - ^{39}Ar ages ranging from 4.52 to 4.08 Ma (Maury et al., 2006).
189 Between 4.00 and 3.62 Ma (unspiked ^{40}K - ^{40}Ar data), the Taiohae inner (post-shield) volcano grew inside the
190 caldera of the Tekao shield, after the southern part of the latter collapsed along a $\text{N}75^\circ\text{E}$ trending normal
191 fault parallel to the MFZ. This collapse event at ca 4.0 Ma (Fig. 4) has been attributed to the lateral
192 spreading of a weak hydrothermal zone located in the central part of the Tekao shield over an unconfined
193 boundary, corresponding to the lower compartment of this fault (Merle et al., 2006). Mapping relationships
194 allow us to estimate the volume of the Taiohae post-shield volcano to $45 \pm 5 \text{ km}^3$, i.e. 28% of the emerged
195 volume of the edifice (160 km^3), but only 0.6% of its total volume ($6,950 \text{ km}^3$, Chauvel et al., 2012). Lavas

196 from the Taiohae volcano include, from bottom to top: olivine tholeiites more enriched in incompatible
197 element than those of the Tekao shield; alkali basalts and a few basanites; and large amounts of hawaiites
198 and mugearites, which cover 47% of its surface, together with benmoreites and trachytes (25% of its
199 surface). In addition, parasitic vents erupted hawaiitic (3.93 Ma) and trachytic (3.92 Ma) flows on the
200 external slopes of the Tekao shield. All the Taiohae post-shield lavas are more radiogenic in Sr and Nd and
201 less radiogenic in Nd than the Tekao ones. Hawaiites and mugearites likely derived from the fractional
202 crystallization from mafic magmas involving separation of amphibole (Legendre et al., 2005b). The isotopic
203 signature of benmoreites and trachytes is closer to the enriched mantle II (EM II) end-member than that of
204 mafic lavas, a feature inconsistent with simple fractionation processes.

205

206 *2.2.3. Ua Huka*

207 Despite its moderate size (83 km²), Ua Huka Island (Legendre et al., 2006; Blais et al., 2008, Chauvel et
208 al., 2012) displays a relatively prolonged, multi-phase geological evolution. Like Nuku Hiva, it has a
209 semicircular shape due to the collapse of the southern half of its outer shield, the Hikitau volcano. It is made
210 up of olivine tholeiitic flows emplaced between 3.24 and 2.94 Ma. The Hane inner (post-shield) volcano was
211 built inside the central caldera of the Hikitau shield between 2.97 and 2.43 Ma (Fig. 4). Its alkali basaltic
212 flows derived from a spinel lherzolite source similar to that of the Hikitau tholeiites but having experienced
213 smaller degrees of melting (Legendre et al., 2006). Associated benmoreitic flows and trachytic and phonolitic
214 domes were simultaneously emplaced (between 2.93 and 2.71 Ma) within the Hane post-shield volcano and
215 from parasitic vents located on the outer slopes of the Hikitau shield. Then, after a 1.3 Myr long quiescence
216 period (Fig. 2), volcanic activity resumed, building over the inner slopes of the Hane volcano two basanitic
217 strombolian cones, the Teepoepo (1.15-0.96 Ma) and the Tahoatikikau (0.82-0.76 Ma). Their lavas
218 originated from temporally decreasing melting degrees of a garnet lherzolite source deeper and isotopically
219 more depleted than that of the older Ua Huka tholeiitic and alkali basalts (Chauvel et al., 2012). The origin of
220 this rejuvenated volcanism (the single case identified so far in the archipelago) has been attributed to a
221 secondary melting zone located downstream the Marquesas plume (Legendre et al., 2006), similar to that
222 envisioned by Ribe and Christensen (1999) for the Hawaiian islands. The volumes (estimated from mapping
223 relationships) of the Hane post-shield volcano (6±1 km³) and the rejuvenated cones (0.6±0.1 km³)
224 correspond respectively to 21% and 2% of the total emerged volume of Ua Huka (28 km³), and less than
225 0.2% only of the bulk volume of the edifice (3,250 km³).

226

227 *2.2.4. Ua Pou*

228 The 105 km² diamond-shaped island of Ua Pou (Legendre et al., 2005a; Guille et al., 2010) is famous
229 for the exceptional abundance of phonolites (Figs. 3 and 4), which cover 65% of its surface and include
230 spectacular phonolitic spines (Ua Pou means “The Pillars” in Marquesan). Its oldest lavas are olivine
231 tholeiite flows derived from a young HIMU-type mantle source (Duncan et al., 1986, Vidal et al., 1987). They
232 outcrop in a very small area near Hakahau village in the northeast part of the island. The base of their ca 40
233 m thick pile (Guille et al., 2010) is not accessible presently but has been dated at 5.61, 4.51 and 4.46 Ma by

234 the ^{40}K - ^{40}Ar method on whole rocks (Duncan et al., 1986). Its presently exposed top flow was dated at 4.00
235 Ma by the unspiked ^{40}K - ^{40}Ar method on groundmass (Legendre et al., 2005a). These Hakahau tholeiitic
236 flows are overlain either by up to 100 m thick laharic deposits or by trachytic and phonolitic domes dated at
237 3.86 and 3.27 Ma (Guille et al., 2010). The latter sequence is in turn overlain by a strongly silica-
238 undersaturated lava suite forming the bulk of the island and dated between 2.95 and 2.35 Ma (unspiked ^{40}K -
239 ^{40}Ar ages). It includes from bottom to top: (1) basanitic and tephritic lava flows with intercalated laharic
240 deposits, (2) lower phonolitic flows and intrusions, (3) basanitic and intermediate (tephritic, tephriphonolitic
241 and benmoreitic) flows with occasional interbedded phonolites, (4) upper phonolitic flows, up to 500 m thick,
242 and finally (5) phonolitic domes and spines, the summit of which tower several hundred meters above the
243 older units. The basanitic magmas of this suite derived from low degrees of melting of an heterogeneous
244 mantle source intermediate between EM II and HIMU end-members, and evolved towards tephritic liquids by
245 fractional crystallization (Legendre et al., 2005a). The origin of tephriphonolitic and benmoreitic magmas was
246 ascribed to the remelting at depth of basanitic rocks, leaving an amphibole-rich residuum (Legendre et al.,
247 2005a). These liquids evolved by either closed-system or more commonly open-system fractionation
248 towards phonolitic and trachytic magmas.

249 In contrast with the other Marquesas Islands, the main Ua Pou volcanic sequence (2.95-2.35 Ma) does
250 not include a basaltic shield. We therefore support Duncan et al.'s (1986) suggestion that the Ua Pou shield
251 is mainly below sea level, with only its uppermost tholeiitic part presently exposed, and that the rest of the
252 island belongs to the post-shield phase. This interpretation is supported by the occurrence of thick laharic
253 deposits overlying the tholeiitic flows, which indicate an erosional event. However, the temporal hiatus
254 between the shield and post-shield phases (only between 4.00 and 3.86 Ma according to Guille et al., 2010)
255 is much shorter than that proposed by former authors: 1.58 Myr calculated using Duncan et al.'s (1986) data
256 and 2.34 Myr according to Woodhead (1992).

257

258 **3. New geological, geochemical and K-Ar age data on the southern Marquesas islands.**

259

260 *3.1. Methods*

261 The analytical techniques are identical to those used to study the northern islands. Unspiked ^{40}K -
262 ^{40}Ar ages were obtained at the LSCE (Laboratoire des Sciences du Climat et de l'environnement) in
263 Gif-sur-Yvette. Fresh and well-crystallized samples were selected for dating after macroscopic and
264 microscopic inspections allowing us to check the lack of post-magmatic mineral phases. In addition,
265 the degree of alteration of these samples was estimated from their loss on ignition value (LOI). For 40
266 out of 45 dated samples (Tables 2 and 4) LOI ranges from -0.39 to 1.56 wt% and these samples are
267 considered as essentially unaltered. The 5 other samples (HV81, HV99, MT11, TH35 and FH30) have
268 LOI between 1.90 and 2.77 wt%. Despite their higher LOI, we selected them because of their critical
269 geological position or their unusual composition (tephriphonolitic sample TH35). The samples were
270 crushed and sieved to 0.250-0.125 mm size fractions, and ultrasonically washed in acetic acid (1N)
271 during 45 minutes at a temperature of 60°C to remove unsuspected minute amounts of secondary
272 mineral phases. Potassium and argon were measured on the microcrystalline groundmass, after
273 removal of phenocrysts using heavy liquids and magnetic separations. This process removes at least

274 some potential sources of systematic error due to the presence of excess ^{40}Ar in olivine and feldspar
275 phenocrysts (Laughlin et al., 1994). The K content of the separated groundmass was measured by
276 ICP-AES in Plouzané using the same method as for major elements while Ar analyses were
277 performed in Gif-sur-Yvette using the procedures of Guillou et al. (2011). Ages given in Tables 1 and 3
278 were calculated using the constants recommended by Steiger and Jäger (1977). Unspiked K-Ar
279 analysis of each sample involved three independent determinations of potassium and two of argon.
280 Based on replicate analysis of material references, the potassium concentrations were determined
281 with an uncertainty of 1% (1σ). These potassium concentrations were averaged to yield a mean value.
282 Age determinations of each sample were made using this mean value and the weighted mean of the
283 two independent measurements of $^{40}\text{Ar}^*$ (radiogenic argon). Analytical uncertainties for the Ar data are
284 1σ , and consist of propagated and quadratically averaged experimental uncertainties arising from the
285 ^{40}Ar (total) and $^{40}\text{Ar}^*$ determinations (see Westaway et al., 2005 for more details). Uncertainties on the
286 ages are given at 2σ .

287 Before chemical analyses, all samples were crushed using an agate mortar. Major and trace element
288 data (Tables 2 and 4) were obtained by Inductively Coupled Plasma-Atomic Emission Spectrometry (ICP-
289 AES) at IUEM, Plouzané using the method of Cotten et al. (1995). The international standards used for
290 calibration were ACE, BEN, JB-2, PM-S and WS-E and the relative standard deviations are $\pm 1\%$ for SiO_2 ,
291 and $\pm 2\%$ for other major elements except P_2O_5 and MnO (absolute precision $\pm 0.01\%$). Samples were
292 classified according to their position in the TAS diagram (Fig. 3). Within the basalt group, silica-saturated or -
293 oversaturated lavas (normative *hy + ol* or *hy + Q*) were called tholeiitic basalts while nepheline-normative
294 samples were called alkali basalts (normative compositions given in Tables 2 and 4). Some tholeiitic basalts
295 plot close to or even above the Macdonald and Katsura's (1964) boundary in Figure 3 and could therefore
296 be considered as transitional basalts. We did not include the latter category in our classification chart
297 because it has not been previously used in the Marquesas and is not defined rigorously.

298

299 3.2. Hiva Oa

300 Hiva Oa (320 km^2), the second largest Marquesas island and the highest one (1276 m at Mt Temetiu),
301 has a WSW-ENE elongated shape parallel to the MFZ (Fig. 1). New field data (Fig. 5) combined with 20 new
302 unspiked ^{40}K - ^{40}Ar ages (Table 1) show that the island consists in four coalescent volcanoes whose age
303 decreases eastwards from 2.55 ± 0.05 to $1.46\text{-}1.44 \pm 0.03$ Ma (Figs. 4 and 5). All of them are made up of
304 tholeiitic basalts, some of which display a transitional affinity, and hawaiites (Table 2). Alkali basalts and
305 basanites were not identified in our set of 87 newly collected samples (Maury et al., 2012) nor in previous
306 samplings by R. Brousse (Chauvel et al., 2012, their Supplementary file D). Mugearites, benmoreites and
307 trachytes (Table 2) occur only in the post-shield Ootua volcano, or as dykes and plugs crosscutting the
308 Puamau shield.

309 The oldest volcano, Taaoa, is located on the western coast of Hiva Oa (Fig. 5). It represents the
310 crescent-shaped remnants of a largely collapsed shield, which are unconformably overlain by the flows of
311 the much bigger Temetiu shield. The Taaoa edifice is formed by a monotonous pile of meter-thick tholeiitic
312 flows interbedded with strombolian ashes and lapilli. The lowermost flow of this pile, located in Taaoa

313 village, was dated at 2.55 ± 0.05 Ma (HV64, Table 1 and Fig. 4). Taaoa basalts have lower K contents, lower
314 $^{87}\text{Sr}/^{86}\text{Sr}$ and higher $^{206}\text{Pb}/^{204}\text{Pb}$ ratios compared to all other Hiva Oa basalts, and their trace element and
315 isotopic signatures are closer to HIMU (Chauvel et al., 2012). They plot within the “Ua Pou” trend unlike all
316 other lavas that plot in the “Ua Huka” trend. Accordingly, the N65°W limit between the two isotopic stripes
317 defined by Chauvel et al. (2012) has been set at Taaoa village.

318 The Temetiu shield (Fig. 5) is the largest volcano of Hiva Oa. It is made of a more than 1,200 m thick
319 pile of meter-thick quartz or olivine normative tholeiites and hawaiites (Table 2). The construction of its
320 exposed part started around 2.27 ± 0.05 Ma (HV87, foot of Mt Temetiu) and 2.25 ± 0.05 Ma (HV84, northern
321 slopes near Hanaiapa village). Its major activity occurred between 2.13 ± 0.05 and 1.91 ± 0.04 Ma, based on
322 seven unspiked ^{40}K - ^{40}Ar ages (Table 1 and Fig. 4). Its well-exposed semicircular caldera facing south
323 collapsed before 2.01 Ma. Indeed, this event was followed by landslides which generated avalanche and
324 debris flow deposits, later crosscut by a number of dykes, including HV99 (2.01 ± 0.04 Ma) south of Atuona
325 village. Volcanic activity of the Temetiu shield ended at 1.83 ± 0.04 Ma (sample HV81 north of Hanapaaoa
326 village). It was almost immediately followed by the emplacement at 1.80 ± 0.04 Ma (sample HV65) of a thick
327 pile of post-shield tholeiitic flows (the Atuona flows) within the caldera, east and north of Atuona village.
328 Temetiu shield and Atuona post-shield tholeiitic flows share the same isotopic signature typical of the “Ua
329 Huka” stripe (Chauvel et al., 2012). The origin of the collapse of the southern part of these edifices is
330 attributed to the lateral spreading of an hydrothermal zone located beneath the Temetiu caldera over an
331 unconfined boundary corresponding to the lower compartment of a fault parallel to the MFZ (Maury et al.,
332 2013), such as in the case of Nuku Hiva.

333 The Puamau shield forms the eastern part of Hiva Oa (Fig. 5). Its lower part is made up of an up to 500
334 m thick pile of meter-thick flows of quartz tholeiites, olivine tholeiites and interbedded hawaiites dipping
335 gently towards the Temetiu shield or the southern coast. They are dated at 1.65 ± 0.04 (HV70) and $1.62 \pm$
336 0.04 Ma (HV62). They are overlain by a 200 m thick pile of tholeiitic basalts and minor interbedded hawaiites
337 occurring as thicker (5-20 m) and usually columnar-jointed flows (Puamau shield upper flows in Fig. 5).
338 Although this unit is younger (1.46 ± 0.03 Ma, sample HV88) than the main shield, we do not consider it as
339 belonging to the post-shield stage. Indeed, both were affected by the collapse event that led to a caldera
340 open NE, with its center near the village of Puamau (Fig. 5). Post-caldera volcanic edifices have not been
341 identified within this caldera, but several small benmoreitic and trachytic dykes and plugs (not shown in the
342 simplified geologic map of Fig. 5) crosscut the Puamau shield pile. They are usually altered and therefore
343 unsuitable for ^{40}K - ^{40}Ar dating.

344 The Ootua post-shield edifice was emplaced on the eastern slopes of the Temetiu shield. Its central unit,
345 ca 200 m thick, is exclusively made up of intermediate (mugearitic, benmoreitic and phonotephritic) and
346 silica-oversaturated trachytic flows and N-S trending dykes. It culminates at Mt Ootua, a 500 m wide and
347 200 m high columnar-jointed dome of quartz normative trachyte. This unit is dated at 1.73 ± 0.04 Ma (HV56
348 mugearitic flow) and 1.64 ± 0.03 Ma (HV54 benmoreitic dyke). Its peripheral unit consists of an up to 400
349 m thick pile of fissure erupted tholeiitic and hawaiitic flows. Most of these flows display well-developed basal
350 autoclastic breccias. They flow over either (1) the northern and southern slopes of the Temetiu shield, (2) its
351 caldera within which they overlie the Atuona post-shield flows, and finally (3) towards the topographic trough

352 separating the Temetiu and Puamau shields (Fig. 5). They fill most of this trough, flowing either towards the
353 northern coast or the southern coast where a tholeiitic basalt (HV107) yields the youngest age measured in
354 Hiva Oa (1.44 ± 0.03 Ma). Another young age of 1.51 ± 0.03 Ma has been obtained on an hawaiitic flow
355 (HV86) overlying the Temetiu shield.

356 The volumes (estimated from mapping relationships) of the Atuona and Ootua post-shield lavas (14 ± 1
357 km^3) correspond to 9.5% of the total emerged volume of Hiva Oa (145 km^3), and 0.2% of the bulk volume of
358 the edifice ($6,900 \text{ km}^3$, Chauvel et al., 2012).

359

360 3.3. Motane and Tahuata

361 Motane (Figs. 1 and 5) is a small (13 km^2) crescent-shaped uninhabited island located southeast of Hiva
362 Oa and east of Tahuata. Like Eiao, it corresponds to a sector of the caldera wall (up to 500 m high) and the
363 upper external slopes of a largely collapsed shield volcano. It is made up of a monotonous pile of meter-
364 thick quartz and olivine tholeiitic flows, interbedded with picobasalts and minor hawaiites. This pile is
365 crosscut by a dense network of radial dykes, which include alkali basalts and basanites (Fig. 4) displaying
366 incompatible element patterns more fractionated than those of the tholeiites. Two tholeiitic flows from the
367 middle part of the pile are dated at 1.59 ± 0.04 Ma (MT04, altitude 120 m) and 1.53 ± 0.03 Ma (MT08,
368 altitude 190 m) (see Table 3). An alkali basaltic dyke collected at sea level yields an older age (1.96 ± 0.04
369 Ma, MT11 in Table 3) that is barely consistent with the others and may indicate sample contamination by
370 seawater (also consistent with its relatively high LOI of 2.53 wt%). The isotopic Sr, Nd, Pb compositions of
371 tholeiites MT04 and MT08 are typical of the “Ua Pou” stripe (Chauvel et al., 2012), as well as that of
372 basanitic sample MT12 that is clearly more radiogenic in Sr and less radiogenic in Nd than the tholeiites.

373 Tahuata (69 km^2) corresponds to the northwestern half of a large shield known as the Vaitahu shield
374 (Maury et al., 2013). Its southern part has collapsed over an unconfined boundary. The latter probably
375 corresponds to the SE down-faulted block, lowered by 1,000 m, of a major N35°E fault lineament well-
376 identified off the SE coast of the island (Maury et al., 2013). This collapse event led to the formation of an 8
377 km large caldera opened toward SE (Fig. 5). A small edifice, the inner Hanatetena volcano (Figs. 4 and 5)
378 grew inside this caldera. The caldera wall was later affected by large landslides, which generated an up to
379 300 m thick pile of avalanche and debris flow deposits. The latter partly filled up the topographic trough
380 separating the foot of the caldera wall from the Hanatetena post-shield edifice.

381 The 700 m thick lower unit of the Vaitahu shield consists of meter-thick basaltic and hawaiitic flows. The
382 unspiked ^{40}K - ^{40}Ar ages (Table 3) indicate that it was emplaced rather quickly, between 2.11 ± 0.05 Ma
383 (TH39 tholeiitic basalt, western coast south of Hapatoni village) and 1.81 ± 0.04 Ma (TH14 alkali basalt,
384 northern coast). Three ages clustering around 1.90 Ma (TH37, TH38 and TH18 tholeiitic basalts, central part
385 of the island) may record the paroxysmal event. This lower unit is overlain by a pile of thick (>10 m) and
386 usually columnar-jointed tholeiitic flows. This upper unit forms the central ridge of the island, and is up to 500
387 m thick. Its basal flow has an age of 1.88 ± 0.04 Ma (TH13). We consider it as the upper part of the Vaitahu
388 shield, because (1) it conformably overlies the top of the lower unit, (2) its age is similar to that of the main

389 building phase of the lower unit between 1.91 ± 0.04 and 1.88 ± 0.04 Ma, and (3) it was obviously affected
390 by the caldera collapse event, as it forms presently the uppermost slopes of the caldera wall (Fig. 5).

391 A specific feature of the Vaitahu shield is its chemical heterogeneity. It is mostly tholeiitic (18 quartz
392 tholeiites and olivine tholeiites in our sample set), but also includes alkali basalts (2 samples), basanites (3
393 samples) and hawaiites (3 samples). Alkali basalts and basanites are more sodic and more enriched in the
394 most incompatible elements compared to the tholeiites (Table 4), and they display consistently higher
395 $^{87}\text{Sr}/^{86}\text{Sr}$ and lower $^{143}\text{Nd}/^{144}\text{Nd}$ and $^{206}\text{Pb}/^{207}\text{Pb}$ ratios according to data obtained on the same samples
396 (Chauvel et al., 2012).

397 The small (less than 200 m high) post-caldera Hanatetena volcano is composed exclusively of tholeiitic
398 and hawaiitic flows. The basal flows display pahoehoe and lava tube features; they are overlain by highly
399 weathered flows of meter thickness. Their trace element and isotopic compositions plot within the range of
400 the Vaitahu shield tholeiites (Chauvel et al., 2012). Two flows are dated at 1.80 ± 0.04 Ma (TH31) and $1.74 \pm$
401 0.04 Ma (TH8). The exposed volume of the Hanatetena edifice ($0.5 \pm 0.1 \text{ km}^3$) represents only 2% of the
402 volume of Tahuata island (25 km^3).

403 The single intermediate/evolved lava documented in Tahuata is a columnar-jointed tephriphonolitic
404 spine, 200 m in diameter, which crosscuts the northern slopes of the Vaitahu shield and forms the summit of
405 Mt Tumu Meae Ufa (1,050 m). Because of its young age (1.78 ± 0.04 Ma, sample TH35), we relate its
406 emplacement to the post-shield stage.

407

408 3.4. *Fatu Hiva*

409 Fatu Hiva Island (84 km^2) displays a typical semicircular shape. It includes an external (outer) shield, the
410 Touaouoho volcano, truncated by a 8 km wide caldera opening westwards, inside which grew a smaller
411 post-caldera edifice, the Omoa volcano (Fig. 5). As in Tahuata, the caldera wall was affected by landslides
412 which generated avalanche and debris flow deposits up to 250 m thick. These deposits now outcrop within
413 the topographic trough separating the outer shield from the inner Omoa post-shield edifice. The drowning of
414 the western half of the island and the development of the caldera are probably related to major sector
415 collapse events, marked in the regional bathymetry by a 15 km wide trough (at 2,500 m depth) located west
416 of Fatu Hiva, downslope from the Omoa volcano.

417 The Touaouoho shield has an up to 1,100 m thick rather monotonous pile of meter-thick flows of olivine
418 tholeiites, tholeiitic picobasalts and minor hawaiites (Table 4), crosscut by a dense network of radial
419 inframetric tholeiitic dykes. Their unspiked ^{40}K - ^{40}Ar ages (Table 3) range from 1.81 ± 0.04 Ma (FH13) to 1.35
420 ± 0.03 Ma (FH18). The Omoa post-caldera edifice is composed of a 700 m thick pile of inframetric tholeiitic
421 flows, with lava tubes in pahoehoe composite flows. Their ages (Table 3) range from 1.43 ± 0.03 Ma (FH08)
422 to 1.23 ± 0.04 Ma (FH05). In addition, a tholeiitic dyke (FH30) crosscutting the debris flow deposits at
423 Hanavave village yielded an age of 1.41 ± 0.03 Ma, consistent with the end of volcanic activity in Touaouoho
424 shield and the initiation of that of the post-shield Omoa edifice. These two stages led to the emplacement of
425 rather similar tholeiitic basalts and hawaiites (Table 4). Their major, trace element (Table 4) and isotopic Sr

426 Nd Pb and Hf compositions largely overlap, and both are typical of the predominantly EM II-HIMU sources of
427 the southwestern trend, which has been labelled the “Fatu Hiva group” (Chauvel et al., 2012).

428 The youngest Fatu Hiva lavas are two well-preserved trachytic domes (Figs. 4 and 5) crosscutting and
429 overlying the Touaouoho shield flows on the northern coast (FH16, 1.11 ± 0.02 Ma) and east of Omoa
430 village (FH06, 1.22 ± 0.03 Ma). In addition, a 15 m wide trachytic dyke (FH12) crosscutting the basal flows of
431 Omoa post-shield edifice is dated at 1.38 ± 0.03 Ma, and was therefore emplaced during the post-shield
432 stage. The volumes (estimated from mapping relationships) of the Omoa post-shield lavas (5 ± 1 km³)
433 correspond to 28% of the total emerged volume of Fatu Hiva (28 km³), and 0.2% only of the bulk volume of
434 the edifice (2,800 km³).

435

436 **4. Discussion**

437 *4.1. Timing of eruptions: no gap between shield-building and post-caldeira stages*

438 The new unspiked ⁴⁰K-⁴⁰Ar ages plotted against the distances of the islands to the MFZR along the
439 N65°W direction of movement of the Pacific plate (Fig. 2) are reasonably consistent with its local motion rate
440 of 10.5 cm/year, as previously pointed out by Legendre et al. (2006). These new ages display much less
441 scatter than the age-distance to the MFZR plots using the main N30-40°W trend of the chain and all the
442 available ⁴⁰K-⁴⁰Ar ages measured on bulk rocks (Brousse et al., 1990; Desonie et al., 1993; Guille et al.,
443 2002). The dashed line in Fig. 2, which corresponds to distances to the unexplored seamount chain located
444 ca 50 km north of the MFZR (Fig. 1), provides a better fit to the start of activity in some islands. Thus, this
445 seamount chain is a strong candidate for the present-day location of the Marquesas hotspot. Overall, Ua
446 Huka differs from all the other islands by the fact that the emplacement of the exposed part of its shield
447 started clearly later than predicted by the hotspot hypothesis (Fig. 2). It is also the only Marquesas Island
448 showing a rejuvenated volcanic stage (Legendre et al., 2006).

449 Data plotted in Figures 2 and 4 show that there is no consistent temporal hiatus between the shield-
450 building and post-caldeira activities. Usually the two stages either slightly overlap (Nuku Hiva, Ua Huka, Fatu
451 Hiva) or the gap between them is within the range of analytical uncertainties (Temetiu shield and Atuona
452 post-caldeira lavas in Hiva Oa, Tahuata). In Ua Pou, a marginal hiatus (Guille et al., 2010) is observed
453 between the youngest shield tholeiitic basalt (4.00 ± 0.06 Ma) and the oldest post-shield phonolite (3.86 ± 0.06
454 Ma). However, this might be due to sampling bias because of the very small size of the emergent part of the
455 shield that is mostly overlain by lahar deposits. Such a temporal continuity implies that the growth of post-
456 shield edifices started immediately after the main caldera collapse event, while eruptive activity was still
457 occurring at least in some parts of the shield volcano. Another striking feature of the data shown in Figure 2
458 is that contemporaneous volcanism occurred in islands located more than 100 km away from each other
459 (Fig. 1), e.g. around 2.5 Ma (Ua Huka, Ua Pou, Hiva Oa) or between 2.0 and 1.5 Ma (Hiva Oa, Tahuata,
460 Motane and Fatu Hiva). This feature is consistent with a “classical” plume model involving a 200 km large
461 summital melting zone (Farnetani and Hoffmann, 2010), and it is also observed in other hotspot-related
462 islands such as the Hawaiian chain (Clague and Dalrymple, 1987), the Society archipelago (Guillou et al.,
463 2005) and the Canaries (Carracedo et al., 1998). However, rejuvenated volcanism is much less common in

464 the Marquesas (Ua Huka) than in the Hawaiian chain, the Canaries, Mauritius (Paul et al., 2005) and Samoa
465 (Konter and Jackson, 2012).

466

467 *4.2. Evidence for post-shield emplacement of nearly all the intermediate and evolved lavas*

468 The TAS diagram (Fig. 3) and the age versus SiO₂ plot (Fig. 6) show that nearly all the dated lavas more
469 evolved than tholeiitic and alkali basalts, basanites and hawaiites were erupted during the post-shield stage
470 of Marquesan volcanoes. These include rare tephrites (Ua Pou), mugearites (Hiva Oa), benmoreites (Nuku
471 Hiva, Ua Pou, Hiva Oa) and tephriphonolites (Ua Pou, Tahuata), and more abundant trachytes (Nuku Hiva,
472 Ua Huka, Ua Pou, Hiva Oa, Fatu Hiva) and phonolites (Ua Pou, Ua Huka). The only exception is Eiao, in
473 which coring has recovered a 10 m thick trachytic flow in the Dominique drill hole (Caroff et al., 1995; Maury
474 et al., 2009), at depths of 462 to 472 m below sea level. It has been dated at 5.44±0.04 Ma, an age perfectly
475 consistent with its position within the Eiao shield pile. This trachyte represents only a very small fraction of
476 the 2,100 m long cored volcanic sequences recovered from the three Eiao deep drillings. However,
477 mugearites (undated) also occur in the three cored sequences, in which they have a total thickness of ca 70
478 m (Maury et al., 2009). The origin of Eiao mugearites and trachytes has been ascribed to open-system
479 fractional crystallization of associated alkali basaltic magmas, coupled with assimilation of the oceanic crust
480 underlying the shield (Caroff et al., 1999).

481 In the other islands, the intermediate and evolved lavas erupted within the post-shield volcanoes (Nuku
482 Hiva, Ua Huka, Ua Pou, Ootua edifice in Hiva Oa). However, some of them outcrop as parasitic domes,
483 spines, plugs or dykes crosscutting the older (outer) volcanic shields: trachytes in Nuku Hiva, Ua Huka, Hiva
484 Oa (within the Puamau shield) and Fatu Hiva, and the tephriphonolitic spine of Mt Tumu Meae Ufa in
485 Tahuata. In Nuku Hiva, Ua Huka and Ua Pou, these trachytes or phonolites and the associated intermediate
486 lavas outcrop together with alkali basalts and/or basanites. Their ⁴⁰K-⁴⁰Ar ages fall within the range of those
487 of the latter or are slightly younger. In the case of Nuku Hiva, petrogenetic studies (Legendre et al., 2005b)
488 led to the conclusion that trachytes derived from open system fractional crystallization of alkali basalt
489 magmas coupled with assimilation of enriched oceanic crust with an EM II signature. The origin of the
490 unusually abundant phonolites from Ua Pou is thought to result from the fractionation of tephriphonolitic and
491 benmoreitic magmas derived from the remelting of basanitic rocks (Legendre et al., 2005a). In Fatu Hiva,
492 the emplacement of trachytes was contemporaneous with or post-dated that of post-caldera tholeiitic
493 basalts, but the possible petrogenetic relationships between them have not been investigated. The same
494 situation pertains to the Ootua post-shield volcano in Hiva Oa, where a spatial and temporal association of
495 tholeiitic basalts (some of which display a transitional affinity), hawaiites, mugearites, benmoreites and
496 trachytes is exposed (Maury et al., 2013). Evolved lavas were emplaced during the known entire history of
497 the archipelago (Fig. 6): Eiao trachyte is one of the oldest lavas of our set of data and Fatu Hiva ones count
498 among the youngest. Nuku Hiva and Ua Huka trachytes as well as the very abundant Ua Pou phonolites
499 were emplaced between ca 4.0 and 2.5 Ma (Fig. 6).

500 *4.3. Chemical diversity of shield and post-shield basaltic lavas*

501 In the Hawaiian model, basaltic magmas derive from temporally decreasing melt fractions of the mantle
502 sources: the emplacement of tholeiitic shield basalts is followed by that of post-shield alkali basalts and then

503 by rejuvenated basanites or nephelinites, and Sr isotopic ratios decrease during this evolution (Garcia et al.,
504 2010; Hanano et al., 2010). In the Marquesas, Ua Huka island volcanism followed this trend, with the
505 successive emplacement of Hikitau shield tholeiites, Hane post-shield alkali basalts and associated
506 benmoreites, trachytes and phonolites, and finally Teepoepo and Tahoatikikau rejuvenated basanitic cones.
507 However, Hikitau and Hane basalts display similar radiogenic Sr isotopic compositions, and only the
508 basanites from the rejuvenated cones are less radiogenic (Chauvel et al., 2012). In Ua Pou, the small
509 emergent remnants of an HIMU-type tholeiitic shield are overlain by a thick post-shield pile of basanites,
510 phonolites and other silica-undersaturated lavas more radiogenic in Sr, with a dominant EM II signature
511 (Duncan et al., 1986; Vidal et al., 1987; Legendre et al., 2005a).

512 The temporal petrologic evolution of other islands is more complex. Most shield lavas are tholeiitic, but
513 minor amounts of alkali basalts and basanites displaying higher enrichments in incompatible elements and
514 more radiogenic Sr isotopic ratios are interbedded with them in the shields of Eiao and Tahuata, or occur as
515 dykes crosscutting them in the Motane shield. In Nuku Hiva, the large post-shield Taiohae volcano includes
516 olivine tholeiites, alkali basalts and basanites more radiogenic in Sr than the Tekao shield tholeiites
517 (Legendre et al., 2005b). Post-shield basaltic lavas are exclusively tholeiitic or transitional in Hiva Oa
518 (Atuona and Ootua units), Tahuata (Hanatetena) and Fatu Hiva (Omoa). Although displaying a rather large
519 isotopic variability, they fall within the range of shield tholeiites from the same islands (Chauvel et al., 2012).

520 As a whole, the claim by Woodhead (1992) and Castillo et al. (2007) that Marquesas shield lavas have
521 systematically lower $^{87}\text{Sr}/^{86}\text{Sr}$ ratios than post-shield lavas is not supported by isotopic studies conducted on
522 our sample set (Chauvel et al., 2012). This conclusion applies to islands from the two isotopic groups, e.g. to
523 Eiao and Ua Huka in the “Ua Huka group” and Hiva Oa, Tahuata and Fatu Hiva in the “Fatu Hiva group”
524 (Chauvel et al., 2012). The isotopic features of the sources of the Marquesas lavas are therefore not related
525 to the temporal pattern of volcanism (shield/post-shield activities) in a given island. The mafic lavas from the
526 two groups display similar La/Yb ratios (Fig. 7), while the Ua Huka rejuvenated basanites exhibit higher
527 ones. Post-shield intermediate and evolved lavas are more scattered in Fig. 7, probably because of their
528 complex petrogenesis (open-system fractionation or remelting of mafic magmas). In a similar La/Yb versus
529 La plot in which samples are sorted by petrographic type, alkali basalts display La/Yb ratios higher than
530 those of tholeiites (Chauvel et al., 2012, their Figure 6).

531 *4.4. Implications for Marquesas plume heterogeneity and hotspot models*

532 Hotspot models previously proposed for the Marquesas (Duncan et al., 1986; Woodhead, 1992; Desonie
533 et al., 1993; Castillo et al., 2007) involved melting of a heterogeneous zoned mantle plume and of the
534 overlying oceanic lithosphere, or interactions between ascending plume-derived melts and this lithosphere.
535 These models were based on the assumption that the archipelago followed an “Hawaiian-type” temporal
536 evolution, the main difference being that in the Marquesas shield tholeiitic basalts were less radiogenic in Sr
537 (closer to DMM and/or HIMU) than the post-shield alkalic lavas (closer to EM end-members). In addition,
538 some authors used the tholeiitic or alkalic compositions of the basalts (Woodhead, 1992) or even their Sr
539 isotopic ratios (Castillo et al., 2007) to classify them as shield or post-shield, which led to additional
540 confusion.

541 In the present study and in the Chauvel et al. paper (2012), we used exclusively geological (field
542 relationships determined from detailed mapping) and chronological (unspiked ^{40}K - ^{40}Ar ages) data to
543 determine the shield or post-shield position of the samples. Our results show that: (1) there was usually no
544 temporal gap between shield and post-shield activities at a given island; (2) eruptions occurred
545 simultaneously in islands distant as much as 100 km one from another; (3) although most shields are
546 tholeiitic, several of them (Eiao, Tahuata) contain interbedded alkali basaltic and basanitic flows; (4) while
547 post-shield intermediate and evolved lavas derive usually from alkali basaltic or basanitic magmas, several
548 post-shield volcanoes are tholeiitic (Hiva Oa, Tahuata, Fatu Hiva); (5) the trace element and isotopic
549 compositions of shield and post-shield tholeiites display large variations, but the two groups overlap in most
550 diagrams (Chauvel et al., 2012); and finally (6) the “Ua Huka” and “Fatu Hiva” isotopic groups involve
551 mixtures of different mantle components, all of them likely located within the plume itself (Chauvel et al.,
552 2012) as also envisioned for Hawaii (Frey et al., 2005; Fekiacova et al., 2007; Garcia et al., 2010; Hanano et
553 al., 2011).

554 The Sr and Nd isotopic differences between tholeiitic basalts and alkali basalts/basanites from
555 Marquesas Islands are shown in Figure 8. This plot shows all the data from the GEOROC database on
556 basaltic lavas whose major element and isotopic data were available. The sources of alkali basalts and
557 basanites are generally more enriched than those of the tholeiites at the scale of the archipelago. This is
558 also true within a given island, although the isotopic contrasts range from huge at Ua Pou to large at
559 Tahuata, Nuku Hiva, and Motane and small at Eiao and Ua Huka. These contrasts are consistent with the
560 hypothesis of an extremely heterogeneous character of the Marquesas plume. The nearly contemporaneous
561 emplacement of tholeiites and alkali basalts with different isotopic compositions in Tahuata (Chauvel et al.,
562 2012) suggests the occurrence of heterogeneous mantle domains 10 km or less in diameter, as envisioned
563 for several other plumes including Hawaii (Marske et al., 2007; Hanano et al., 2010), Mauritius (Paul et al.,
564 2005) and the Galápagos (Gibson et al., 2012). When affected by the same high thermal regime in the
565 central part of a plume, domains with contrasted lithologies could experience variable degrees of melting,
566 generating the observed diversity of basaltic magmas. Especially, low-degree melts might sample
567 preferentially fertile (and isotopically enriched) pyroxenite while the signature of the more depleted peridotitic
568 source dominates in high-degree melts (Sobolev et al., 2005, 2007; Jackson and Dasgupta, 2008; Day et
569 al., 2009; Dasgupta et al., 2010; White, 2010; Davis et al., 2011; Herzberg, 2011).

570 The occurrence of tholeiitic post-shield basalts in several islands is not surprising given the temporal
571 continuity between the shield and post-shield stages and the usually short period of emplacement of these
572 post-shield tholeiites (<0.1 Ma in Tahuata, Nuku Hiva and for Ootua basaltic flows in Hiva Oa; 0.2 Ma in Fatu
573 Hiva, Fig. 5 and Tables 1 and 3). It is likely that during such short time spans the extent of melting of the
574 plume at depth did not change significantly, while the volcano structure was considerably modified after the
575 caldera collapse event. Longer post-shield activities might record a decrease of melting and possible
576 preferential sampling of enriched materials. In the Taiohae inner edifice (Nuku Hiva) where post-shield
577 activity lasted ca 0.4 Ma (from 4.00 to 3.62 Ma; Maury et al., 2006), a brief tholeiitic episode was followed by
578 the emplacement of alkali basalts and basanites, and then by that of mugearites, benmoreites and trachytes
579 derived from an enriched mantle source. A rather similar evolution has been documented in the post-shield
580 volcanism of Mauna Kea, Hawaii (Frey et al., 1990), where the initial emplacement of tholeiites and alkali

581 basalts (basaltic substage) was followed by that of intermediate and evolved lavas (hawaiitic substage).
582 Finally, the emplacement of the rejuvenated basanitic strombolian cones in Ua Huka after a 1.3 Myr long
583 quiescence period (Fig. 2) was accompanied by major petrogenetic changes, involving very low melting
584 degrees of a garnet lherzolite source deeper and isotopically more depleted than that of the older tholeiitic
585 and alkali basalts (Legendre et al., 2006).

586 The petrologic and geochemical diversity of Marquesas lavas is rather exceptional given the modest
587 size of the archipelago, as appreciated since the pioneer works of A. Lacroix (1928) and L.J. Chubb (1930).
588 It can be related to the “weak” character of the Marquesas plume (McNutt et al., 1989), which produced
589 “only” 7,700 km³ of magma per Myr in the Marquesas (Chauvel et al., 2012), compared to 213,000 km³ for
590 the Big Island of Hawaii (Robinson and Eakins, 2006). Indeed, low degrees of partial melting resulted in the
591 preservation in the Marquesas basaltic magmas of geochemical features inherited from small-size source
592 heterogeneities, while high degrees of partial melting and resulting high magma production rate tend to
593 blend these features. The complex petrogenesis (open-system processes or remelting of mafic precursors)
594 of post-shield intermediate and evolved lavas contributed further to increase this diversity.

595 **5. Conclusions**

596 The study of 110 Marquesas lavas located on detailed geological maps and dated by the unspiked ⁴⁰K-
597 ⁴⁰Ar method on separated groundmass allows us to demonstrate that the temporal evolution of the
598 archipelago is rather different with respect to that of Hawaii and many other hotspot-related chains. There is
599 usually no temporal gap between shield and post-shield activities in a given island, and rejuvenated
600 volcanism is uncommon. Although most shields are tholeiitic, several of them (Eiao, Tahuata) contain
601 interbedded alkali basaltic and basanitic flows. The occurrence of intermediate and evolved lavas is
602 restricted to the post-shield stage, with one exception (Eiao). Although these lavas are usually associated
603 with alkali basaltic or basanitic magmas, several post-shield volcanoes are tholeiitic (Hiva Oa, Tahuata, Fatu
604 Hiva) or include tholeiites (Nuku Hiva). In a given island, the trace element and isotopic compositions of
605 shield and post-shield tholeiites overlap although both display large variations (Chauvel et al., 2012).

606 These features are inconsistent with former models (Duncan et al., 1986; Woodhead, 1992; Desonie et
607 al., 1993; Castillo et al., 2007) that postulated that the Marquesas followed a “Hawaiian-type” evolution.
608 They are consistent with the hypothesis of an extremely heterogeneous character of the Marquesas plume.
609 The “weak” character of this plume led to low degrees of partial melting, which in turn resulted in the
610 preservation in the basaltic magmas of geochemical features inherited from such small-size source
611 heterogeneities.

612 **Acknowledgements**

613 This study has been funded by CNRS (INSU and UMR 8212, 6538, 5275, 6518), BRGM and CEA-
614 DASE-DSM. We thank two anonymous reviewers for their very constructive comments that helped us to
615 improve the overall content of the manuscript. We also thank Mayors Guy Rauzy and Etienne Tehaamoana
616 (Hiva Oa), Henri Tuieinui (Fatu Hiva) and Félix Barsinas (Tahuata) who provided logistic support during
617 fieldwork. We are very grateful to Andy Teiki Richmond and the team of the Service du Développement
618 Rural of Atuona-Hiva Oa for their considerable help in the field, especially during coastal sampling and work

619 in densely forested areas. Joseph Cotten's contribution to analytical work is greatly appreciated. Jean
620 François Tannau and Vincent Scao provided helpful technical assistance. This is LSCE contribution N°5115.

621

622 **References**

- 623 Blais, S., Legendre, C., Maury, R.C., Guille, G., Guillou, H., Rossi, P., Chauvel, C., 2008.
624 Notice explicative, carte géologique de France, feuille de Ua Huka, Polynésie française, 102 pp, scale 1:
625 50,000, Bureau de Recherches Géologiques et Minières, Orléans, France.
- 626
- 627 Brousse, R., Barszczus, H.G., Bellon, H., Cantagrel, J.M., Diraison, C., Guillou, H., Léotot,
628 C., 1990. Les Marquises (Polynésie française): volcanologie, géochronologie, discussion d'un modèle de
629 point chaud [The Marquesas alignment (French Polynesia) – Volcanology, geochronology, a hotspot model].
630 Bulletin de la Société géologique de France 6, 933-949.
- 631
- 632 Cadio, C., Panet, I., Davaille, A., Diament, M., Métivier, L., de Viron, O., 2011. Pacific geoid
633 anomalies revisited in light of thermochemical oscillating domes in the lower mantle. Earth
634 Planetary Science Letters 306, 123-135.
- 635
- 636 Caress, D.V., McNutt, M.K., Detrick, R.S., Mutter, J.C., 1995. Seismic imaging of hotspot
637 related crustal underplating beneath the Marquesas Islands. Nature 373, 600-603.
- 638
- 639 Caroff, M., Maury, R.C., Vidal, P., Guille, G., Dupuy, C., Cotten, J., Guillou, H., Gillot, P.Y.,
640 1995. Rapid temporal changes in ocean island basalt composition – evidence from an 800 m
641 deep drill hole in Eiao shield (Marquesas). Journal of Petrology 36, 1333-1365.
- 642
- 643 Caroff, M., Guillou, H., Lamiaux, M.I., Maury, R.C., Guille, G., Cotten, J., 1999.
644 Assimilation of ocean crust by hawaiitic and mugearitic magmas: an example from Eiao
645 (Marquesas). Lithos 46, 235-258.
- 646
- 647 Carracedo, J.C., Day, S., Guillou, H., Badiola, E.R., Canas, J.A., Pérez Torrado, F.J., 1998.
648 Hotspot volcanism close to a passive continental margin: The Canary Islands. Geological Magazine 135,
649 591-604.
- 650
- 651 Castillo, P.R., Scarsi, P., Craig, H., 2007. He, Sr, Nd and Pb isotopic constraints on the origin
652 of the Marquesas and other linear volcanic chains. Chemical Geology 240, 205-221.
- 653
- 654 Chauvel, C., Maury, R.C., Blais, S., Lewin, E., Guillou, H., Guille, G., Rossi, P., Gutscher, M.-A., 2012. The
655 size of plume heterogeneities constrained by Marquesas isotopic stripes. Geochemistry Geophysics
656 Geosystems 13(1), Q07005, doi: 10.129/2012GC004123.
- 657
- 658 Chubb, L.J., 1930. The geology of the Marquesas islands. Bernice P. Bishop Museum Bulletin, 68, 1-71.
- 659
- 660 Clague, D.A., 1987. Hawaiian xenolith populations, magma supply rates, and development of magma
661 chambers. Bulletin of Volcanology 49, 577-587.
- 662
- 663 Clague, D.A., Dalrymple, G.B., 1987. The Hawaiian-Emperor volcanic chain. Part 1. Geological evolution.
664 United States Geological Survey Professional Paper 1350, 5-54.
- 665
- 666 Cotten, J., Le Dez, A., Bau, M., Caroff, M., Maury, R.C., Dulski, P., Fourcade, S., Bohn, M.,
667 Brousse, R., 1995. Origin of anomalous rare-earth element and yttrium enrichments in
668 subaerially exposed basalts: Evidence from French Polynesia. Chemical Geology 119, 115-138.
- 669
- 670 Courtillot, V., Davaille, A., Besse, J., Stock, J., 2003. Three distinct types of hotspots in the
671 Earth's mantle. Earth and Planetary Science Letters 205, 295-308.
- 672
- 673 Crough, S.T., Jarrard, R.D., 1981. The Marquesas-line swell. Journal of Geophysical Research 86, 1763-
674 1771.
- 675
- 676 Dasgupta, R., Jackson, M.G., Lee, C.T.A., 2010. Major element chemistry of ocean island

677 basalts - Conditions of mantle melting and heterogeneity of mantle source. *Earth and Planetary Science*
678 *Letters* 289, 377-392.

679

680 Davaille, A., Girard, F., Le Bars, M., 2002. How to anchor hotspots in a convecting mantle ? *Earth and*
681 *Planetary Science Letters* 203, 621-634.

682

683 Davis, F.A., Hirschmann, M.M., Humayun, M., 2011. The composition of the incipient partial melt of garnet
684 peridotite at 3 GPa and the origin of OIB. *Earth and Planetary Science Letters* 308, 380-390.

685

686 Day, J.M.D., Pearson, D.G., Macpherson, C.G., Lowry, D., Carracedo, J.C., 2009.
687 Pyroxenite-rich mantle formed by recycled oceanic lithosphere: Oxygen-osmium isotope
688 evidence from Canary Island lavas. *Geology* 37, 555-558.

689

690 Desonie, D.L., Duncan, R.A., Natland, J.H., 1993. Temporal and geochemical variability of
691 volcanic products of the Marquesas hotspot. *Journal of Geophysical Research* 98,
692 17649-17665.

693

694 Devey, C.W., Haase, K.M., 2003. The sources for hotspot volcanism in the South Pacific
695 Ocean, in: R. Hékinian, P.S., J.L. Cheminée (Ed.), *Oceanic hotspots: intraplate submarine*
696 *magmatism and tectonism*. Springer Verlag, Berlin, pp. 253-284.

697

698 Duncan, R.A., 1975. Linear volcanism in French Polynesia. Unpublished PhD Thesis, Australian National
699 University.

700

701 Duncan, R.A., McDougall, I., 1974. Migration of volcanism with time in the Marquesas
702 Islands, French Polynesia. *Earth and Planetary Science Letters* 21, 414-420.

703

704 Duncan, R.A., McCulloch, M.T., Barczus, H.G., Nelson, D.R., 1986. Plume versus
705 lithospheric sources for the melts at Ua Pou, Marquesas Island. *Nature* 303, 142-146.

706

707 Farnetani, C.G., Hofmann, A.W., 2010. Dynamics and internal structure of the Hawaiian
708 plume. *Earth and Planetary Science Letters* 295, 231-240.

709

710 Fekiacova, Z., Abouchami, W., Galer, S.J.G., Garcia, M.O., Hofmann, A.W., 2007. Origin
711 and temporal evolution of Ko'olau Volcano, Hawai'i: Inferences from isotope data on the
712 Ko'olau Scientific Drilling Project (KSDP), the Honolulu Volcanics and ODP Site 843. *Earth*
713 *and Planetary Science Letters* 261, 65-83.

714

715 Filmer, P.E., McNutt, M.K., Wolfe, C.J., 1993. Elastic thickness of the lithosphere in the
716 Marquesas and Society Islands. *Journal of Geophysical Research* 98, 19565-
717 19577.

718

719 Frey, F.A., Wise, W.S., Garcia, M.O., West, H., Kwon, S.-T., Kennedy, A., 1990. Evolution of Mauna Kea
720 volcano, Hawaii: petrologic and geochemical constraints on postshield volcanism. *Journal of Geophysical*
721 *Research* 95, 1271-1300.

722

723 Frey, F.A., Huang, J., Blichert-Toft, J., Regelous, M., Boyet, M., 2005. Origin of depleted components in
724 basalt related to the Hawaiian hot spot: Evidence from isotopic and incompatible element ratios.
725 *Geochemistry Geophysics Geosystems* 6, Q02107, doi:10.129/2004GC000757.

726

727 Garcia, M.O., Swinnard, L., Weis, D., Greene, A.R., Tagami, T., Sano, H., Gandy, C.E.,
728 2010. Petrology, geochemistry and geochronology of Kaua'i lavas over 4.5 Myr: implications
729 for the origin of rejuvenated volcanism and the evolution of the Hawaiian plume. *Journal of Petrology* 51,
730 1507-1540.

731

732 Gibson, S.A., Geist, D.G., Day, J.A., Dale, C.W., 2012. Short wavelength heterogeneity in the Galápagos
733 plume: evidence from compositionally diverse basalts on Isla Santiago.. *Geochemistry Geophysics*
734 *Geosystems* 13(1), Q09007, doi: 10.129/2012GC004244.

735

736 Guille, G., Legendre, C., Maury, R.C., Caroff, M., Munsch, M., Blais, S., Chauvel, C.,

737 Cotten, J., Guillou, H., 2002. Les Marquises (Polynésie française): un archipel intraocéanique
738 atypique. *Géologie de la France* 2, 5-36.
739

740 Guille, G., Legendre, C., Maury, R.C., Guillou, H., Rossi, P., Blais, S., 2010. Notice explicative, carte
741 géologique de France, feuille de Ua Pou, Polynésie française, 133 pp, scale 1: 30,000, Bureau de
742 Recherches Géologiques et Minières, Orléans, France, in press.
743

744 Guille, G., Maury, R.C., (coordinators), 2013. Carte géologique de la feuille Groupe Sud de l'archipel des
745 Iles Marquises (Hiva Oa – Tahuata – Motane et Fatu Hiva), Polynésie française, scale 1: 100,000, Bureau
746 de Recherches Géologiques et Minières, Orléans, France, in press.
747

748 Guillou, H, Maury, R.C., Blais, S., Cotten, J., Legendre, C., Guille, G., Caroff, M., 2005. Age progression
749 along the Society hot spot chain (French Polynesia) based on new unspiked K-Ar ages. *Bulletin de la*
750 *Société géologique Française* 176, 135-150.
751

752 Guillou, H., Nomade, S., Carracedo, J.C., Kissel, C., Laj, C., Perez Torrado, F.J., Wandres,
753 C., 2011. Effectiveness of combined unspiked K-Ar and ⁴⁰Ar/³⁹Ar dating methods in the
754 ¹⁴C age range. *Quaternary Geochronology* 6, 530-538.
755

756 Gutscher, M.A., Olivet, J.L., Aslanian, D., Eissen, J.P., Maury, R., 1999. The "lost Inca
757 Plateau": cause of flat subduction beneath Peru? *Earth and Planetary Science Letters* 171, 335-341.
758

759 Hanano, D., Weis, D., Scoates, J.S., Aciego, S., DePaolo, D.J., 2010. Horizontal and vertical
760 zoning of heterogeneities in the Hawaiian mantle plume from the geochemistry of consecutive
761 postshield volcano pairs: Kohala-Mahukona and Mauna Kea-Hualalai. *Geochemistry*
762 *Geophysics Geosystems* 11, Q01004, doi:10.129/2009GC002782.
763

764 Herzberg, C., 2011. Identification of Source Lithology in the Hawaiian and Canary Islands:
765 Implications for Origins. *Journal of Petrology* 52, 113-146.
766

767 Jackson, M.G., Dasgupta, R., 2008. Compositions of HIMU, EM1, and EM2 from global
768 trends between radiogenic isotopes and major elements in ocean island basalts. *Earth Planetary Science*
769 *Letters* 276, 175-186.
770

771 Jordahl, K.A., McNutt, M.K., Webb, H.F., Kruse, S.E., Kuykendall, M.G., 1995. Why there
772 are no earthquakes on the Marquesas Fracture Zone. *Journal of Geophysical Research* 100, 24431-24447.
773

774 Konter, J.G., Jackson, M.G., 2012. Large volumes of rejuvenated volcanism in Samoa: evidence supporting
775 a tectonic influence on late-stage volcanism. *Geochemistry Geophysics Geosystems* 13, Q0AM04,
776 doi:10.129/2011GC003974.
777

778 Lacroix, A., 1928. Nouvelles observations sur les laves des îles Marquises et de l'île Tubuai (Polynésie
779 australe). *Comptes Rendus de l'Académie des Sciences Paris* 187, 365-369.
780

781 Laughlin, A.W., Poths, J., Healey, H.A., Reneau, S., Woldegabriel, G., 1994. Dating of Quaternary basalts
782 using the cosmogenic He-3 and C-14 methods with implications for excess Ar-40. *Geology* 22, 135-138.
783

784 Le Bas, M.J., Le Maitre, R.W., Streckeisen, A., Zanettin, B., 1986. A chemical classification of volcanic rocks
785 based on the total-alkali-silica diagram. *Journal of Petrology* 27, 745-750.
786

787 Legendre, C., Maury, R.C., Caroff, M., Guillou, H., Cotten, J., Chauvel, C., Bollinger, C.,
788 Hémond, C., Guille, G., Blais, S., Rossi, P., Savanier, D., 2005a. Origin of exceptionally
789 abundant phonolites on Ua Pou island (Marquesas, french Polynesia): partial melting of
790 basanites followed by crustal contamination. *Journal of Petrology* 46, 1925-1962.
791

792 Legendre, C., Maury, R.C., Savanier, D., Cotten, J., Chauvel, C., Hémond, C., Bollinger, C.,
793 Guille, G., Blais, S., Rossi, P., 2005b. The origin of intermediate and evolved lavas in the
794 Marquesas archipelago: an example from Nuku Hiva island (French Polynesia). *Journal of Volcanology and*
795 *Geothermal Research* 143, 293-317.
796

797 Legendre, C., Maury, R.C., Blais, S., Guillou, H., Cotten, J., 2006. Atypical hotspot chains:
798 evidence for a secondary melting zone below the Marquesas (French Polynesia). *Terra Nova*
799 18, 210-216.

800
801 Macdonald, G.A., Katsura, T., 1964. Chemical composition of Hawaiian lavas. *Journal of Petrology* 5, 82-
802 133.

803
804 Marske, J.P., Pietruszka, A.J., Weis, D., Garcia, M.O., Rhodes, J.M., 2007. Rapid passage of a small-scale
805 mantle heterogeneity through the melting regions of Kilauea and Mauna Loa volcanoes. *Earth and Planetary*
806 *Science Letters* 259, 34-50.

807
808 Maury, R.C., Guille, G., Legendre, C., Savanier, D., Guillou, H., Rossi, P., Blais, S., 2006.
809 Notice explicative, carte géologique de France, feuille de Nuku Hiva, Polynésie française.
810 116 pp, scale 1: 50,000, Bureau de Recherches Géologiques et Minières, Orléans, France.

811
812 Maury, R.C., Legendre, C., Guille, G., Demange, J., Caroff, M., 2009. Notice explicative, carte géologique de
813 France, feuille d'Eiao, Polynésie française, 89 pp, scale 1: 25,000, Bureau de Recherches Géologiques et
814 Minières, Orléans, France.

815
816 Maury, R.C., Guille, G., Guillou, H., Rossi, P., Legendre, C., Chauvel, C., Blais, S., Ottino,
817 P., Meyer, J.-Y., Deroussi, S., Tegye, M., Cabioch, G., 2013. Notice explicative, carte
818 géologique de France, feuille Groupe Sud de l'archipel des Iles Marquises (Hiva Oa – Tahuata – Motane et
819 Fatu Hiva), Polynésie française, XX pp, scale 1: 100,000, Bureau de Recherches Géologiques et Minières,
820 Orléans, France, in press.

821
822 McDougall, I., Duncan, R.A., 1980. Linear volcanic chains: recording plate motions? *Tectonophysics* 63,
823 275-295.

824
825 McNutt, M., Bonneville, A., 2000. A shallow, chemical origin for the Marquesas Swell.
826 *Geochemistry Geophysics Geosystems* 1, 1999GC000028.

827
828 McNutt, M., Fischer, K., Kruse, S., Natland, J., 1989. The origin of the Marquesas fracture
829 zone ridge and its implications for the nature of hot spots. *Earth and Planetary Science Letters* 91, 381-393.

830
831 Merle, O., Barde-Cabusson, S., Maury, R.C., Legendre, C., Guille, G., Blais, S., 2006. Volcano core collapse
832 triggered by regional faulting. *Journal of Volcanology and Geothermal Research* 158, 269-280.

833
834 Paul, D., White, W.M., Blichert-Toft, J., 2005. Geochemistry of Mauritius and the origin of rejuvenescent
835 volcanism on oceanic island volcanoes. *Geochemistry Geophysics Geosystems* 6, Q06007, doi:
836 10.129/2004GC000883.

837
838 Pautot, G., Dupont, J., 1974. La zone de fracture des Marquises. *Comptes Rendus de l'Académie des*
839 *Sciences Paris* 279, 1519-1523.

840
841 Ribe N.M., Christensen U.R., 1999. The dynamical origin of Hawaiian volcanism. *Earth and Planetary*
842 *Science Letters* 171, 517-531.

843
844 Shafer, J.T., Neal, C.R., Regelous, M. 2005. Petrogenesis of Hawaiian postshield lavas: evidence from
845 Nintoku Seamount, Emperor Seamount Chain. *Geochemistry Geophysics Geosystems* 6, Q05L09, doi:
846 10.129/2004GC000875.

847
848 Smith, W.H.F., Sandwell, D.T., 1997. Global sea floor topography from satellite altimetry and
849 ship depth soundings. *Science* 277, 1956-1962.

850
851 Sobolev, A.V., Hofmann, A.W., Sobolev, S.V., Nikogosian, I.K., 2005. An olivine-free
852 mantle source of Hawaiian shield basalts. *Nature* 434, 590-597.

853
854 Sobolev, A.V., Hofmann, A.W., Kuzmin, D.V., Yaxley, G.M., Arndt, N.T., Chung, S.-L., Danyushevsky, L.V.,
855 Elliott, T., Frey, F.A., Garcia, M.O., Gurenko, A.A., Kamenetsky, V.S., Kerr, A.C., Krivolutskaia, N.A.,

856 Matvienkov, V.V., Nikogosian, I.K., Rocholl, A., Sigurdsson, I.A., Sushchevskaya, N.M., Teklay, M., 2007.
857 The Amount of Recycled Crust in Sources of Mantle-Derived Melts. *Science* 316, 412-417.
858
859 Stearns, H.T., 1966. *Geology of the State of Hawaii*: Palo Alto. Pacific Books, 266 p.
860
861 Steiger, R.H., Jäger, E., 1977. Subcommittee on geochronology: convention on the use of
862 decay constants in geo- and cosmo-chronology. *Earth and Planetary Science Letters* 36, 359-362.
863
864 Vidal, P., Chauvel, C., Brousse, R., 1984. Large mantle heterogeneity beneath French
865 Polynesia. *Nature* 307, 536-538.
866
867 Vidal, P., Dupuy, C., Barszczus, H.G., Chauvel, C., 1987. Hétérogénéités du manteau et
868 origine des basaltes des Marquises (Polynésie). *Bulletin de la Société géologique de France* 4, 633-642.
869
870 Westaway, R., Guillou, H., Yurtmen, S., Demir, T., Scaillet, S., Rowbotham, G., 2005. Constraints on
871 the timing and regional conditions at the start of the present phase of crustal extension in western
872 Turkey, from observations in and around the Denizli region. *Geodinamica Acta*. 18/3-4, 209-238.
873
874 White, W.M., 2010. Oceanic Island Basalts and Mantle Plumes: The Geochemical
875 Perspective, in: Jeanloz, R., Freeman, K.H. (Eds.), *Annual Review of Earth and Planetary*
876 *Sciences*, Vol 38. Annual Reviews, Palo Alto, pp. 133-160.
877
878 Woodhead, J.D., 1992. Temporal geochemical evolution in oceanic intra-plate volcanics: a
879 case study from the Marquesas (French Polynesia) and comparison with other hotspots.
880 *Contributions to Mineralogy and Petrology* 111, 458-467.
881
882
883
884

885 **Figure captions**

886
887 **Fig. 1.** Location map of Marquesas Islands. The bathymetry comes from the global altimetry data set of
888 Smith and Sandwell (1997). The main trend of the Marquesas chain is N40°W. Current Pacific plate motion
889 is 10.5 cm/yr at N65°W, corresponding to the line shown in white. The names of the southern islands are in
890 large print. MFZ: Marquesas Fracture Zone.

891
892 **Fig. 2.** Age versus distance plot for the Marquesas. The distances to the MFZ Ridge (MFZR) along
893 N65°W trend corresponding to the 10.5 cm/yr motion of the Pacific plate are from Chauvel et al. (2012). The
894 dashed line starts from the unexplored chain of seamounts located 50 km NW of the MFZR. Shield ages are
895 denoted by open symbols, post-shield ages by filled symbols and rejuvenated ages by grey symbols.
896 Sources of unspiked ^{40}K - ^{40}Ar ages on groundmass: Tables 1 and 3 for southern islands; Caroff et al. (1995)
897 and Maury et al. (2009) for Eiao; Maury et al. (2006) for Nuku Hiva; Legendre et al. (2006) and Blais et al.
898 (2008) for Ua Huka; Legendre et al. (2005a) and Guille et al. (2010) for Ua Pou.

899
900 **Fig. 3.** Total-Alkali-Silica (TAS) diagram (Le Bas et al., 1986) for the dated Marquesas lavas. The
901 dashed line separating the fields of tholeiitic (Thol.) and alkali (Alk.) basalts is from Macdonald and Katsura
902 (1964). Shield ages are denoted by open symbols, post-shield ages by filled symbols and rejuvenated ages
903 by grey symbols. Sources of major and trace element analyses: Tables 2 and 4 for southern islands; Caroff
904 et al. (1995) and Maury et al. (2009) for Eiao; Maury et al. (2006) for Nuku Hiva; Legendre et al. (2006) and
905 Blais et al. (2008) for Ua Huka; Legendre et al. (2005a) and Guille et al. (2010) for Ua Pou.

906
907 **Fig. 4.** Sketches of the Marquesas volcanic successions, showing caldera collapse events (red dashed
908 lines) and simplified distributions of tholeiitic basalts, alkali basalts and basanites, and felsic lavas (trachytes
909 and phonolites). Intermediate lavas have been omitted for clarity. Vertical scales are arbitrary. Abbreviated
910 volcano names: Ha: Hane; Hi: Hikitau; Hk: Hakahau; Hn: Hanatetena; Om: Omoa; Oo: Ootua; Pu: Puamau;
911 Ta: Taaoa; Te: Temetiu; Th: Taiohae; Tk: Tekao; To: Touaouoho; Va: Vaitahu. In Ua Huka, a temporal gap
912 separates the end of building of the Hane volcano from the rejuvenated volcanic phase which emplaced the
913 Teepoepo (1.15-0.96 Ma) and Tahoatikikau (0.82-0.76 Ma) basanitic cones. In Tahuata, the horizontal line
914 below the red dashed line separates the upper from the lower tholeiitic flows of Vaitahu shield.

915
916 **Fig. 5.** Geological sketch maps of the southern Marquesas islands, simplified from Guille and Maury
917 (2013) and Maury et al. (2013). The locations of the dated samples are shown by small red crosses
918 (corresponding ages in Ma from Tables 1 and 3). Most flow dips range from 8 to 12°. See text for
919 explanations.

920
921 **Fig. 6.** Plot of unspiked ^{40}K - ^{40}Ar ages against SiO_2 for dated samples. Symbols and sources of data as
922 in Figs. 2 and 3.

923
924 **Fig. 7.** Plot of La/Yb against La (ppm) for dated samples. Symbols and sources of data as in Fig. 3.

925
926 **Fig. 8.** $^{87}\text{Sr}/^{86}\text{Sr}$ versus $^{143}\text{Nd}/^{144}\text{Nd}$ diagram showing the differences between tholeiitic basalts and alkali
927 basalts/basanites from Marquesas islands. Data from the GEOROC database and Chauvel et al. (2012).
928 The Fatu Hiva sample plotting away from the main trend (low $^{143}\text{Nd}/^{144}\text{Nd}$) is from Woodhead (1992).
929

930 **Table captions**

931
932 **Table 1.** Unspiked ^{40}K - ^{40}Ar ages measured on groundmass for Hiva Oa lavas. See text for analytical
933 methods and Fig. 4 for sample locations. SH: shield; PS: post-shield. Mugear.: mugearite; benmor.:
934 benmoreite. *: ages already given in Chauvel et al. (2012) but without details.
935

936 **Table 2.** Major and trace element ICP-AES analyses of dated lavas from Hiva Oa. Major element oxides
937 in wt%, trace elements in ppm. Fe_2O_3^* : total iron as Fe_2O_3 . See text for analytical methods, Table 1 for ages
938 and Fig. 4 for sample locations. Samples are ranked by order of decreasing ages. SH: shield; PS: post-
939 shield. Thol: tholeiite; haw: hawaiiite; mug: mugearite; ben: benmoreite; tra: trachyte. The rare earth element
940 and Y concentrations of sample HV54 have been modified by supergene alteration involving crystallization
941 of rhabdophane (Cotten et al., 1995), and therefore this sample has not been plotted in Fig. 6. *: Major
942 element analyses given in Chauvel et al. (2012) together with ICP-MS trace element analyses.
943

944 **Table 3.** Unspiked ^{40}K - ^{40}Ar ages measured on groundmass for Motane, Tahuata and Fatu Hiva lavas.
945 See text for analytical methods and Fig. 4 for sample locations. SH: shield; PS: post-shield. Alk. bas.: alkali
946 basalt. *: ages already given in Chauvel et al. (2012) but without details.
947

948 **Table 4.** Major and trace element ICP-AES analyses of dated lavas from Motane, Tahuata and Fatu
949 Hiva. Major element oxides in wt%, trace elements in ppm. Fe_2O_3^* : total iron as Fe_2O_3 . See text for
950 analytical methods, Table 3 for ages and Fig. 4 for sample locations. For each island, samples are ranked
951 by order of decreasing ages. SH: shield; PS: post-shield. Thol: tholeiite; alb: alkali basalt; bas: basanite;
952 haw: hawaiiite; teph: tephriphonolite; tra: trachyte. *: Major element analyses given in Chauvel et al. (2012)
953 together with ICP-MS trace element analyses.
954

Volcanic successions in Marquesas eruptive centers: A departure from the Hawaiian model

Hervé Guillou ^{a*}, René C. Maury ^b, Gérard Guille ^c, Catherine Chauvel ^{d,e}, Philippe Rossi ^f, Carlos Pallares ^{b,g}, Christelle Legendre ^b, Sylvain Blais ^h, Céline Liorzou ^b, Sébastien Deroussi ⁱ

^aUMR 8212 LSCE-IPSL/CEA-CNRS-UVSQ, Domaine du CNRS, 12 avenue de la Terrasse, 91198 Gif-sur-Yvette, France

^bUniversité de Brest; Université Européenne de Bretagne, CNRS; UMR 6538 Domaines Océaniques; Institut Universitaire Européen de la Mer, Place N. Copernic, 29280 Plouzané, France.

^cLaboratoire de Géophysique, CEA-DASE, 91680 Bruyères-le-Chatel, France.

^dUniv. Grenoble Alpes, ISTERre, F-38041 Grenoble, France

^eCNRS, ISTERre, F-38041 Grenoble, France

^fBRGM, SGN-CGF, 3 avenue Claude-Guillemin, BP 36009, 45060 Orléans cedex 2, France.

^gUniversité de Paris-Sud, Laboratoire IDES, UMR 8148, Orsay, F-91405, France; CNRS, Orsay, F-91405, France.

^hUniversité de Rennes 1; Université Européenne de Bretagne, CNRS; UMR 6518 Géosciences Rennes; Campus de Beaulieu, Avenue du Général Leclerc, 35042 Rennes Cedex, France.

ⁱObservatoire Volcanologique et Sismologique de Guadeloupe, IPGP, 97113 Courbeyre, La Guadeloupe, France.

* Corresponding author. Tel.: + 33169823556; fax: +33169823568

E-mail address: herve.guillou@lsce.ispl.fr

Abstract

The temporal and geochemical evolution of Marquesas hotspot volcanoes have often been interpreted with reference to the Hawaiian model, where a tholeiitic shield-building stage is followed by an alkali basaltic post-shield stage, followed after a 0.4 to 2.5 Myr long quiescence period, by a rejuvenated basanitic/nephelinitic stage. Here we discuss geochemical data on 110 Marquesas lavas also dated using the unspiked ⁴⁰K-⁴⁰Ar method on separated groundmass (including 45 new ages measured on the southern islands of Hiva Oa, Motane, Tahuata and Fatu Hiva). Sample locations were positioned on detailed geological maps to determine their shield or post-shield position with respect to the caldera collapse event(s), without taking into account their geochemical features. A rather regular decrease of the ages towards SE, consistent with the Pacific plate motion, is observed from Eiao (5.52 Ma) to Fatu Hiva (1.11 Ma), and rejuvenated basanitic volcanism occurs only in Ua Huka (1.15-0.76 Ma). The occurrence of intermediate and evolved lavas is restricted to the post-caldera stage, with the exception of Eiao island. However, many other features of the Marquesas chain are rather atypical with respect to those of Hawaii.

41 Although Marquesas shields are tholeiitic, several of them (Eiao, Tahuata) contain interbedded alkali
42 basaltic and basanitic flows. Moreover, post-shield volcanoes are either alkali basalts (Ua Huka), tholeiites
43 (Hiva Oa, Tahuata, Fatu Hiva) or both (Nuku Hiva). This feature is consistent with the temporal continuity of
44 the two stages and the usually short length of the post-shield period (<0.2 Myr). In a given island, the trace
45 element and isotopic compositions of shield and post-shield lavas overlap, although both display large
46 variations. The sources of alkali basalts and basanites are more enriched than those of the
47 contemporaneous tholeiites. These specific features support the hypothesis of an extremely heterogeneous
48 Marquesas plume. The “weak” character of this plume led to low partial melting degrees, which in turn
49 resulted in the preservation in the basaltic magmas of geochemical features inherited from small-size source
50 heterogeneities.

51

52 *Keywords:* Shield, Post-shield, Tholeiite, Alkali basalt, Trachyte, ^{40}K - ^{40}Ar age, Hotspot, Marquesas.

53

54

55

56 1. Introduction

57

58 The temporal evolution of plume-related oceanic intraplate volcanoes has often been investigated with
59 reference to the classical Hawaiian model, in which four successive growth stages are distinguished (Clague
60 and Dalrymple, 1987; Clague, 1987; Hanano et al., 2010): (1) a small volume (ca. 3%) alkalic pre-shield
61 stage, emplacing mostly submarine alkali basalts and basanites; (2) the main shield-building stage, during
62 which the majority (95-98%) of the volcano is rapidly constructed, culminating in subaerial flows of tholeiitic
63 basalts; (3) the alkalic post-shield phase, during which small volumes (1-2%) of alkali basalts and related
64 intermediate/evolved lavas (hawaiites, mugearites, benmoreites and trachytes) are erupted; and finally (4)
65 the alkalic rejuvenated stage, during which very small volumes (<<1%) of basanites, alkali basalts and
66 nephelinites are emplaced after a quiescence period. In the Hawaiian chain, shield tholeiitic basalts are less
67 enriched in incompatible elements and derive from larger melting rates than the post-shield and rejuvenated
68 alkalic lavas; in addition, the mantle sources of the latter are isotopically depleted with respect to those of
69 the tholeiites (lower $^{87}\text{Sr}/^{86}\text{Sr}$ and $^{206}\text{Pb}/^{204}\text{Pb}$, higher $^{143}\text{Nd}/^{144}\text{Nd}$: Frey et al., 1990, 2005; Shafer et al., 2005;
70 Fekiacova et al., 2007; Garcia et al., 2010; Hanano et al., 2010).

71 For Hawaiian volcanoes, the main criterion used for the distinction between the shield-building and post-
72 shield stages is the change from tholeiites to alkali basalts. Indeed, Clague and Dalrymple (1987) stated
73 (their page 7) that “the shield stage usually includes caldera collapse and eruptions of caldera-filling tholeiitic
74 basalt. During the next stage, the alkalic postshield stage, alkalic basalt also may fill the caldera and form a
75 thin cap of alkalic basalt and associated differentiated lava that covers the main shield”. They also
76 mentioned (their page 8) that “we have omitted the main caldera-collapse stage of Stearns (1966) from the
77 eruption sequence because it can occur either during the shield stage or near the beginning of the alkalic
78 postshield stage. The lava erupted may therefore be tholeiitic or alkali basalt, or of both types”.

79 Large major, trace element and isotopic variations in Marquesas lavas have been known for decades
80 (Vidal et al., 1984, 1987; Duncan et al., 1986). They have been interpreted with reference to the shield/post-
81 shield Hawaiian model by several authors (Duncan et al., 1986; Woodhead, 1992; Desonie et al., 1993;
82 Castillo et al., 2007). However, most of these works were based on the pioneer (and hence limited) sampling
83 of Marquesas Islands made during the 1970's by R.A. Duncan (Duncan and McDougall, 1974; Duncan,
84 1975; McDougall and Duncan, 1980) and R. Brousse (Vidal et al., 1984; Brousse et al., 1990). No geological
85 maps of the islands were available at that time, and therefore the distinction between shield and post-shield
86 lavas was usually made using geochemical **criteria**. For instance, the observation that the oldest lavas from
87 Nuku Hiva, Ua Pou and Hiva Oa are tholeiitic basalts (Duncan, 1975; Duncan et al., 1986) led Woodhead
88 (1992) to classify hypersthene-normative Marquesas lavas as shield-related and alkali basalts/basanites as
89 post-shield. Later, Castillo et al. (2007) studied samples collected by H. Craig, and used $^{87}\text{Sr}/^{86}\text{Sr}$ (>0.7041)
90 and $^{143}\text{Nd}/^{144}\text{Nd}$ (<0.51285) ratios to characterize post-shield lavas, based on the isotopic data of Woodhead
91 (1992) obtained on R.A. Duncan's samples.

92 A mapping program of the Marquesas **archipelago (2001-2009)** led us to collect a number of new
93 samples and draw detailed geological maps of the islands. The trace element and Sr, Nd, Pb and Hf isotopic
94 features of these samples (Chauvel et al., 2012) point towards relationships between shield and post-shield
95 lavas **more complex** than previously thought. Here, we use geological **settings combined with** unspiked ^{40}K -
96 ^{40}Ar ages measured on groundmass and petrologic/geochemical features of this new sample set to
97 demonstrate that the temporal evolution of the Marquesas volcanoes is rather different from that of Hawaiian
98 volcanoes. We also discuss the constraints that they set on the corresponding plume/hotspot model.

99

100

101 **2. Geological setting and previous work**

102

103 *2.1. The Marquesas archipelago*

104 The ca. 350 km-long Marquesas archipelago, located in northern French Polynesia, includes eight main
105 islands (**Fig. 1**) that cluster into a northern group (Eiao, Nuku Hiva, Ua Huka and Ua Pou) and a southern
106 group (Hiva Oa, Tahuata, Motane, Fatu Hiva); few islets ("motu"), banks and seamounts also exist (**Fig. 1**).
107 The age of the islands decreases towards the SE (Duncan and McDougall, 1974; Brousse et al., 1990) from
108 5.5 Ma in Eiao to 0.6-0.35 Ma on the DH12 seamount south of Fatu Hiva (Desonie et al., 1993). However,
109 no active volcanoes are known at the southeastern edge of the chain. ^{40}K - ^{40}Ar ages younger than 1 Ma **have**
110 **been obtained** only on DH12 and on the Teepoepo (1.15-0.96 Ma) and Tahoatikikau (0.82-0.76 Ma)
111 **strombolian cones** on Ua Huka (Legendre et al., 2006; Blais et al., 2008). These cones were emplaced after
112 a 1.3 Myr quiescence period, and are considered as the only example of rejuvenated volcanism in the
113 Marquesas (Legendre et al., 2006; Chauvel et al., 2012). Most authors believe that the Marquesas Fracture
114 Zone (MFZ; Pautot and Dupont, 1974) overlies the present position of the hotspot activity (McNutt et al.,
115 1989; Brousse et al., 1990; Guille et al., 2002). However, the MFZ is aseismic (Jordahl et al., 1995) and no
116 young volcanic rock has been recovered from the adjacent Marquesas Fracture Zone Ridge (MFZR; **Fig. 1**).
117 The seamount chain parallel to the MFZ ridge ca. 50 km to the north (**Fig. 1**) has not yet been dredged and it
118 could possibly mark the present location of Marquesas hotspot activity.

119 The Marquesas archipelago is atypical in many respects (Brousse et al., 1990; Guille et al., 2002; Devey
120 and Haase, 2003). It lies on an anomalously shallow (less than 4,000 m deep) 53-49 Ma old oceanic crust
121 generated at the axis of the Pacific-Farallon ridge (Crough and Jarrard, 1981), and its crustal thickness
122 reaches 15-20 km below the central part of the chain (Filmer et al., 1993; Caress et al., 1995). This
123 abnormally thick crust is attributed either to underplating of plume magmas below the Moho (Caress et al.,
124 1995; McNutt and Bonneville, 2000) or to the construction of the archipelago over a small 50-45 Ma old
125 oceanic plateau that formed near the axis of the Pacific-Farallon ridge (Gutscher et al., 1999). In addition,
126 the N30-40°W direction of the archipelago is oblique to that of the current N65°W motion of the Pacific plate
127 (Fig. 1), but parallel to the spreading axis of the Pacific-Farallon ridge prior to the current orientation of
128 accretion along the East Pacific Rise. This feature suggests that zones of weakness in the underlying
129 Pacific-Farallon plate might have controlled the emplacement of the Marquesas magmas (Crough and
130 Jarrard, 1981; McNutt et al., 1989). Age-distance to the MFZR plots using the main N30-40°W trend of the
131 chain and all available ^{40}K - ^{40}Ar ages display considerable scatter (Brousse et al., 1990; Desonie et al., 1993;
132 Guille et al., 2002). Similar plots using the N65°W trend give better fits (Legendre et al., 2006; Chauvel et al.,
133 2012), especially when considering only unspiked ^{40}K - ^{40}Ar ages measured on separated groundmass (Fig.
134 2), which are more accurate and reliable than conventional ^{40}K - ^{40}Ar data on whole rocks. Recently, Chauvel
135 et al. (2012) showed that the chain is made of two adjacent rows of islands with distinct Sr, Nd, Pb isotopic
136 features, delineating two isotopic stripes. At any given $^{143}\text{Nd}/^{144}\text{Nd}$ value, the northeastern row (the “Ua Huka
137 group”) has systematically higher $^{87}\text{Sr}/^{86}\text{Sr}$ and lower $^{206}\text{Pb}/^{204}\text{Pb}$ ratios than the southwestern row (the “Fatu
138 Hiva group”). These rows are thought to originate from the partial melting of two adjacent filaments
139 contained in an elongated ascending plumelet or secondary plume, rooted in a larger dome located at the
140 base of the upper mantle (Davaille et al., 2002; Courtillot et al., 2003; Cadio et al., 2011).

141 The common occurrence of nested volcanoes in the Marquesas was first reported by L.J. Chubb (1930).
142 Half of the islands (Nuku Hiva, Ua Huka, Tahuata, Fatu Hiva) are made up of a large external (outer) shield
143 volcano with a central caldera. A younger and smaller internal (inner) post-shield volcanic edifice has grown
144 inside this caldera. Hiva Oa comprises three adjacent shields: the larger one is unconformably overlain by
145 post-shield flows, which also filled up part of its caldera. Ua Pou is rather unusual, because this island lacks
146 a well-exposed outer shield and is mostly made up of phonolitic flows interbedded with basanitic and
147 tephritic flows (Fig. 3), and crosscut by huge phonolitic spines (Legendre et al., 2005a). The two smallest
148 islands, Eiao and Motane, represent crescent-shaped remnants of the caldera wall and external upper
149 slopes of much larger collapsed shield volcanoes (Brousse et al., 1990; Guille et al., 2002). Therefore, the
150 shield-building or post-shield character of a given Marquesan sample with respect to caldera collapse events
151 (see Stearns, 1966, for the case of Hawaii) can be determined using only its geological position deduced
152 from field relationships and its ^{40}K - ^{40}Ar age, without making any assumption based on its petrologic and
153 geochemical features. We choose this approach because no well-defined temporal change from tholeiitic to
154 alkali volcanism is observed in most Marquesas volcanoes. In the present work, we use a coherent set of
155 110 lava samples to investigate the temporal geochemical evolution of the Marquesas volcanoes, with
156 special attention to the respective features of shield-building, post-shield and rejuvenated (Ua Huka) stages
157 of volcanic activity. All samples were collected during the 2001-2009 mapping program, dated by the

158 unspiked ^{40}K - ^{40}Ar method on groundmass at Gif-sur-Yvette laboratory and analyzed for major and trace
159 elements by ICP-AES at Plouzané (Brest) laboratory.

160

161 2.2. Summary of the geological and geochemical features of the northern group islands

162 The four islands from the northern group (Eiao, Nuku Hiva, Ua Huka and Ua Pou) were studied
163 previously using the same methods (Caroff et al., 1995, 1999; Legendre et al., 2005a, 2005b, 2006; Maury
164 et al., 2006, 2009; Blais et al., 2008; Guille et al., 2010). Their volcanic successions are shown schematically
165 in Figure 4. Below we provide a short description of their main features.

166 2.2.1. Eiao

167 Eiao (Maury et al., 2009) is the northernmost (Fig. 1) and largest (44 km^2) uninhabited island in French
168 Polynesia. It corresponds to the northwestern crescent-shaped remains of the caldera wall and of the
169 external upper slopes of a 20 km large collapsed volcano. Its coastal cliffs expose a ca 400 m thick pile of
170 tholeiitic basaltic flows interbedded with less common alkali basalts and crosscut by a dense network of
171 radial dykes. Three deep core drillings have sampled the upper 1,200 m thick sequence of the Eiao shield,
172 down to -700 m below sea level (Caroff et al., 1995, 1999). The base of this sequence, dated at 5.52-5.48
173 Ma (Fig. 2), is made up of quartz-normative tholeiitic flows overlain by olivine tholeiitic flows (Fig. 3). These
174 are in turn overlain by a ca 250 m thick sequence of hawaiites and mugearites, with a single intercalated
175 trachytic flow 5.44 Ma old (Fig. 4). The middle (dated at 5.36-5.25 Ma) and upper (4.98-4.95 Ma) parts of the
176 drilled pile are mostly made up of olivine tholeiites intercalated with picobasaltic and alkali basaltic flows
177 (Caroff et al., 1995, 1999; Maury et al., 2009). The old quartz tholeiites are less enriched in incompatible
178 elements than the overlying olivine tholeiites and alkali basalts, and their Sr, Nd, Pb isotopic composition
179 tends towards a HIMU end-member. Hawaiites and mugearites result from open-system fractional
180 crystallization of the latter basaltic magmas, coupled with variable extents of assimilation of materials from
181 the underlying oceanic crust (Caroff et al., 1999).

182 2.2.2. Nuku Hiva

183 Nuku Hiva (Legendre et al., 2005b; Maury et al., 2006) is the largest island of the archipelago (339 km^2).
184 It has a semicircular shape, and its northern, western and eastern parts correspond to the northern half of a
185 huge shield, the Tekao volcano (Fig. 4). It is exclusively made up of olivine tholeiites (Fig. 2) derived from a
186 mantle source containing a depleted MORB mantle (DMM) component. Its upper flows were emplaced
187 between 4.01 and 3.83 Ma according to unspiked ^{40}K - ^{40}Ar data (Fig. 3), although altered flows from the
188 lower part of the exposed pile yielded ^{40}Ar - ^{39}Ar ages ranging from 4.52 to 4.08 Ma (Maury et al., 2006).
189 Between 4.00 and 3.62 Ma (unspiked ^{40}K - ^{40}Ar data), the Taiohae inner (post-shield) volcano grew inside the
190 caldera of the Tekao shield, after the southern part of the latter collapsed along a N75°E trending normal
191 fault parallel to the MFZ. This collapse event at ca 4.0 Ma (Fig. 4) has been attributed to the lateral
192 spreading of a weak hydrothermal zone located in the central part of the Tekao shield over an unconfined
193 boundary, corresponding to the lower compartment of this fault (Merle et al., 2006). Mapping relationships
194 allow us to estimate the volume of the Taiohae post-shield volcano to $45 \pm 5 \text{ km}^3$, i.e. 28% of the emerged
195 volume of the edifice (160 km^3), but only 0.6% of its total volume ($6,950 \text{ km}^3$, Chauvel et al., 2012). Lavas

196 from the Taiohae volcano include, from bottom to top: olivine tholeiites more enriched in incompatible
197 element than those of the Tekao shield; alkali basalts and a few basanites; and large amounts of hawaiites
198 and mugearites, which cover 47% of its surface, together with benmoreites and trachytes (25% of its
199 surface). In addition, parasitic vents erupted hawaiitic (3.93 Ma) and trachytic (3.92 Ma) flows on the
200 external slopes of the Tekao shield. All the Taiohae post-shield lavas are more radiogenic in Sr and Nd and
201 less radiogenic in Nd than the Tekao ones. Hawaiites and mugearites likely derived from the fractional
202 crystallization from mafic magmas involving separation of amphibole (Legendre et al., 2005b). The isotopic
203 signature of benmoreites and trachytes is closer to the [enriched mantle II](#) (EM II) end-member than that of
204 mafic lavas, a feature inconsistent with simple fractionation processes.

205

206 *2.2.3. Ua Huka*

207 Despite its moderate size (83 km²), Ua Huka Island (Legendre et al., 2006; Blais et al., 2008, Chauvel et
208 al., 2012) displays a relatively [prolonged, multi-phase geological evolution](#). Like Nuku Hiva, it has a
209 semicircular shape due to the collapse of the southern half of its outer shield, the Hikitau volcano. [It is made](#)
210 up of olivine tholeiitic flows emplaced between 3.24 and 2.94 Ma. The Hane inner (post-shield) volcano was
211 built inside the central caldera of the Hikitau shield between 2.97 and 2.43 Ma ([Fig. 4](#)). Its alkali basaltic
212 flows derived from a spinel lherzolite source similar to that of the Hikitau tholeiites but having experienced
213 smaller degrees of melting ([Legendre et al., 2006](#)). Associated benmoreitic flows and trachytic and phonolitic
214 domes were simultaneously emplaced (between 2.93 and 2.71 Ma) within the Hane post-shield volcano and
215 from parasitic vents located on the outer slopes of the Hikitau shield. Then, after a 1.3 Myr long quiescence
216 period ([Fig. 2](#)), volcanic activity resumed, building over the inner slopes of the Hane volcano two basanitic
217 strombolian cones, the Teepoepo (1.15-0.96 Ma) and the Tahoatikikau (0.82-0.76 Ma). Their lavas
218 originated from temporally decreasing melting degrees of a garnet lherzolite source deeper and isotopically
219 more depleted than that of the older Ua Huka tholeiitic and alkali basalts (Chauvel et al., 2012). The origin of
220 this rejuvenated volcanism (the single case identified so far in the archipelago) has been attributed to a
221 secondary melting zone located downstream the Marquesas plume (Legendre et al., 2006), similar to that
222 envisioned by Ribe and Christensen (1999) for the Hawaiian islands. The volumes (estimated from [mapping](#)
223 relationships) of the Hane post-shield volcano (6±1 km³) and the rejuvenated cones (0.6±0.1 km³)
224 correspond respectively to 21% and 2% of the total emerged volume of Ua Huka (28 km³), and less than
225 0.2% only of the bulk volume of the edifice (3,250 km³).

226

227 *2.2.4. Ua Pou*

228 The 105 km² diamond-shaped island of Ua Pou (Legendre et al., 2005a; Guille et al., 2010) is famous
229 for the exceptional abundance of phonolites ([Figs. 3 and 4](#)), which cover 65% of its surface and include
230 spectacular phonolitic [spines](#) (Ua Pou means “The Pillars” in Marquesan). Its oldest lavas are olivine
231 tholeiite flows derived from a young HIMU-type mantle source (Duncan et al., 1986, Vidal et al., 1987). They
232 outcrop in a very small area near Hakahau village in the northeast part of the island. The base of their ca 40
233 m thick pile (Guille et al., 2010) [is not accessible presently](#) but has been dated at 5.61, 4.51 and 4.46 Ma by

234 the ^{40}K - ^{40}Ar method on whole rocks (Duncan et al., 1986). Its presently exposed top flow was dated at 4.00
235 Ma by the unspiked ^{40}K - ^{40}Ar method on groundmass (Legendre et al., 2005a). These [Hakahau](#) tholeiitic
236 flows are overlain either by up to 100 m thick laharic deposits or by trachytic and phonolitic domes dated at
237 3.86 and 3.27 Ma (Guille et al., 2010). The latter sequence is in turn overlain by a strongly silica-
238 undersaturated lava suite forming the bulk of the island and dated between 2.95 and 2.35 Ma (unspiked ^{40}K -
239 ^{40}Ar ages). It includes from bottom to top: (1) basanitic and tephritic lava flows with intercalated laharic
240 deposits, (2) lower phonolitic flows and intrusions, (3) basanitic and intermediate (tephritic, tephriphonolitic
241 and benmoreitic) flows with occasional interbedded phonolites, (4) upper phonolitic flows, up to 500 m thick,
242 and finally (5) phonolitic domes and [spines](#), the summit of which tower several hundred meters above the
243 older units. The basanitic magmas of this suite derived from low degrees of melting of an heterogeneous
244 mantle source intermediate between EM II and HIMU end-members, and evolved towards tephritic liquids by
245 fractional crystallization (Legendre et al., 2005a). The origin of tephriphonolitic and benmoreitic magmas was
246 ascribed to the remelting at depth of basanitic rocks, leaving an amphibole-rich residuum (Legendre et al.,
247 2005a). These liquids evolved by either closed-system or more commonly open-system fractionation
248 towards phonolitic and trachytic magmas.

249 In contrast with the other Marquesas Islands, the main Ua Pou volcanic sequence (2.95-2.35 Ma) does
250 not include [a basaltic shield](#). We therefore support Duncan et al.'s (1986) [suggestion that the Ua Pou shield](#)
251 [is mainly below sea level](#), with only its uppermost tholeiitic part presently exposed, and that the rest of the
252 island belongs to the post-shield phase. This interpretation is supported by the occurrence of thick laharic
253 deposits overlying the tholeiitic flows, which indicate an erosional [event](#). However, the temporal hiatus
254 between the shield and post-shield phases ([only between 4.00 and 3.86 Ma according to Guille et al., 2010](#))
255 is much shorter than that proposed by former authors: 1.58 Myr calculated using Duncan et al.'s (1986) data
256 and 2.34 Myr according to Woodhead (1992).

257

258 **3. New geological, geochemical and K-Ar age data on the southern Marquesas islands.**

259

260 *3.1. Methods*

261 The analytical techniques are [identical](#) to those used to study the northern islands. Unspiked ^{40}K -
262 ^{40}Ar ages were obtained at the LSCE (Laboratoire des Sciences du Climat et de l'environnement) in
263 Gif-sur-Yvette. [Fresh and well-crystallized samples were selected for dating after macroscopic and](#)
264 [microscopic inspections allowing us to check the lack of post-magmatic mineral phases. In addition,](#)
265 [the degree of alteration of these samples was estimated from their loss on ignition value \(LOI\). For 40](#)
266 [out of 45 dated samples \(Tables 2 and 4\) LOI ranges from -0.39 to 1.56 wt% and these samples are](#)
267 [considered as essentially unaltered. The 5 other samples \(HV81, HV99, MT11, TH35 and FH30\) have](#)
268 [LOI between 1.90 and 2.77 wt%. Despite their higher LOI, we selected them because of their critical](#)
269 [geological position or their unusual composition \(tephriphonolitic sample TH35\). The samples were](#)
270 [crushed and sieved to 0.250-0.125 mm size fractions, and ultrasonically washed in acetic acid \(1N\)](#)
271 [during 45 minutes at a temperature of 60°C to remove unsuspected minute amounts of secondary](#)
272 [mineral phases.](#) Potassium and argon were measured on the microcrystalline groundmass, after
273 removal of phenocrysts using heavy liquids and magnetic separations. This process removes at least

274 some potential sources of systematic error due to the presence of excess ^{40}Ar in olivine and feldspar
275 phenocrysts (Laughlin et al., 1994). The K content of the separated groundmass was measured by
276 ICP-AES in Plouzané using the same method as for major elements while Ar analyses were
277 performed in Gif-sur-Yvette using the procedures of Guillou et al. (2011). Ages given in Tables 1 and 3
278 were calculated using the constants recommended by Steiger and Jäger (1977). **Unspiked K-Ar**
279 **analysis of each sample involved three independent determinations of potassium and two of argon.**
280 **Based on replicate analysis of material references, the potassium concentrations were determined**
281 **with an uncertainty of 1% (1σ). These potassium concentrations were averaged to yield a mean value.**
282 **Age determinations of each sample were made using this mean value and the weighted mean of the**
283 **two independent measurements of $^{40}\text{Ar}^*$ (radiogenic argon). Analytical uncertainties for the Ar data are**
284 **1σ , and consist of propagated and quadratically averaged experimental uncertainties arising from the**
285 **^{40}Ar (total) and $^{40}\text{Ar}^*$ determinations (see Westaway et al., 2005 for more details). Uncertainties on the**
286 **ages are given at 2σ .**

287 Before chemical analyses, all samples were crushed using an agate mortar. Major and trace element
288 data (Tables 2 and 4) were obtained by Inductively Coupled Plasma-Atomic Emission Spectrometry (ICP-
289 AES) at IUEM, Plouzané using the method of Cotten et al. (1995). The international standards used for
290 calibration were ACE, BEN, JB-2, PM-S and WS-E and the relative standard deviations are $\pm 1\%$ for SiO_2 ,
291 and $\pm 2\%$ for other major elements except P_2O_5 and MnO (absolute precision $\pm 0.01\%$). **Samples were**
292 **classified according to their position in the TAS diagram (Fig. 3). Within the basalt group, silica-saturated or -**
293 **oversaturated lavas (normative *hy + ol* or *hy + Q*) were called tholeiitic basalts while nepheline-normative**
294 **samples were called alkali basalts (normative compositions given in Tables 2 and 4). Some tholeiitic basalts**
295 **plot close to or even above the Macdonald and Katsura's (1964) boundary in Figure 3 and could therefore**
296 **be considered as transitional basalts. We did not include the latter category in our classification chart**
297 **because it has not been previously used in the Marquesas and is not defined rigorously.**

298

299 3.2. Hiva Oa

300 Hiva Oa (320 km^2), the second largest Marquesas island and the highest one (1276 m at Mt Temetiu),
301 has a WSW-ENE elongated shape parallel to the MFZ (Fig. 1). New field data (Fig. 5) combined with 20 new
302 unspiked ^{40}K - ^{40}Ar ages (Table 1) show that the island consists in four coalescent volcanoes whose age
303 decreases eastwards from 2.55 ± 0.05 to $1.46\text{-}1.44 \pm 0.03$ Ma (Figs. 4 and 5). All of them are made up of
304 tholeiitic basalts, some of which display a transitional affinity, and hawaiiites (Table 2). Alkali basalts and
305 basanites were not identified in our set of 87 newly collected samples (Maury et al., 2012) nor in previous
306 samplings by R. Brousse (Chauvel et al., 2012, their Supplementary file D). Mugearites, benmoreites and
307 trachytes (Table 2) occur only in the post-shield Ootua volcano, or as dykes and plugs crosscutting the
308 Puamau shield.

309 The oldest volcano, Taaoa, is located on the western coast of Hiva Oa (Fig. 5). It represents the
310 crescent-shaped remnants of a largely collapsed shield, which are unconformably overlain by the flows of
311 the much bigger Temetiu shield. The Taaoa edifice is formed by a monotonous pile of meter-thick tholeiitic
312 flows interbedded with strombolian ashes and lapilli. The lowermost flow of this pile, located in Taaoa

313 village, was dated at 2.55 ± 0.05 Ma (HV64, Table 1 and Fig. 4). Taaoa basalts have lower K contents, lower
314 $^{87}\text{Sr}/^{86}\text{Sr}$ and higher $^{206}\text{Pb}/^{204}\text{Pb}$ ratios compared to all other Hiva Oa basalts, and their trace element and
315 isotopic signatures are closer to HIMU (Chauvel et al., 2012). They plot within the “Ua Pou” trend unlike all
316 other lavas that plot in the “Ua Huka” trend. Accordingly, the N65°W limit between the two isotopic stripes
317 defined by Chauvel et al. (2012) has been set at Taaoa village.

318 The Temetiu shield (Fig. 5) is the largest volcano of Hiva Oa. It is made of a more than 1,200 m thick
319 pile of meter-thick quartz or olivine normative tholeiites and hawaiites (Table 2). The construction of its
320 exposed part started around 2.27 ± 0.05 Ma (HV87, foot of Mt Temetiu) and 2.25 ± 0.05 Ma (HV84, northern
321 slopes near Hanaiapa village). Its major activity occurred between 2.13 ± 0.05 and 1.91 ± 0.04 Ma, based on
322 seven unspiked ^{40}K - ^{40}Ar ages (Table 1 and Fig. 4). Its well-exposed semicircular caldera facing south
323 collapsed before 2.01 Ma. Indeed, this event was followed by landslides which generated avalanche and
324 debris flow deposits, later crosscut by a number of dykes, including HV99 (2.01 ± 0.04 Ma) south of Atuona
325 village. Volcanic activity of the Temetiu shield ended at 1.83 ± 0.04 Ma (sample HV81 north of Hanapaaoa
326 village). It was almost immediately followed by the emplacement at 1.80 ± 0.04 Ma (sample HV65) of a thick
327 pile of post-shield tholeiitic flows (the Atuona flows) within the caldera, east and north of Atuona village.
328 Temetiu shield and Atuona post-shield tholeiitic flows share the same isotopic signature typical of the “Ua
329 Huka” stripe (Chauvel et al., 2012). The origin of the collapse of the southern part of these edifices is
330 attributed to the lateral spreading of an hydrothermal zone located beneath the Temetiu caldera over an
331 unconfined boundary corresponding to the lower compartment of a fault parallel to the MFZ (Maury et al.,
332 2013), such as in the case of Nuku Hiva.

333 The Puamau shield forms the eastern part of Hiva Oa (Fig. 5). Its lower part is made up of an up to 500
334 m thick pile of meter-thick flows of quartz tholeiites, olivine tholeiites and interbedded hawaiites dipping
335 gently towards the Temetiu shield or the southern coast. They are dated at 1.65 ± 0.04 (HV70) and $1.62 \pm$
336 0.04 Ma (HV62). They are overlain by a 200 m thick pile of tholeiitic basalts and minor interbedded hawaiites
337 occurring as thicker (5-20 m) and usually columnar-jointed flows (Puamau shield upper flows in Fig. 5).
338 Although this unit is younger (1.46 ± 0.03 Ma, sample HV88) than the main shield, we do not consider it as
339 belonging to the post-shield stage. Indeed, both were affected by the collapse event that led to a caldera
340 open NE, with its center near the village of Puamau (Fig. 5). Post-caldera volcanic edifices have not been
341 identified within this caldera, but several small benmoreitic and trachytic dykes and plugs (not shown in the
342 simplified geologic map of Fig. 5) crosscut the Puamau shield pile. They are usually altered and therefore
343 unsuitable for ^{40}K - ^{40}Ar dating.

344 The Ootua post-shield edifice was emplaced on the eastern slopes of the Temetiu shield. Its central unit,
345 ca 200 m thick, is exclusively made up of intermediate (mugearitic, benmoreitic and phonotephritic) and
346 silica-oversaturated trachytic flows and N-S trending dykes. It culminates at Mt Ootua, a 500 m wide and
347 200 m high columnar-jointed dome of quartz normative trachyte. This unit is dated at 1.73 ± 0.04 Ma (HV56
348 mugearitic flow) and 1.64 ± 0.03 Ma (HV54 benmoreitic dyke). Its peripheral unit consists of an up to 400
349 m thick pile of fissure erupted tholeiitic and hawaiitic flows. Most of these flows display well-developed basal
350 autoclastic breccias. They flow over either (1) the northern and southern slopes of the Temetiu shield, (2) its
351 caldera within which they overlie the Atuona post-shield flows, and finally (3) towards the topographic trough

352 separating the Temetiu and Puamau shields (Fig. 5). They fill most of this trough, flowing either towards the
353 northern coast or the southern coast where a tholeiitic basalt (HV107) yields the youngest age measured in
354 Hiva Oa (1.44 ± 0.03 Ma). Another young age of 1.51 ± 0.03 Ma has been obtained on an hawaiitic flow
355 (HV86) overlying the Temetiu shield.

356 The volumes (estimated from mapping relationships) of the Atuona and Ootua post-shield lavas (14 ± 1
357 km^3) correspond to 9.5% of the total emerged volume of Hiva Oa (145 km^3), and 0.2% of the bulk volume of
358 the edifice ($6,900 \text{ km}^3$, Chauvel et al., 2012).

359

360 3.3. Motane and Tahuata

361 Motane (Figs. 1 and 5) is a small (13 km^2) crescent-shaped uninhabited island located southeast of Hiva
362 Oa and east of Tahuata. Like Eiao, it corresponds to a sector of the caldera wall (up to 500 m high) and the
363 upper external slopes of a largely collapsed shield volcano. It is made up of a monotonous pile of meter-
364 thick quartz and olivine tholeiitic flows, interbedded with picobasalts and minor hawaiites. This pile is
365 crosscut by a dense network of radial dykes, which include alkali basalts and basanites (Fig. 4) displaying
366 incompatible element patterns more fractionated than those of the tholeiites. Two tholeiitic flows from the
367 middle part of the pile are dated at 1.59 ± 0.04 Ma (MT04, altitude 120 m) and 1.53 ± 0.03 Ma (MT08,
368 altitude 190 m) (see Table 3). An alkali basaltic dyke collected at sea level yields an older age (1.96 ± 0.04
369 Ma, MT11 in Table 3) that is barely consistent with the others and may indicate sample contamination by
370 seawater (also consistent with its relatively high LOI of 2.53 wt%). The isotopic Sr, Nd, Pb compositions of
371 tholeiites MT04 and MT08 are typical of the “Ua Pou” stripe (Chauvel et al., 2012), as well as that of
372 basanitic sample MT12 that is clearly more radiogenic in Sr and less radiogenic in Nd than the tholeiites.

373 Tahuata (69 km^2) corresponds to the northwestern half of a large shield known as the Vaitahu shield
374 (Maury et al., 2013). Its southern part has collapsed over an unconfined boundary. The latter probably
375 corresponds to the SE down-faulted block, lowered by 1,000 m, of a major N35°E fault lineament well-
376 identified off the SE coast of the island (Maury et al., 2013). This collapse event led to the formation of an 8
377 km large caldera opened toward SE (Fig. 5). A small edifice, the inner Hanatetena volcano (Figs. 4 and 5)
378 grew inside this caldera. The caldera wall was later affected by large landslides, which generated an up to
379 300 m thick pile of avalanche and debris flow deposits. The latter partly filled up the topographic trough
380 separating the foot of the caldera wall from the Hanatetena post-shield edifice.

381 The 700 m thick lower unit of the Vaitahu shield consists of meter-thick basaltic and hawaiitic flows. The
382 unspiked ^{40}K - ^{40}Ar ages (Table 3) indicate that it was emplaced rather quickly, between 2.11 ± 0.05 Ma
383 (TH39 tholeiitic basalt, western coast south of Hapatoni village) and 1.81 ± 0.04 Ma (TH14 alkali basalt,
384 northern coast). Three ages clustering around 1.90 Ma (TH37, TH38 and TH18 tholeiitic basalts, central part
385 of the island) may record the paroxysmal event. This lower unit is overlain by a pile of thick (>10 m) and
386 usually columnar-jointed tholeiitic flows. This upper unit forms the central ridge of the island, and is up to 500
387 m thick. Its basal flow has an age of 1.88 ± 0.04 Ma (TH13). We consider it as the upper part of the Vaitahu
388 shield, because (1) it conformably overlies the top of the lower unit, (2) its age is similar to that of the main

389 building phase of the lower unit between 1.91 ± 0.04 and 1.88 ± 0.04 Ma, and (3) it was obviously affected
390 by the caldera collapse event, as it forms presently the uppermost slopes of the caldera wall (Fig. 5).

391 A specific feature of the Vaitahu shield is its chemical heterogeneity. It is mostly tholeiitic (18 quartz
392 tholeiites and olivine tholeiites in our sample set), but also includes alkali basalts (2 samples), basanites (3
393 samples) and hawaiites (3 samples). Alkali basalts and basanites are more sodic and more enriched in the
394 most incompatible elements compared to the tholeiites (Table 4), and they display consistently higher
395 $^{87}\text{Sr}/^{86}\text{Sr}$ and lower $^{143}\text{Nd}/^{144}\text{Nd}$ and $^{206}\text{Pb}/^{207}\text{Pb}$ ratios according to data obtained on the same samples
396 (Chauvel et al., 2012).

397 The small (less than 200 m high) post-caldera Hanatetena volcano is composed exclusively of tholeiitic
398 and hawaiitic flows. The basal flows display pahoehoe and lava tube features; they are overlain by highly
399 weathered flows of meter thickness. Their trace element and isotopic compositions plot within the range of
400 the Vaitahu shield tholeiites (Chauvel et al., 2012). Two flows are dated at 1.80 ± 0.04 Ma (TH31) and $1.74 \pm$
401 0.04 Ma (TH8). The exposed volume of the Hanatetena edifice ($0.5 \pm 0.1 \text{ km}^3$) represents only 2% of the
402 volume of Tahuata island (25 km^3).

403 The single intermediate/evolved lava documented in Tahuata is a columnar-jointed tephriphonolitic
404 spine, 200 m in diameter, which crosscuts the northern slopes of the Vaitahu shield and forms the summit of
405 Mt Tumu Meae Ufa (1,050 m). Because of its young age (1.78 ± 0.04 Ma, sample TH35), we relate its
406 emplacement to the post-shield stage.

407

408 3.4. Fatu Hiva

409 Fatu Hiva Island (84 km^2) displays a typical semicircular shape. It includes an external (outer) shield, the
410 Touaouoho volcano, truncated by a 8 km wide caldera opening westwards, inside which grew a smaller
411 post-caldera edifice, the Omoa volcano (Fig. 5). As in Tahuata, the caldera wall was affected by landslides
412 which generated avalanche and debris flow deposits up to 250 m thick. These deposits now outcrop within
413 the topographic trough separating the outer shield from the inner Omoa post-shield edifice. The drowning of
414 the western half of the island and the development of the caldera are probably related to major sector
415 collapse events, marked in the regional bathymetry by a 15 km wide trough (at 2,500 m depth) located west
416 of Fatu Hiva, downslope from the Omoa volcano.

417 The Touaouoho shield has an up to 1,100 m thick rather monotonous pile of meter-thick flows of olivine
418 tholeiites, tholeiitic picobasalts and minor hawaiites (Table 4), crosscut by a dense network of radial
419 inframetric tholeiitic dykes. Their unspiked ^{40}K - ^{40}Ar ages (Table 3) range from 1.81 ± 0.04 Ma (FH13) to 1.35
420 ± 0.03 Ma (FH18). The Omoa post-caldera edifice is composed of a 700 m thick pile of inframetric tholeiitic
421 flows, with lava tubes in pahoehoe composite flows. Their ages (Table 3) range from 1.43 ± 0.03 Ma (FH08)
422 to 1.23 ± 0.04 Ma (FH05). In addition, a tholeiitic dyke (FH30) crosscutting the debris flow deposits at
423 Hanavave village yielded an age of 1.41 ± 0.03 Ma, consistent with the end of volcanic activity in Touaouoho
424 shield and the initiation of that of the post-shield Omoa edifice. These two stages led to the emplacement of
425 rather similar tholeiitic basalts and hawaiites (Table 4). Their major, trace element (Table 4) and isotopic Sr

426 Nd Pb and Hf compositions largely overlap, and both are typical of the predominantly EM II-HIMU sources of
427 the southwestern trend, which has been labelled the “Fatu Hiva group” (Chauvel et al., 2012).

428 The youngest Fatu Hiva lavas are two well-preserved trachytic domes (Figs. 4 and 5) crosscutting and
429 overlying the Touaouoho shield flows on the northern coast (FH16, 1.11 ± 0.02 Ma) and east of Omoa
430 village (FH06, 1.22 ± 0.03 Ma). In addition, a 15 m wide trachytic dyke (FH12) crosscutting the basal flows of
431 Omoa post-shield edifice is dated at 1.38 ± 0.03 Ma, and was therefore emplaced during the post-shield
432 stage. The volumes (estimated from mapping relationships) of the Omoa post-shield lavas (5 ± 1 km³)
433 correspond to 28% of the total emerged volume of Fatu Hiva (28 km³), and 0.2% only of the bulk volume of
434 the edifice (2,800 km³).

435

436 4. Discussion

437 4.1. Timing of eruptions: no gap between shield-building and post-caldeira stages

438 The new unspiked ⁴⁰K-⁴⁰Ar ages plotted against the distances of the islands to the MFZR along the
439 N65°W direction of movement of the Pacific plate (Fig. 2) are reasonably consistent with its local motion rate
440 of 10.5 cm/year, as previously pointed out by Legendre et al. (2006). These new ages display much less
441 scatter than the age-distance to the MFZR plots using the main N30-40°W trend of the chain and all the
442 available ⁴⁰K-⁴⁰Ar ages measured on bulk rocks (Brousse et al., 1990; Desonie et al., 1993; Guille et al.,
443 2002). The dashed line in Fig. 2, which corresponds to distances to the unexplored seamount chain located
444 ca 50 km north of the MFZR (Fig. 1), provides a better fit to the start of activity in some islands. Thus, this
445 seamount chain is a strong candidate for the present-day location of the Marquesas hotspot. Overall, Ua
446 Huka differs from all the other islands by the fact that the emplacement of the exposed part of its shield
447 started clearly later than predicted by the hotspot hypothesis (Fig. 2). It is also the only Marquesas Island
448 showing a rejuvenated volcanic stage (Legendre et al., 2006).

449 Data plotted in Figures 2 and 4 show that there is no consistent temporal hiatus between the shield-
450 building and post-caldeira activities. Usually the two stages either slightly overlap (Nuku Hiva, Ua Huka, Fatu
451 Hiva) or the gap between them is within the range of analytical uncertainties (Temetiu shield and Atuona
452 post-caldeira lavas in Hiva Oa, Tahuata). In Ua Pou, a marginal hiatus (Guille et al., 2010) is observed
453 between the youngest shield tholeiitic basalt (4.00 ± 0.06 Ma) and the oldest post-shield phonolite (3.86 ± 0.06
454 Ma). However, this might be due to sampling bias because of the very small size of the emergent part of the
455 shield that is mostly overlain by lahar deposits. Such a temporal continuity implies that the growth of post-
456 shield edifices started immediately after the main caldera collapse event, while eruptive activity was still
457 occurring at least in some parts of the shield volcano. Another striking feature of the data shown in Figure 2
458 is that contemporaneous volcanism occurred in islands located more than 100 km away from each other
459 (Fig. 1), e.g. around 2.5 Ma (Ua Huka, Ua Pou, Hiva Oa) or between 2.0 and 1.5 Ma (Hiva Oa, Tahuata,
460 Motane and Fatu Hiva). This feature is consistent with a “classical” plume model involving a 200 km large
461 summital melting zone (Farnetani and Hoffmann, 2010), and it is also observed in other hotspot-related
462 islands such as the Hawaiian chain (Clague and Dalrymple, 1987), the Society archipelago (Guillou et al.,
463 2005) and the Canaries (Carracedo et al., 1998). However, rejuvenated volcanism is much less common in

464 the Marquesas (Ua Huka) than in the Hawaiian chain, the Canaries, Mauritius (Paul et al., 2005) and Samoa
465 (Konter and Jackson, 2012).

466

467 *4.2. Evidence for post-shield emplacement of nearly all the intermediate and evolved lavas*

468 The TAS diagram (Fig. 3) and the age versus SiO₂ plot (Fig. 6) show that nearly all the dated lavas more
469 evolved than tholeiitic and alkali basalts, basanites and hawaiites were erupted during the post-shield stage
470 of Marquesan volcanoes. These include rare tephrites (Ua Pou), mugearites (Hiva Oa), benmoreites (Nuku
471 Hiva, Ua Pou, Hiva Oa) and tephriphonolites (Ua Pou, Tahuata), and more abundant trachytes (Nuku Hiva,
472 Ua Huka, Ua Pou, Hiva Oa, Fatu Hiva) and phonolites (Ua Pou, Ua Huka). The only exception is Eiao, in
473 which coring has recovered a 10 m thick trachytic flow in the Dominique drill hole (Caroff et al., 1995; Maury
474 et al., 2009), at depths of 462 to 472 m below sea level. It has been dated at 5.44±0.04 Ma, an age perfectly
475 consistent with its position within the Eiao shield pile. This trachyte represents only a very small fraction of
476 the 2,100 m long cored volcanic sequences recovered from the three Eiao deep drillings. However,
477 mugearites (undated) also occur in the three cored sequences, in which they have a total thickness of ca 70
478 m (Maury et al., 2009). The origin of Eiao mugearites and trachytes has been ascribed to open-system
479 fractional crystallization of associated alkali basaltic magmas, coupled with assimilation of the oceanic crust
480 underlying the shield (Caroff et al., 1999).

481 In the other islands, the intermediate and evolved lavas erupted within the post-shield volcanoes (Nuku
482 Hiva, Ua Huka, Ua Pou, Ootua edifice in Hiva Oa). However, some of them outcrop as parasitic domes,
483 spines, plugs or dykes crosscutting the older (outer) volcanic shields: trachytes in Nuku Hiva, Ua Huka, Hiva
484 Oa (within the Puamau shield) and Fatu Hiva, and the tephriphonolitic spine of Mt Tumu Meae Ufa in
485 Tahuata. In Nuku Hiva, Ua Huka and Ua Pou, these trachytes or phonolites and the associated intermediate
486 lavas outcrop together with alkali basalts and/or basanites. Their ⁴⁰K-⁴⁰Ar ages fall within the range of those
487 of the latter or are slightly younger. In the case of Nuku Hiva, petrogenetic studies (Legendre et al., 2005b)
488 led to the conclusion that trachytes derived from open system fractional crystallization of alkali basalt
489 magmas coupled with assimilation of enriched oceanic crust with an EM II signature. The origin of the
490 unusually abundant phonolites from Ua Pou is thought to result from the fractionation of tephriphonolitic and
491 benmoreitic magmas derived from the remelting of basanitic rocks (Legendre et al., 2005a). In Fatu Hiva,
492 the emplacement of trachytes was contemporaneous with or post-dated that of post-caldera tholeiitic
493 basalts, but the possible petrogenetic relationships between them have not been investigated. The same
494 situation pertains to the Ootua post-shield volcano in Hiva Oa, where a spatial and temporal association of
495 tholeiitic basalts (some of which display a transitional affinity), hawaiites, mugearites, benmoreites and
496 trachytes is exposed (Maury et al., 2013). Evolved lavas were emplaced during the known entire history of
497 the archipelago (Fig. 6): Eiao trachyte is one of the oldest lavas of our set of data and Fatu Hiva ones count
498 among the youngest. Nuku Hiva and Ua Huka trachytes as well as the very abundant Ua Pou phonolites
499 were emplaced between ca 4.0 and 2.5 Ma (Fig. 6).

500 *4.3. Chemical diversity of shield and post-shield basaltic lavas*

501 In the Hawaiian model, basaltic magmas derive from temporally decreasing melt fractions of the mantle
502 sources: the emplacement of tholeiitic shield basalts is followed by that of post-shield alkali basalts and then

503 by [rejuvenated basanites](#) or nephelinites, and Sr isotopic ratios decrease during this evolution (Garcia et al.,
504 2010; Hanano et al., 2010). In the Marquesas, Ua Huka island volcanism followed this trend, with the
505 successive emplacement of Hikitau shield tholeiites, Hane post-shield alkali basalts and associated
506 benmoreites, trachytes and phonolites, and finally Teepoepo and Tahoatikikau rejuvenated basanitic cones.
507 However, Hikitau and Hane basalts display similar radiogenic Sr isotopic compositions, and only the
508 basanites from the rejuvenated cones are less radiogenic (Chauvel et al., 2012). In Ua Pou, the small
509 [emergent](#) remnants of an HIMU-type tholeiitic shield are overlain by a thick post-shield pile of basanites,
510 phonolites and other silica-undersaturated lavas more radiogenic in Sr, with a dominant EM II signature
511 (Duncan et al., 1986; Vidal et al., 1987; Legendre et al., 2005a).

512 The temporal petrologic evolution of other islands is more complex. Most shield lavas are tholeiitic, but
513 minor amounts of alkali basalts and basanites displaying higher enrichments in incompatible elements and
514 more radiogenic Sr isotopic ratios are interbedded [with](#) them in the shields of Eiao and Tahuata, or occur as
515 dykes crosscutting them in the Motane shield. In Nuku Hiva, the large post-shield Taiohae volcano includes
516 olivine tholeiites, alkali basalts and basanites more radiogenic in Sr than the Tekao shield tholeiites
517 (Legendre et al., 2005b). Post-shield basaltic lavas are exclusively tholeiitic or transitional in Hiva Oa
518 (Atuona and Ootua units), Tahuata (Hanatetena) and Fatu Hiva (Omoa). Although displaying a rather large
519 isotopic variability, they fall within the range of shield tholeiites from the same islands (Chauvel et al., 2012).

520 As a whole, [the claim by Woodhead \(1992\) and Castillo et al. \(2007\) that Marquesas shield lavas have](#)
521 [systematically lower \$^{87}\text{Sr}/^{86}\text{Sr}\$ ratios than post-shield lavas is not supported by isotopic studies conducted on](#)
522 [our sample set \(Chauvel et al., 2012\)](#). This conclusion applies to islands from the two isotopic [groups](#), e.g. to
523 Eiao and Ua Huka in the “Ua Huka group” and Hiva Oa, Tahuata and Fatu Hiva in the “Fatu Hiva group”
524 (Chauvel et al., 2012). The isotopic features of the sources of the Marquesas lavas are therefore not related
525 to the temporal pattern of volcanism (shield/post-shield activities) in a given island. The mafic lavas from the
526 two groups display similar La/Yb ratios ([Fig. 7](#)), while the Ua Huka rejuvenated basanites exhibit higher
527 ones. Post-shield intermediate and evolved lavas are more scattered in [Fig. 7](#), probably because of their
528 complex petrogenesis (open-system fractionation or remelting of mafic magmas). [In a similar La/Yb versus](#)
529 [La plot in which samples are sorted by petrographic type, alkali basalts display La/Yb ratios higher than](#)
530 [those of tholeiites \(Chauvel et al., 2012, their Figure 6\)](#).

531 *4.4. Implications for Marquesas plume heterogeneity and hotspot models*

532 Hotspot models previously proposed for the Marquesas (Duncan et al., 1986; Woodhead, 1992; Desonie
533 et al., 1993; Castillo et al., 2007) involved melting of a heterogeneous zoned mantle plume and of the
534 overlying oceanic lithosphere, or interactions between ascending plume-derived melts and this lithosphere.
535 These models were based on the assumption that the archipelago followed an “Hawaiian-type” temporal
536 evolution, the main difference being that in the Marquesas shield tholeiitic basalts were less radiogenic in Sr
537 (closer to DMM and/or HIMU) than the post-shield alkalic lavas (closer to EM end-members). In addition,
538 some authors used the tholeiitic or alkalic compositions of the basalts (Woodhead, 1992) or even their Sr
539 isotopic ratios (Castillo et al., 2007) to classify them as shield or post-shield, which led to additional
540 confusion.

541 In the present study and [in the Chauvel et al. paper \(2012\)](#), we used exclusively geological (field
542 relationships determined from detailed mapping) and chronological (unspiked ^{40}K - ^{40}Ar ages) data to
543 determine the shield or post-shield position of the samples. Our results show that: (1) there was usually no
544 temporal gap between shield and post-shield activities [at](#) a given island; (2) eruptions occurred
545 simultaneously in islands distant [as much as](#) 100 km one from another; (3) although most shields are
546 tholeiitic, several of them (Eiao, Tahuata) contain interbedded alkali basaltic and basanitic flows; (4) while
547 post-shield intermediate and evolved lavas derive usually from alkali basaltic or basanitic magmas, several
548 post-shield volcanoes are tholeiitic (Hiva Oa, Tahuata, Fatu Hiva); (5) the trace element and isotopic
549 compositions of shield and post-shield tholeiites display large variations, but the two groups overlap in most
550 diagrams (Chauvel et al., 2012); and finally (6) the “Ua Huka” and “Fatu Hiva” isotopic [groups](#) involve
551 mixtures of different mantle components, all of them likely located within the plume itself (Chauvel et al.,
552 2012) as also envisioned for Hawaii (Frey et al., 2005; Fekiacova et al., 2007; Garcia et al., 2010; Hanano et
553 al., 2011).

554 [The Sr and Nd isotopic differences between tholeiitic basalts and alkali basalts/basanites from](#)
555 [Marquesas Islands are shown in Figure 8. This plot shows all the data from the GEOROC database on](#)
556 [basaltic lavas whose major element and isotopic data were available. The sources of alkali basalts and](#)
557 [basanites are generally more enriched than those of the tholeiites at the scale of the archipelago. This is](#)
558 [also true within a given island, although the isotopic contrasts range from huge at Ua Pou to large at](#)
559 [Tahuata, Nuku Hiva, and Motane and small at Eiao and Ua Huka. These contrasts are consistent with the](#)
560 [hypothesis of an extremely heterogeneous character of the Marquesas plume. The nearly contemporaneous](#)
561 [emplacement of tholeiites and alkali basalts with different isotopic compositions in Tahuata \(Chauvel et al.,](#)
562 [2012\) suggests the occurrence of heterogenous mantle domains 10 km or less in diameter, as envisioned](#)
563 [for several other plumes including Hawaii \(Marske et al., 2007; Hanano et al., 2010\), Mauritius \(Paul et al.,](#)
564 [2005\) and the Galápagos \(Gibson et al., 2012\). When affected by the same high thermal regime in the](#)
565 [central part of a plume, domains with contrasted lithologies](#) could experience variable degrees of melting,
566 generating the observed diversity of basaltic magmas. Especially, low-degree melts might sample
567 preferentially fertile (and isotopically enriched) pyroxenite while the signature of the more depleted peridotitic
568 source dominates in high-degree melts (Sobolev et al., 2005, 2007; Jackson and Dasgupta, 2008; Day et
569 al., 2009; Dasgupta et al., 2010; White, 2010; Davis et al., 2011; Herzberg, 2011).

570 The occurrence of tholeiitic post-shield basalts in several islands is not surprising given the temporal
571 continuity between the shield and post-shield stages and the usually short period of emplacement of these
572 post-shield tholeiites (<0.1 Ma in Tahuata, Nuku Hiva and for Ootua basaltic flows in Hiva Oa; 0.2 Ma in Fatu
573 Hiva, [Fig. 5](#) and Tables 1 and 3). It is likely that during such short time spans [the extent of](#) melting of the
574 plume at depth did not change significantly, while the volcano structure was considerably modified after the
575 caldera collapse event. Longer post-shield activities might record a decrease [of melting](#) and [possible](#)
576 preferential sampling of [enriched materials](#). In the Taiohae inner edifice (Nuku Hiva) where post-shield
577 activity lasted ca 0.4 Ma (from 4.00 to 3.62 Ma; Maury et al., 2006), a brief tholeiitic episode was followed by
578 the emplacement of alkali basalts and basanites, and then by that of mugearites, benmoreites and trachytes
579 derived from an enriched mantle source. A rather similar evolution [has](#) been documented in the post-shield
580 volcanism of Mauna Kea, Hawaii (Frey et al., 1990), where the initial emplacement of tholeiites [and alkali](#)

581 **basalts** (basaltic substage) was followed by that of intermediate and evolved lavas (hawaiitic substage).
582 Finally, the emplacement of the rejuvenated basanitic strombolian cones in Ua Huka after a 1.3 Myr long
583 quiescence period (Fig. 2) was accompanied by major petrogenetic changes, involving very low melting
584 degrees of a garnet lherzolite source deeper and isotopically more depleted than that of the older tholeiitic
585 and alkali basalts (Legendre et al., 2006).

586 The petrologic and geochemical diversity of Marquesas lavas is rather exceptional given the modest
587 size of the archipelago, **as appreciated** since the pioneer works of A. Lacroix (1928) and L.J. Chubb (1930).
588 It can be related to the “weak” character of the Marquesas plume (McNutt et al., 1989), which produced
589 “only” 7,700 km³ of magma per Myr in the Marquesas (Chauvel et al., 2012), compared to 213,000 km³ **for**
590 **the Big Island of Hawaii** (Robinson and Eakins, 2006). Indeed, low degrees of partial melting resulted in the
591 preservation in the Marquesas basaltic magmas of geochemical features inherited from small-size source
592 heterogeneities, while high degrees of partial melting and resulting high magma production rate tend to
593 **blend** these features. The complex petrogenesis (open-system processes or remelting of mafic precursors)
594 of post-shield intermediate and evolved lavas contributed further to increase this diversity.

595 **5. Conclusions**

596 The study of 110 Marquesas lavas **located** on detailed geological maps and dated by the unspiked ⁴⁰K-
597 ⁴⁰Ar method on separated groundmass allows us to demonstrate that the temporal evolution of the
598 archipelago is rather **different** with respect to that of Hawaii and many other hotspot-related chains. There is
599 usually no temporal gap between shield and post-shield activities in a given island, and rejuvenated
600 volcanism is uncommon. Although most shields are tholeiitic, several of them (Eiao, Tahuata) contain
601 interbedded alkali basaltic and basanitic flows. The occurrence of intermediate and evolved lavas is
602 restricted to the post-shield stage, with one exception (Eiao). Although these lavas are usually associated
603 **with** alkali basaltic or basanitic magmas, several post-shield volcanoes are tholeiitic (Hiva Oa, Tahuata, Fatu
604 Hiva) or include tholeiites (Nuku Hiva). In a given island, the trace element and isotopic compositions of
605 shield and post-shield tholeiites overlap although both display large variations (Chauvel et al., 2012).

606 These features are inconsistent with former models (Duncan et al., 1986; Woodhead, 1992; Desonie et
607 al., 1993; Castillo et al., 2007) that postulated that the Marquesas followed a “Hawaiian-type” evolution.
608 They are consistent with the hypothesis of an extremely heterogeneous character of the Marquesas plume.
609 The “weak” character of **this** plume led to **low degrees of partial melting**, which in turn resulted in the
610 preservation in the basaltic magmas of geochemical features inherited from such small-size source
611 heterogeneities.

612 **Acknowledgements**

613 This study has been funded by CNRS (INSU and UMR 8212, 6538, 5275, 6518), BRGM and CEA-
614 DASE-DSM. **We thank two anonymous reviewers for their very constructive comments that helped us to**
615 **improve the overall content of the manuscript. We also** thank Mayors Guy Rauzy and Etienne Tehaamoana
616 (Hiva Oa), Henri Tuieinui (Fatu Hiva) and Félix Barsinas (Tahuata) who provided logistic support during
617 fieldwork. We are very grateful to Andy Teiki Richmond and the team of the Service du Développement
618 Rural of Atuona-Hiva Oa for their considerable help in the field, especially during coastal sampling and work

619 in densely forested areas. Joseph Cotten's contribution to analytical work is greatly appreciated. [Jean](#)
620 [François Tannau](#) and [Vincent Scao](#) provided helpful technical assistance. This is LSCE contribution N°5115.

621

622 **References**

- 623 Blais, S., Legendre, C., Maury, R.C., Guille, G., Guillou, H., Rossi, P., Chauvel, C., 2008.
624 Notice explicative, carte géologique de France, feuille de Ua Huka, Polynésie française, 102 pp, scale 1:
625 50,000, Bureau de Recherches Géologiques et Minières, Orléans, France.
- 626
- 627 Brousse, R., Barszczus, H.G., Bellon, H., Cantagrel, J.M., Diraison, C., Guillou, H., Léotot,
628 C., 1990. Les Marquises (Polynésie française): volcanologie, géochronologie, discussion d'un modèle de
629 point chaud [The Marquesas alignment (French Polynesia) – Volcanology, geochronology, a hotspot model].
630 Bulletin de la Société géologique de France 6, 933-949.
- 631
- 632 Cadio, C., Panet, I., Davaille, A., Diament, M., Métivier, L., de Viron, O., 2011. Pacific geoid
633 anomalies revisited in light of thermochemical oscillating domes in the lower mantle. Earth
634 Planetary Science Letters 306, 123-135.
- 635
- 636 Caress, D.V., McNutt, M.K., Detrick, R.S., Mutter, J.C., 1995. Seismic imaging of hotspot
637 related crustal underplating beneath the Marquesas Islands. Nature 373, 600-603.
- 638
- 639 Caroff, M., Maury, R.C., Vidal, P., Guille, G., Dupuy, C., Cotten, J., Guillou, H., Gillot, P.Y.,
640 1995. Rapid temporal changes in ocean island basalt composition – evidence from an 800 m
641 deep drill hole in Eiao shield (Marquesas). Journal of Petrology 36, 1333-1365.
- 642
- 643 Caroff, M., Guillou, H., Lamiaux, M.I., Maury, R.C., Guille, G., Cotten, J., 1999.
644 Assimilation of ocean crust by hawaiitic and mugearitic magmas: an example from Eiao
645 (Marquesas). Lithos 46, 235-258.
- 646
- 647 Carracedo, J.C., Day, S., Guillou, H., Badiola, E.R., Canas, J.A., Pérez Torrado, F.J., 1998.
648 Hotspot volcanism close to a passive continental margin: The Canary Islands. Geological Magazine 135,
649 591-604.
- 650
- 651 Castillo, P.R., Scarsi, P., Craig, H., 2007. He, Sr, Nd and Pb isotopic constraints on the origin
652 of the Marquesas and other linear volcanic chains. Chemical Geology 240, 205-221.
- 653
- 654 Chauvel, C., Maury, R.C., Blais, S., Lewin, E., Guillou, H., Guille, G., Rossi, P., Gutscher, M.-A., 2012. The
655 size of plume heterogeneities constrained by Marquesas isotopic stripes. Geochemistry Geophysics
656 Geosystems 13(1), Q07005, doi: 10.129/2012GC004123.
- 657
- 658 Chubb, L.J., 1930. The geology of the Marquesas islands. Bernice P. Bishop Museum Bulletin, 68, 1-71.
- 659
- 660 Clague, D.A., 1987. Hawaiian xenolith populations, magma supply rates, and development of magma
661 chambers. Bulletin of Volcanology 49, 577-587.
- 662
- 663 Clague, D.A., Dalrymple, G.B., 1987. The Hawaiian-Emperor volcanic chain. Part 1. Geological evolution.
664 United States Geological Survey Professional Paper 1350, 5-54.
- 665
- 666 Cotten, J., Le Dez, A., Bau, M., Caroff, M., Maury, R.C., Dulski, P., Fourcade, S., Bohn, M.,
667 Brousse, R., 1995. Origin of anomalous rare-earth element and yttrium enrichments in
668 subaerially exposed basalts: Evidence from French Polynesia. Chemical Geology 119, 115-138.
- 669
- 670 Courtillot, V., Davaille, A., Besse, J., Stock, J., 2003. Three distinct types of hotspots in the
671 Earth's mantle. Earth and Planetary Science Letters 205, 295-308.
- 672
- 673 Crough, S.T., Jarrard, R.D., 1981. The Marquesas-line swell. Journal of Geophysical Research 86, 1763-
674 1771.
- 675
- 676 Dasgupta, R., Jackson, M.G., Lee, C.T.A., 2010. Major element chemistry of ocean island

677 basalts - Conditions of mantle melting and heterogeneity of mantle source. *Earth and Planetary Science*
678 *Letters* 289, 377-392.

679

680 Davaille, A., Girard, F., Le Bars, M., 2002. How to anchor hotspots in a convecting mantle ? *Earth and*
681 *Planetary Science Letters* 203, 621-634.

682

683 Davis, F.A., Hirschmann, M.M., Humayun, M., 2011. The composition of the incipient partial melt of garnet
684 peridotite at 3 GPa and the origin of OIB. *Earth and Planetary Science Letters* 308, 380-390.

685

686 Day, J.M.D., Pearson, D.G., Macpherson, C.G., Lowry, D., Carracedo, J.C., 2009.
687 Pyroxenite-rich mantle formed by recycled oceanic lithosphere: Oxygen-osmium isotope
688 evidence from Canary Island lavas. *Geology* 37, 555-558.

689

690 Desonie, D.L., Duncan, R.A., Natland, J.H., 1993. Temporal and geochemical variability of
691 volcanic products of the Marquesas hotspot. *Journal of Geophysical Research* 98,
692 17649-17665.

693

694 Devey, C.W., Haase, K.M., 2003. The sources for hotspot volcanism in the South Pacific
695 Ocean, in: R. Hékinian, P.S., J.L. Cheminée (Ed.), *Oceanic hotspots: intraplate submarine*
696 *magmatism and tectonism*. Springer Verlag, Berlin, pp. 253-284.

697

698 Duncan, R.A., 1975. Linear volcanism in French Polynesia. Unpublished PhD Thesis, Australian National
699 University.

700

701 Duncan, R.A., McDougall, I., 1974. Migration of volcanism with time in the Marquesas
702 Islands, French Polynesia. *Earth and Planetary Science Letters* 21, 414-420.

703

704 Duncan, R.A., McCulloch, M.T., Barczus, H.G., Nelson, D.R., 1986. Plume versus
705 lithospheric sources for the melts at Ua Pou, Marquesas Island. *Nature* 303, 142-146.

706

707 Farnetani, C.G., Hofmann, A.W., 2010. Dynamics and internal structure of the Hawaiian
708 plume. *Earth and Planetary Science Letters* 295, 231-240.

709

710 Fekiacova, Z., Abouchami, W., Galer, S.J.G., Garcia, M.O., Hofmann, A.W., 2007. Origin
711 and temporal evolution of Ko'olau Volcano, Hawai'i: Inferences from isotope data on the
712 Ko'olau Scientific Drilling Project (KSDP), the Honolulu Volcanics and ODP Site 843. *Earth*
713 *and Planetary Science Letters* 261, 65-83.

714

715 Filmer, P.E., McNutt, M.K., Wolfe, C.J., 1993. Elastic thickness of the lithosphere in the
716 Marquesas and Society Islands. *Journal of Geophysical Research* 98, 19565-
717 19577.

718

719 Frey, F.A., Wise, W.S., Garcia, M.O., West, H., Kwon, S.-T., Kennedy, A., 1990. Evolution of Mauna Kea
720 volcano, Hawaii: petrologic and geochemical constraints on postshield volcanism. *Journal of Geophysical*
721 *Research* 95, 1271-1300.

722

723 Frey, F.A., Huang, J., Blichert-Toft, J., Regelous, M., Boyet, M., 2005. Origin of depleted components in
724 basalt related to the Hawaiian hot spot: Evidence from isotopic and incompatible element ratios.
725 *Geochemistry Geophysics Geosystems* 6, Q02107, doi:10.129/2004GC000757.

726

727 Garcia, M.O., Swinnard, L., Weis, D., Greene, A.R., Tagami, T., Sano, H., Gandy, C.E.,
728 2010. Petrology, geochemistry and geochronology of Kaua'i lavas over 4.5 Myr: implications
729 for the origin of rejuvenated volcanism and the evolution of the Hawaiian plume. *Journal of Petrology* 51,
730 1507-1540.

731

732 Gibson, S.A., Geist, D.G., Day, J.A., Dale, C.W., 2012. Short wavelength heterogeneity in the Galápagos
733 plume: evidence from compositionally diverse basalts on Isla Santiago.. *Geochemistry Geophysics*
734 *Geosystems* 13(1), Q09007, doi: 10.129/2012GC004244.

735

736 Guille, G., Legendre, C., Maury, R.C., Caroff, M., Munsch, M., Blais, S., Chauvel, C.,

737 Cotten, J., Guillou, H., 2002. Les Marquises (Polynésie française): un archipel intraocéanique
738 atypique. *Géologie de la France* 2, 5-36.
739

740 Guille, G., Legendre, C., Maury, R.C., Guillou, H., Rossi, P., Blais, S., 2010. Notice explicative, carte
741 géologique de France, feuille de Ua Pou, Polynésie française, 133 pp, scale 1: 30,000, Bureau de
742 Recherches Géologiques et Minières, Orléans, France, in press.
743

744 Guille, G., Maury, R.C., (coordinators), 2013. Carte géologique de la feuille Groupe Sud de l'archipel des
745 Iles Marquises (Hiva Oa – Tahuata – Motane et Fatu Hiva), Polynésie française, scale 1: 100,000, Bureau
746 de Recherches Géologiques et Minières, Orléans, France, in press.
747

748 Guillou, H, Maury, R.C., Blais, S., Cotten, J., Legendre, C., Guille, G., Caroff, M., 2005. Age progression
749 along the Society hot spot chain (French Polynesia) based on new unspiked K-Ar ages. *Bulletin de la*
750 *Société géologique Française* 176, 135-150.
751

752 Guillou, H., Nomade, S., Carracedo, J.C., Kissel, C., Laj, C., Perez Torrado, F.J., Wandres,
753 C., 2011. Effectiveness of combined unspiked K-Ar and ⁴⁰Ar/³⁹Ar dating methods in the
754 ¹⁴C age range. *Quaternary Geochronology* 6, 530-538.
755

756 Gutscher, M.A., Olivet, J.L., Aslanian, D., Eissen, J.P., Maury, R., 1999. The "lost Inca
757 Plateau": cause of flat subduction beneath Peru? *Earth and Planetary Science Letters* 171, 335-341.
758

759 Hanano, D., Weis, D., Scoates, J.S., Aciego, S., DePaolo, D.J., 2010. Horizontal and vertical
760 zoning of heterogeneities in the Hawaiian mantle plume from the geochemistry of consecutive
761 postshield volcano pairs: Kohala-Mahukona and Mauna Kea-Hualalai. *Geochemistry*
762 *Geophysics Geosystems* 11, Q01004, doi:10.129/2009GC002782.
763

764 Herzberg, C., 2011. Identification of Source Lithology in the Hawaiian and Canary Islands:
765 Implications for Origins. *Journal of Petrology* 52, 113-146.
766

767 Jackson, M.G., Dasgupta, R., 2008. Compositions of HIMU, EM1, and EM2 from global
768 trends between radiogenic isotopes and major elements in ocean island basalts. *Earth Planetary Science*
769 *Letters* 276, 175-186.
770

771 Jordahl, K.A., McNutt, M.K., Webb, H.F., Kruse, S.E., Kuykendall, M.G., 1995. Why there
772 are no earthquakes on the Marquesas Fracture Zone. *Journal of Geophysical Research* 100, 24431-24447.
773

774 Konter, J.G., Jackson, M.G., 2012. Large volumes of rejuvenated volcanism in Samoa: evidence supporting
775 a tectonic influence on late-stage volcanism. *Geochemistry Geophysics Geosystems* 13, Q0AM04,
776 doi:10.129/2011GC003974.
777

778 Lacroix, A., 1928. Nouvelles observations sur les laves des îles Marquises et de l'île Tubuai (Polynésie
779 australe). *Comptes Rendus de l'Académie des Sciences Paris* 187, 365-369.
780

781 Laughlin, A.W., Poths, J., Healey, H.A., Reneau, S., Woldegabriel, G., 1994. Dating of Quaternary basalts
782 using the cosmogenic He-3 and C-14 methods with implications for excess Ar-40. *Geology* 22, 135-138.
783

784 Le Bas, M.J., Le Maitre, R.W., Streckeisen, A., Zanettin, B., 1986. A chemical classification of volcanic rocks
785 based on the total-alkali-silica diagram. *Journal of Petrology* 27, 745-750.
786

787 Legendre, C., Maury, R.C., Caroff, M., Guillou, H., Cotten, J., Chauvel, C., Bollinger, C.,
788 Hémond, C., Guille, G., Blais, S., Rossi, P., Savanier, D., 2005a. Origin of exceptionally
789 abundant phonolites on Ua Pou island (Marquesas, french Polynesia): partial melting of
790 basanites followed by crustal contamination. *Journal of Petrology* 46, 1925-1962.
791

792 Legendre, C., Maury, R.C., Savanier, D., Cotten, J., Chauvel, C., Hémond, C., Bollinger, C.,
793 Guille, G., Blais, S., Rossi, P., 2005b. The origin of intermediate and evolved lavas in the
794 Marquesas archipelago: an example from Nuku Hiva island (French Polynesia). *Journal of Volcanology and*
795 *Geothermal Research* 143, 293-317.
796

797 Legendre, C., Maury, R.C., Blais, S., Guillou, H., Cotten, J., 2006. Atypical hotspot chains:
798 evidence for a secondary melting zone below the Marquesas (French Polynesia). *Terra Nova*
799 18, 210-216.
800
801 Macdonald, G.A., Katsura, T., 1964. Chemical composition of Hawaiian lavas. *Journal of Petrology* 5, 82-
802 133.
803
804 Marske, J.P., Pietruszka, A.J., Weis, D., Garcia, M.O., Rhodes, J.M., 2007. Rapid passage of a small-scale
805 mantle heterogeneity through the melting regions of Kilauea and Mauna Loa volcanoes. *Earth and Planetary*
806 *Science Letters* 259, 34-50.
807
808 Maury, R.C., Guille, G., Legendre, C., Savanier, D., Guillou, H., Rossi, P., Blais, S., 2006.
809 Notice explicative, carte géologique de France, feuille de Nuku Hiva, Polynésie française.
810 116 pp, scale 1: 50,000, Bureau de Recherches Géologiques et Minières, Orléans, France.
811
812 Maury, R.C., Legendre, C., Guille, G., Demange, J., Caroff, M., 2009. Notice explicative, carte géologique de
813 France, feuille d'Eiao, Polynésie française, 89 pp, scale 1: 25,000, Bureau de Recherches Géologiques et
814 Minières, Orléans, France.
815
816 Maury, R.C., Guille, G., Guillou, H., Rossi, P., Legendre, C., Chauvel, C., Blais, S., Ottino,
817 P., Meyer, J.-Y., Deroussi, S., Tegye, M., Cabioch, G., 2013. Notice explicative, carte
818 géologique de France, feuille Groupe Sud de l'archipel des Iles Marquises (Hiva Oa – Tahuata – Motane et
819 Fatu Hiva), Polynésie française, XX pp, scale 1: 100,000, Bureau de Recherches Géologiques et Minières,
820 Orléans, France, in press.
821
822 McDougall, I., Duncan, R.A., 1980. Linear volcanic chains: recording plate motions? *Tectonophysics* 63,
823 275-295.
824
825 McNutt, M., Bonneville, A., 2000. A shallow, chemical origin for the Marquesas Swell.
826 *Geochemistry Geophysics Geosystems* 1, 1999GC000028.
827
828 McNutt, M., Fischer, K., Kruse, S., Natland, J., 1989. The origin of the Marquesas fracture
829 zone ridge and its implications for the nature of hot spots. *Earth and Planetary Science Letters* 91, 381-393.
830
831 Merle, O., Barde-Cabusson, S., Maury, R.C., Legendre, C., Guille, G., Blais, S., 2006. Volcano core collapse
832 triggered by regional faulting. *Journal of Volcanology and Geothermal Research* 158, 269-280.
833
834 Paul, D., White, W.M., Blichert-Toft, J., 2005. Geochemistry of Mauritius and the origin of rejuvenescent
835 volcanism on oceanic island volcanoes. *Geochemistry Geophysics Geosystems* 6, Q06007, doi:
836 10.129/2004GC000883.
837
838 Pautot, G., Dupont, J., 1974. La zone de fracture des Marquises. *Comptes Rendus de l'Académie des*
839 *Sciences Paris* 279, 1519-1523.
840
841 Ribe N.M., Christensen U.R., 1999. The dynamical origin of Hawaiian volcanism. *Earth and Planetary*
842 *Science Letters* 171, 517-531.
843
844 Shafer, J.T., Neal, C.R., Regelous, M. 2005. Petrogenesis of Hawaiian postshield lavas: evidence from
845 Nintoku Seamount, Emperor Seamount Chain. *Geochemistry Geophysics Geosystems* 6, Q05L09, doi:
846 10.129/2004GC000875.
847
848 Smith, W.H.F., Sandwell, D.T., 1997. Global sea floor topography from satellite altimetry and
849 ship depth soundings. *Science* 277, 1956-1962.
850
851 Sobolev, A.V., Hofmann, A.W., Sobolev, S.V., Nikogosian, I.K., 2005. An olivine-free
852 mantle source of Hawaiian shield basalts. *Nature* 434, 590-597.
853
854 Sobolev, A.V., Hofmann, A.W., Kuzmin, D.V., Yaxley, G.M., Arndt, N.T., Chung, S.-L., Danyushevsky, L.V.,
855 Elliott, T., Frey, F.A., Garcia, M.O., Gurenko, A.A., Kamenetsky, V.S., Kerr, A.C., Krivolutskaia, N.A.,

856 Matvienkov, V.V., Nikogosian, I.K., Rocholl, A., Sigurdsson, I.A., Sushchevskaya, N.M., Teklay, M., 2007.
857 The Amount of Recycled Crust in Sources of Mantle-Derived Melts. *Science* 316, 412-417.
858
859 Stearns, H.T., 1966. *Geology of the State of Hawaii*: Palo Alto. Pacific Books, 266 p.
860
861 Steiger, R.H., Jäger, E., 1977. Subcommittee on geochronology: convention on the use of
862 decay constants in geo- and cosmo-chronology. *Earth and Planetary Science Letters* 36, 359-362.
863
864 Vidal, P., Chauvel, C., Brousse, R., 1984. Large mantle heterogeneity beneath French
865 Polynesia. *Nature* 307, 536-538.
866
867 Vidal, P., Dupuy, C., Barszczus, H.G., Chauvel, C., 1987. Hétérogénéités du manteau et
868 origine des basaltes des Marquises (Polynésie). *Bulletin de la Société géologique de France* 4, 633-642.
869
870 [Westaway, R., Guillou, H., Yurtmen, S., Demir, T., Scaillet, S., Rowbotham, G., 2005. Constraints on](#)
871 [the timing and regional conditions at the start of the present phase of crustal extension in western](#)
872 [Turkey, from observations in and around the Denizli region. *Geodinamica Acta*. 18/3-4, 209-238.](#)
873
874 White, W.M., 2010. Oceanic Island Basalts and Mantle Plumes: The Geochemical
875 Perspective, in: Jeanloz, R., Freeman, K.H. (Eds.), *Annual Review of Earth and Planetary*
876 *Sciences*, Vol 38. Annual Reviews, Palo Alto, pp. 133-160.
877
878 Woodhead, J.D., 1992. Temporal geochemical evolution in oceanic intra-plate volcanics: a
879 case study from the Marquesas (French Polynesia) and comparison with other hotspots.
880 *Contributions to Mineralogy and Petrology* 111, 458-467.
881
882
883
884

885 **Figure captions**

886
887 **Fig. 1.** Location map of Marquesas Islands. The bathymetry comes from the global altimetry data set of
888 Smith and Sandwell (1997). The main trend of the Marquesas chain is N40°W. Current Pacific plate motion
889 is 10.5 cm/yr at N65°W, corresponding to the line shown in white. The names of the southern islands are in
890 large print. MFZ: Marquesas Fracture Zone.

891
892 **Fig. 2.** Age versus distance plot for the Marquesas. The distances to the MFZ Ridge (MFZR) along
893 N65°W trend corresponding to the 10.5 cm/yr motion of the Pacific plate are from Chauvel et al. (2012). The
894 dashed line starts from the unexplored chain of seamounts located 50 km NW of the MFZR. Shield ages are
895 denoted by open symbols, post-shield ages by filled symbols and rejuvenated ages by grey symbols.
896 Sources of unspiked ⁴⁰K-⁴⁰Ar ages on groundmass: Tables 1 and 3 for southern islands; Caroff et al. (1995)
897 and Maury et al. (2009) for Eiao; Maury et al. (2006) for Nuku Hiva; Legendre et al. (2006) and Blais et al.
898 (2008) for Ua Huka; Legendre et al. (2005a) and Guille et al. (2010) for Ua Pou.

899
900 **Fig. 3.** Total-Alkali-Silica (TAS) diagram (Le Bas et al., 1986) for the dated Marquesas lavas. The
901 dashed line separating the fields of tholeiitic (Thol.) and alkali (Alk.) basalts is from Macdonald and Katsura
902 (1964). Shield ages are denoted by open symbols, post-shield ages by filled symbols and rejuvenated ages
903 by grey symbols. Sources of major and trace element analyses: Tables 2 and 4 for southern islands; Caroff
904 et al. (1995) and Maury et al. (2009) for Eiao; Maury et al. (2006) for Nuku Hiva; Legendre et al. (2006) and
905 Blais et al. (2008) for Ua Huka; Legendre et al. (2005a) and Guille et al. (2010) for Ua Pou.

906
907 **Fig. 4.** Sketches of the Marquesas volcanic successions, showing caldera collapse events (red dashed
908 lines) and simplified distributions of tholeiitic basalts, alkali basalts and basanites, and felsic lavas (trachytes
909 and phonolites). Intermediate lavas have been omitted for clarity. Vertical scales are arbitrary. Abbreviated
910 volcano names: Ha: Hane; Hi: Hikitau; Hk: Hakahau; Hn: Hanatetena; Om: Omoa; Oo: Ootua; Pu: Puamau;
911 Ta: Taaoa; Te: Temetiu; Th: Taiohae; Tk: Tekao; To: Touaouoho; Va: Vaitahu. In Ua Huka, a temporal gap
912 separates the end of building of the Hane volcano from the rejuvenated volcanic phase which emplaced the
913 Teepoepo (1.15-0.96 Ma) and Tahoatikikau (0.82-0.76 Ma) basanitic cones. In Tahuata, the horizontal line
914 below the red dashed line separates the upper from the lower tholeiitic flows of Vaitahu shield.

915
916 **Fig. 5.** Geological sketch maps of the southern Marquesas islands, simplified from Guille and Maury
917 (2013) and Maury et al. (2013). The locations of the dated samples are shown by small red crosses
918 (corresponding ages in Ma from Tables 1 and 3). Most flow dips range from 8 to 12°. See text for
919 explanations.

920
921 **Fig. 6.** Plot of unspiked ⁴⁰K-⁴⁰Ar ages against SiO₂ for dated samples. Symbols and sources of data as
922 in Figs. 2 and 3.

923
924 **Fig. 7.** Plot of La/Yb against La (ppm) for dated samples. Symbols and sources of data as in Fig. 3.

925
926 **Fig. 8.** $^{87}\text{Sr}/^{86}\text{Sr}$ versus $^{143}\text{Nd}/^{144}\text{Nd}$ diagram showing the differences between tholeiitic basalts and alkali
927 basalts/basanites from Marquesas islands. Data from the GEOROC database and Chauvel et al. (2012).
928 The Fatu Hiva sample plotting away from the main trend (low $^{143}\text{Nd}/^{144}\text{Nd}$) is from Woodhead (1992).
929

930 **Table captions**

931
932 **Table 1.** Unspiked ^{40}K - ^{40}Ar ages measured on groundmass for Hiva Oa lavas. See text for analytical
933 methods and Fig. 4 for sample locations. SH: shield; PS: post-shield. Mugear.: mugearite; benmor.:
934 benmoreite. *: ages already given in Chauvel et al. (2012) but without details.
935

936 **Table 2.** Major and trace element ICP-AES analyses of dated lavas from Hiva Oa. Major element oxides
937 in wt%, trace elements in ppm. Fe_2O_3^* : total iron as Fe_2O_3 . See text for analytical methods, Table 1 for ages
938 and Fig. 4 for sample locations. **Samples are ranked by order of decreasing ages.** SH: shield; PS: post-
939 shield. Thol: tholeiite; haw: hawaiiite; mug: mugearite; ben: benmoreite; tra: trachyte. The rare earth element
940 and Y concentrations of sample HV54 have been modified by supergene alteration involving crystallization
941 of rhabdophane (Cotten et al., 1995), and therefore this sample has not been plotted in Fig. 6. *: Major
942 element analyses given in Chauvel et al. (2012) together with ICP-MS trace element analyses.
943

944 **Table 3.** Unspiked ^{40}K - ^{40}Ar ages measured on groundmass for Motane, Tahuata and Fatu Hiva lavas.
945 See text for analytical methods and Fig. 4 for sample locations. SH: shield; PS: post-shield. Alk. bas.: alkali
946 basalt. *: ages already given in Chauvel et al. (2012) but without details.
947

948 **Table 4.** Major and trace element ICP-AES analyses of dated lavas from Motane, Tahuata and Fatu
949 Hiva. Major element oxides in wt%, trace elements in ppm. Fe_2O_3^* : total iron as Fe_2O_3 . See text for
950 analytical methods, Table 3 for ages and Fig. 4 for sample locations. **For each island, samples are ranked**
951 **by order of decreasing ages.** SH: shield; PS: post-shield. Thol: tholeiite; alb: alkali basalt; bas: basanite;
952 haw: hawaiiite; teph: tephriphonolite; tra: trachyte. *: Major element analyses given in Chauvel et al. (2012)
953 together with ICP-MS trace element analyses.
954

Table
[Click here to download Table: Table 1 Guillou et al.doc](#)

Sample & Experiment	Occurrence & Type	K (wt%) ± 1σ	Mass molten (g)	⁴⁰ Ar* (%)	⁴⁰ Ar* (10 ⁻¹² mol./g) ± 1 σ	Weighted mean ⁴⁰ Ar* (10 ⁻¹² mol./g) ± 1 σ	Age (Ma) ± 2 σ
HV107 7378	PS tholeiite flow	1.978 ± 0.020	1.43274	36.482	4.935 ± 0.026		
7394	Ootua	« »	1.64660	49.561	4.925 ± 0.025	4.930 ± 0.018	1.44 ± 0.03
HV88 7347	SH hawaiite upper flow	1.695 ± 0.017	1.35898	47.011	4.273 ± 0.022		
7361	Puamau	« »	1.50413	60.993	4.311 ± 0.022	4.292 ± 0.016	1.46 ± 0.03
HV86 7308	PS hawaiite flow	1.501 ± 0.015	1.03777	20.778	4.077 ± 0.023		
7324	Ootua	« »	1.69426	56.220	3.823 ± 0.020	3.932 ± 0.015	1.51 ± 0.03
HV62 7323	SH tholeiite flow	1.507 ± 0.015	1.21717	21.901	4.185 ± 0.023		
7339	Puamau	« »	1.08625	33.020	4.300 ± 0.023	4.241 ± 0.016	1.62 ± 0.04
HV54 7548	PS benmor. dyke	2.638 ± 0.026	1.00103	55.652	7.369 ± 0.037		
7564	Ootua	« »	2.07615	63.800	7.640 ± 0.038	7.500 ± 0.027	1.64 ± 0.03
HV70 7302	SH tholeiite flow	1.509 ± 0.015	1.06608	33.920	4.227 ± 0.023		
7316	Puamau	« »	1.07234	19.444	4.418 ± 0.025	4.315 ± 0.017	1.65 ± 0.04
HV56 7541	PS mugear. flow	1.991 ± 0.020	1.13733	16.494	5.993 ± 0.032		
7557	Ootua	« »	1.17474	30.860	5.981 ± 0.033	5.987 ± 0.023	1.73 ± 0.04
HV65 7293	PS tholeiite flow	1.181 ± 0.012	1.16980	27.526	3.676 ± 0.020		
7309	Atuona	« »	1.27950	21.735	3.715 ± 0.020	3.695 ± 0.014	1.80 ± 0.04
HV81 7332	SH hawaiite flow	1.976 ± 0.020	1.08717	18.778	6.232 ± 0.033		
7348	Temetiu	« »	1.35792	17.642	6.316 ± 0.033	6.275 ± 0.023	1.83 ± 0.04
HV82 7315	SH tholeiite flow	1.137 ± 0.011	1.10367	19.184	3.821 ± 0.022		
7331	Temetiu	« »	1.27970	21.827	3.736 ± 0.021	3.777 ± 0.015	1.91 ± 0.04
HV99 7472	SH tholeiite dyke	1.869 ± 0.020	0.56437	36.823	6.539 ± 0.033		
7587	Temetiu	« »	0.61803	6.398	6.525 ± 0.033	6.533 ± 0.024	2.01 ± 0.04
HV76* 7301	SH tholeiite flow	1.254 ± 0.013	1.02679	29.743	4.477 ± 0.025		
7320	Temetiu	« »	1.12163	24.685	4.338 ± 0.024	4.406 ± 0.017	2.02 ± 0.04
HV11 7543	SH tholeiite flow	1.459 ± 0.015	1.38244	33.999	5.325 ± 0.027		
7559	Temetiu	« »	1.26070	4.831	5.157 ± 0.033	5.258 ± 0.021	2.08 ± 0.04
HV38 7549	SH hawaiite flow	1.870 ± 0.019	0.93187	32.635	6.598 ± 0.034		
7565	Temetiu	« »	0.95534	22.934	6.904 ± 0.036	6.744 ± 0.025	2.08 ± 0.04
HV112 7379	SH hawaiite flow	1.824 ± 0.018	1.13791	42.865	6.701 ± 0.035		
7395	Temetiu	« »	1.49233	23.887	6.762 ± 0.035	6.731 ± 0.024	2.13 ± 0.05
HV78 7456	SH tholeiite flow	1.322 ± 0.013	0.99687	25.760	4.916 ± 0.026		
7472	Temetiu	« »	1.50904	23.970	4.865 ± 0.025	4.890 ± 0.018	2.13 ± 0.05
HV77 7325	SH hawaiite flow	1.848 ± 0.018	1.39336	22.254	7.005 ± 0.037		
7340	Temetiu	« »	1.04261	35.918	6.934 ± 0.036	6.969 ± 0.026	2.17 ± 0.05
HV84 7618	SH tholeiite flow	1.150 ± 0.015	1.03595	27.021	4.456 ± 0.023		
7634	Temetiu	« »	1.56657	48.619	4.521 ± 0.023	4.489 ± 0.016	2.25 ± 0.05

HV87	SH tholeiite						
7455	flow	1.403 ± 0.014	1.01446	32.032	5.532 ± 0.029		
7471	Temetiu	« »	1.50142	24.886	5.505 ± 0.028	5.518 ± 0.020	2.27 ± 0.05
HV64*	SH tholeiite						
7341	flow	0.913 ± 0.009	1.23639	24.869	4.046 ± 0.022		
7357	Taaoa	« »	1.12964	25.818	4.036 ± 0.022	4.041 ± 0.016	2.55 ± 0.05

* Age in Chauvel et al. (2012) but no details.

Sample	HV64*	HV87	HV84	HV77	HV78	HV112	HV 38	HV 11	HV76*	HV99	HV82	HV81	HV65	HV 56	HV70	HV54	HV62	HV86	HV88	HV107
Volcano type	Taaoa SH thol	Temetiu SH thol	Temetiu SH thol	Temetiu SH haw	Temetiu SH thol	Temetiu SH haw	Temetiu SH haw	Temetiu SH thol	Temetiu SH thol	Temetiu SH thol	Temetiu SH thol	Temetiu SH haw	Atuona PS thol	Ootua PS mug	Puamau SH thol	Ootua PS ben	Puamau SH thol	Ootua PS haw	Puamau SH haw	Ootua PS thol
SiO2	46.60	46.20	48.40	48.00	48.00	48.40	48.75	47.10	48.50	47.00	48.60	48.00	46.00	50.70	46.75	54.50	48.40	48.60	48.20	47.60
TiO2	3.55	3.26	3.34	3.52	3.22	3.71	3.72	3.61	3.84	2.99	3.78	3.67	3.65	3.12	4.05	2.17	3.01	3.92	3.69	2.85
Al2O3	13.40	11.50	13.55	14.42	13.60	15.54	15.90	13.80	14.65	12.94	14.15	15.35	13.75	15.83	13.15	16.34	13.25	16.00	14.20	12.35
Fe2O3*	13.00	13.60	12.40	11.88	12.80	11.58	11.60	12.35	12.85	11.70	13.00	11.58	13.15	11.10	12.80	8.45	11.90	11.90	12.20	12.40
MnO	0.15	0.17	0.15	0.16	0.17	0.18	0.15	0.16	0.15	0.15	0.16	0.15	0.16	0.17	0.16	0.18	0.14	0.19	0.16	0.16
MgO	8.00	11.40	8.44	7.18	7.86	4.32	3.55	6.20	5.14	9.20	6.12	4.14	8.85	3.70	8.75	2.36	8.95	4.58	6.85	10.67
CaO	9.00	8.30	8.56	8.60	9.75	9.07	8.00	9.75	9.63	7.95	9.00	8.60	10.28	7.50	9.40	5.52	8.40	9.25	8.58	8.90
Na2O	3.18	2.37	3.18	3.30	2.68	3.32	3.85	2.75	2.91	2.63	2.95	3.16	2.60	4.00	2.70	4.91	2.75	3.27	3.20	2.50
K2O	1.08	1.22	1.33	2.08	1.18	2.08	2.26	1.69	1.49	1.94	1.23	2.27	1.45	2.42	1.63	3.19	1.69	1.77	1.94	1.70
P2O5	0.50	0.41	0.53	0.49	0.38	0.56	0.62	0.48	0.43	0.47	0.47	0.63	0.43	0.66	0.50	0.86	0.42	0.49	0.58	0.41
LOI	1.29	0.86	0.22	0.19	0.43	0.87	1.07	1.56	0.32	2.77	0.32	1.90	-0.39	0.61	-0.05	1.33	0.61	0.28	-0.08	0.08
Total	99.75	99.29	99.92	99.44	100.07	99.63	99.47	99.45	99.91	99.74	99.78	99.45	99.93	99.81	99.84	99.81	99.52	100.25	99.52	99.62
Rb	18.3	28.4	27.5	51.0	26.5	62.0	53.5	42.5	51.5	48.0	17.6	62.0	34.0	61.0	36.5	80.0	35.0	42.5	50.0	42.0
Ba	217	238	282	410	224	412	404	334	278	350	325	465	295	485	345	730	295	375	385	332
Th	3.85	3.55	4.90	5.90	2.90	5.80	6.10	4.60	3.20	4.90	4.10	5.40	3.30	6.20	3.75	7.60	3.50	3.90	5.15	3.65
Nb	41.0	34.0	43.0	44.0	29.5	43.0	49.0	38.5	31.0	36.0	35.0	47.5	33.5	48.0	39.0	63.0	30.5	36.0	44.5	32.0
La	33.0	30.5	38.0	40.5	25.0	42.0	44.0	37.0	30.5	35.5	33.0	47.5	28.0	47.0	32.0	78.0	28.0	38.0	39.5	31.0
Ce	72.0	66.0	83.0	86.0	57.0	88.0	98.0	81.0	65.5	77.0	68.5	100	61.5	102	73.0	154.0	60.0	99.0	88.0	63.0
Sr	599	435	650	682	485	670	660	570	586	479	482	746	637	668	635	780	473	625	626	510
Nd	42.0	36.0	45.0	43.0	33.0	47.0	55.0	45.0	40.0	40.5	44.5	52.0	34.0	56.0	43.0	98.0	36.0	61.0	48.0	35.5
Sm	9.40	8.15	9.90	8.75	7.60	10.1	11.0	9.45	9.05	8.75	10.0	10.6	7.70	11.5	9.35	20.0	8.15	15.9	10.2	7.85
Zr	315	262	352	322	245	342	400	292	278	315	305	375	240	375	315	510	260	297	376	249
Eu	2.97	2.53	3.05	2.66	2.38	2.98	3.43	2.80	2.77	2.60	3.13	3.16	2.40	3.46	2.87	5.80	2.48	5.74	3.17	2.32
Gd	8.60	7.70	8.10	7.90	7.10	9.00	10.7	9.15	8.30	7.80	9.55	9.05	6.80	11.1	9.20	21.50	7.50	23.70	9.45	7.20
Dy	6.65	6.15	6.30	6.20	6.10	7.20	8.10	7.00	7.20	6.15	8.40	7.40	5.55	8.70	6.90	18.40	6.05	24.00	7.55	5.80
Y	32.5	31.0	30.0	31.5	31.0	36.0	41.0	34.5	35.5	30.0	43.0	38.5	27.5	46.0	33.0	116.0	31.5	21.0	38.0	29.0
Er	2.80	2.60	2.40	2.60	2.60	3.00	3.60	3.10	3.00	2.60	3.50	3.20	2.20	4.00	2.90	9.40	2.60	14.50	3.20	2.50
Yb	2.16	2.19	1.92	2.10	2.14	2.50	2.72	2.35	2.54	2.07	3.01	2.69	1.86	3.10	2.09	7.16	2.22	13.70	2.60	2.02
Sc	23.0	23.0	19.5	21.0	25.5	19.0	18.5	24.0	24.0	21.5	23.0	19.3	25.0	15.0	23.0	9.5	23.0	22.0	19.5	22.5
V	300	286	265	295	300	328	314	332	341	256	348	329	352	290	325	128	284	337	314	270
Cr	428	386	335	258	326	49.0	10.0	201	69.0	365	191	17.0	357	7.00	301	2	432	55	207	410
Co	52.0	64.0	52.0	43.0	51.0	44.0	31.0	40.0	39.0	47.0	40.0	32.0	53.0	26.0	51.0	8.0	48.0	37.0	41.0	54.0
Ni	272	404	252	165	226	88.0	39.0	98.0	71.0	215	155	53.0	205	7.00	240	1	280	50	164	320
Q	0.00	0.00	0.00	0.00	1.61	1.15	0.52	1.24	3.64	0.00	3.94	1.90	0.00	1.65	0.00	2.68	0.12	1.63	0.00	0.00
ne	0.00	0.00	0.00	0.00	0.00	0.00	0.00	0.00	0.00	0.00	0.00	0.00	0.00	0.00	0.00	0.00	0.00	0.00	0.00	0.00
hy	12.74	20.32	16.89	6.62	14.62	7.96	7.45	10.76	9.31	15.98	12.61	8.38	7.01	7.55	12.19	5.23	18.62	9.23	12.70	14.32
ol	2.38	2.96	0.57	5.51	0.00	0.00	0.00	0.00	0.00	2.64	0.00	0.00	6.86	0.00	3.97	0.00	0.00	0.00	1.06	4.87

* In Chauvel et al., 2012

Table

[Click here to download Table: Table 3 Guillou et al.doc](#)

Sample & Experiment	Occurrence & Type	K (wt%) ± 1σ	Mass molten (g)	⁴⁰ Ar* (%)	⁴⁰ Ar* (10 ⁻¹² mol./g) ± 1 σ	Weighted mean ⁴⁰ Ar* (10 ⁻¹² mol./g) ± 1 σ	Age (Ma) ± 2 σ
MT04*	SH tholeiite						
8026	flow	0.656 ± 0.007	1.00089	9.104	1.794 ± 0.013		
8042	Motane	«»	1.00253	5.592	1.825 ± 0.014	1.808 ± 0.010	1.59 ± 0.04
MT08*	SH tholeiite						
8027	flow	1.112 ± 0.011	1.02209	39.698	2.978 ± 0.018		
8043	Motane	«»	2.00172	33.989	2.943 ± 0.015	2.958 ± 0.012	1.53 ± 0.03
MT11	SH alk. bas.						
8028	dyke	1.685 ± 0.017	1.00579	28.565	5.733 ± 0.029		
8044	Motane	«»	1.00148	20.518	5.745 ± 0.030	5.739 ± 0.021	1.96 ± 0.04
TH8*	PS hawaiiite						
8052	flow	1.563 ± 0.015	1.00087	36.879	4.712 ± 0.025		
8067	Hanatetena	«»	1.50091	47.536	4.744 ± 0.024	4.728 ± 0.017	1.74 ± 0.04
TH35	PS tephriph.						
7796	needle	4.383 ± 0.043	0.49301	45.584	13.219 ± 0.068		
7812	Vaitahu	«»	0.98675	43.218	13.527 ± 0.069	13.523 ± 0.048	1.78 ± 0.04
TH31*	PS tholeiite						
7794	flow	0.631 ± 0.006	1.18672	14.510	2.015 ± 0.013		
7810	Hanatetena	«»	1.23815	6.891	1.908 ± 0.015	1.966 ± 0.010	1.80 ± 0.04
TH14*	SH alk. bas.						
8080	flow	0.847 ± 0.009	1.00344	15.206	2.668 ± 0.016		
8109	Vaitahu	«»	1.00670	19.159	2.648 ± 0.016	2.658 ± 0.011	1.81 ± 0.04
TH18*	SH tholeiite						
8068	flow	1.303 ± 0.013	1.03076	21.981	4.111 ± 0.022		
8084	Vaitahu	«»	1.00141	30.848	4.107 ± 0.021	4.109 ± 0.015	1.82 ± 0.04
TH13*	SH tholeiite						
8069	upper flow	0.852 ± 0.009	1.00095	17.817	2.775 ± 0.011		
8085	Vaitahu	«»	1.00289	16.538	2.783 ± 0.016	2.779 ± 0.011	1.88 ± 0.04
TH38	SH tholeiite						
7899	flow	1.195 ± 0.012	1.09784	41.032	3.849 ± 0.029		
7915	Vaitahu	«»	1.59724	16.812	3.999 ± 0.022	3.944 ± 0.017	1.90 ± 0.04
TH37	SH hawaiiite						
7795	flow	1.959 ± 0.020	1.10225	27.170	6.435 ± 0.034		
7811	Vaitahu	«»	1.01065	20.584	6.546 ± 0.036	6.487 ± 0.025	1.91 ± 0.04
TH41	SH tholeiite						
7910	flow	0.407 ± 0.004	1.05413	11.485	1.419 ± 0.011		
7926	Vaitahu	«»	1.1609	11.309	1.499 ± 0.012	1.456 ± 0.008	2.06 ± 0.05
TH39*	SH tholeiite						
7907	flow	1.212 ± 0.012	0.93740	33.084	4.448 ± 0.025		
7923	Vaitahu	«»	1.72916	25.158	4.418 ± 0.023	4.432 ± 0.017	2.11 ± 0.05
FH16	PS trachyte						
7928	dome	4.043 ± 0.040	0.44685	24.759	7.845 ± 0.048		
7944	Touaouoho	«»	0.60293	70.794	7.782 ± 0.041	7.809 ± 0.031	1.11 ± 0.02
FH06	PS trachyte						
7918	dome	3.719 ± 0.037	0.51412	17.011	7.792 ± 0.051		
7932	Omoa	«»	0.48218	25.537	7.886 ± 0.044	7.845 ± 0.032	1.22 ± 0.03
FH05	PS tholeiite						
7938	flow	0.672 ± 0.007	0.44551	5.529	1.437 ± 0.023		
7954	Omoa	«»	0.55791	3.267	1.441 ± 0.018	1.440 ± 0.014	1.23 ± 0.04
FH11*	PS tholeiite						
7908	flow	0.988 ± 0.010	1.30538	7.853	2.155 ± 0.017		
7924	Omoa	«»	1.18210	27.261	2.157 ± 0.013	2.156 ± 0.010	1.26 ± 0.03
FH18*	SH tholeiite						
7917	flow	1.029 ± 0.010	1.16847	20.673	2.468 ± 0.017		

7933	Touaouoho	«»	1.0733	25.176	2.378 ± 0.014	2.416 ± 0.011	1.35 ± 0.03
FH12	PS trachyte						
7960	dyke	3.238 ± 0.033	0.59089	23.677	7.859 ± 0.043		
7968	Omoa	«»	0.51453	40.616	7.662 ± 0.042	7.557 ± 0.030	1.38 ± 0.03
FH01*	PS tholeiite						
7805	flow	1.146 ± 0.011	1.17441	18.578	2.747 ± 0.016		
7821	Omoa	«»	1.63045	25.899	2.687 ± 0.016	2.718 ± 0.011	1.37 ± 0.03
FH30	PS tholeiite						
8157	dyke	1.021 ± 0.010	1.05080	12.193	2.515 ± 0.015		
8173	Omoa	«»	1.01932	5.904	2.459 ± 0.018	2.491 ± 0.011	1.41 ± 0.03
		»					
FH08	SH tholeiite						
7806	flow	0.755 ± 0.008	1.19866	10.197	1.900 ± 0.014		
7822	Omoa	«»	1.09248	11.745	1.838 ± 0.015	1.869 ± 0.010	1.43 ± 0.03
FH19	SH tholeiite						
7909	flow	1.254 ± 0.012	1.14484	12.529	3.128 ± 0.021		
7925	Touaouoho	«»	1.20202	20.824	3.127 ± 0.019	3.127 ± 0.013	1.44 ± 0.03
FH17*	SH tholeiite						
7802	flow	1.187 ± 0.012	1.32097	21.118	3.105 ± 0.017		
7818	Touaouoho	«»	1.42923	11.183	3.001 ± 0.021	3.064 ± 0.013	1.49 ± 0.03
FH13*	SH tholeiite						
7801	flow	1.229 ± 0.012	1.22071	27.683	3.833 ± 0.021		
7817	Touaouoho	«»	1.51566	4.430	3.920 ± 0.032	3.825 ± 0.017	1.81 ± 0.04

* age in Chauvel et al. (2012) but no details

Table
[Click here to download Table: Table 4 Guillou et al.xls](#)

Sample	MT11	MT04*	MT08*	TH39*	TH41	TH37	TH38	TH13*	TH18*	TH14*
Volcano	Motane	Motane	Motane	Vaitahu						
Type	SH alb	SH thol	SH thol	SH thol	SH thol	SH haw	SH thol	SH thol	SH thol	SH alb
SiO2	44.10	47.90	47.90	47.20	45.80	47.00	46.70	47.70	47.70	46.40
TiO2	3.78	4.28	3.78	3.45	4.26	3.56	3.34	4.15	3.44	3.17
Al2O3	13.75	14.65	14.86	12.70	14.70	16.10	11.90	14.70	14.60	13.17
Fe2O3*	12.90	12.93	12.32	12.80	13.30	12.40	12.80	12.35	12.30	12.66
MnO	0.17	0.16	0.17	0.17	0.17	0.17	0.17	0.16	0.16	0.17
MgO	5.96	5.63	5.53	9.20	6.20	5.10	11.00	6.09	6.40	8.37
CaO	11.42	9.87	10.15	9.80	10.70	10.10	10.70	9.95	9.93	9.96
Na2O	2.55	3.05	3.13	2.70	2.30	3.20	2.30	3.09	2.99	3.36
K2O	1.93	0.72	1.27	1.30	0.44	2.21	1.28	0.91	1.55	0.97
P2O5	0.63	0.50	0.52	0.52	0.52	0.60	0.43	0.51	0.46	0.48
LOI	2.53	0.01	0.00	0.40	1.20	0.50	0.00	-0.06	0.28	1.10
Total	99.72	99.70	99.63	100.24	99.59	100.94	100.62	99.67	99.81	99.81
Rb	51.0	11.2	26.0	32.2	4.9	64.2	25.1	11.7	40.5	9.3
Ba	508	215	507	297	226	577	314	240	342	516
Th	7.40	3.10	4.20	4.71	3.50	7.44	4.28	4.30	4.60	6.9
Nb	54.5	38.4	39.0	41.1	38.3	50.9	37.5	44.0	42.0	50
La	53.0	32.0	35.0	39.5	31.4	54.7	34.3	36.0	38.0	49
Ce	108	71.0	76.0	84.6	72.3	112	75.9	77.0	78	96
Sr	822	577	609	574	539	773	552	612	570	618
Nd	55.0	42.5	45.0	45.6	42.3	49.9	38.2	44.0	41.5	45
Sm	11.0	10.0	10.0	9.79	9.92	9.58	8.15	10.05	9.0	8.85
Zr	358	335	310	279	308	323	250	347	280	295

Figure
[Click here to download Figure: Fig1 Guillou et al.pdf](#)

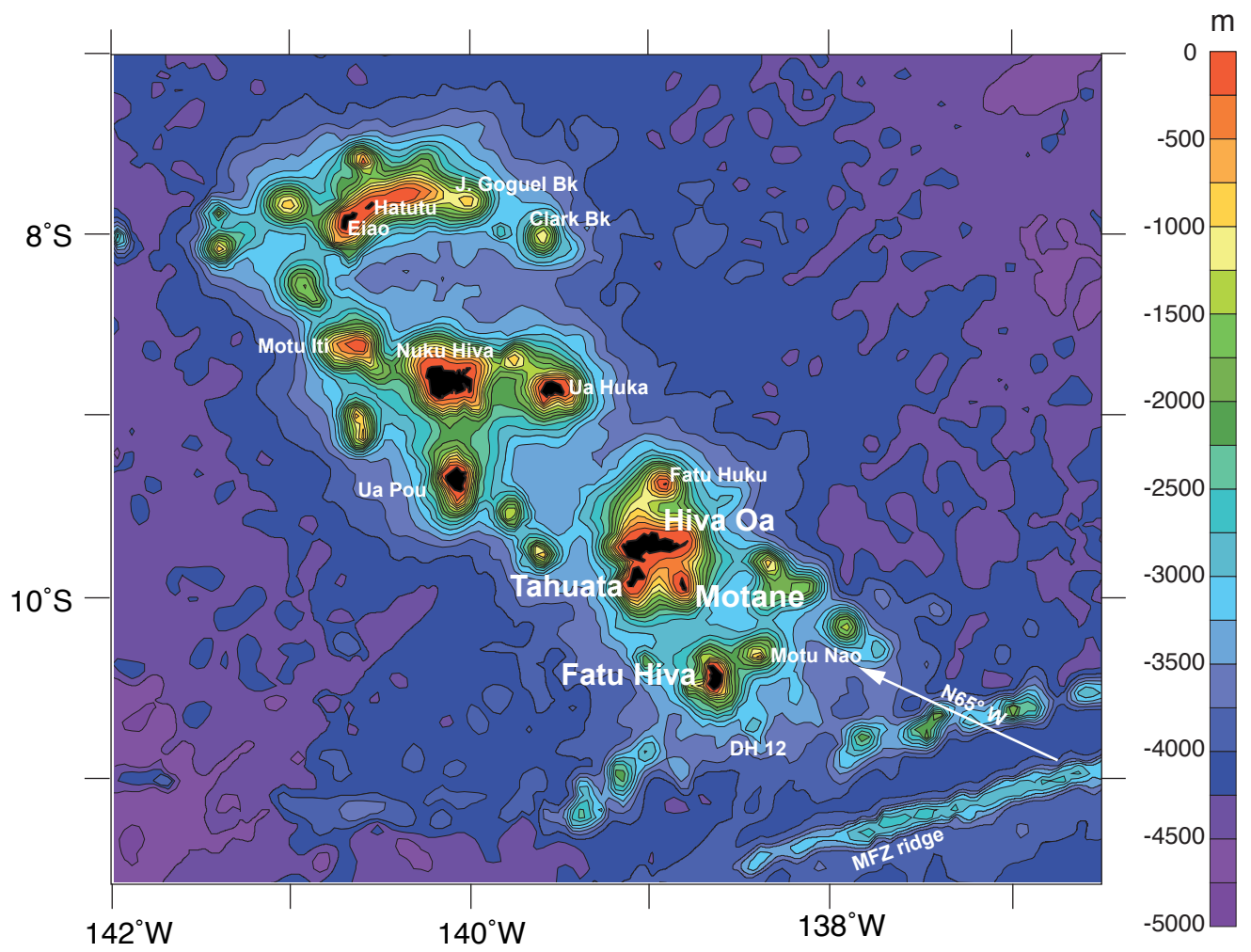
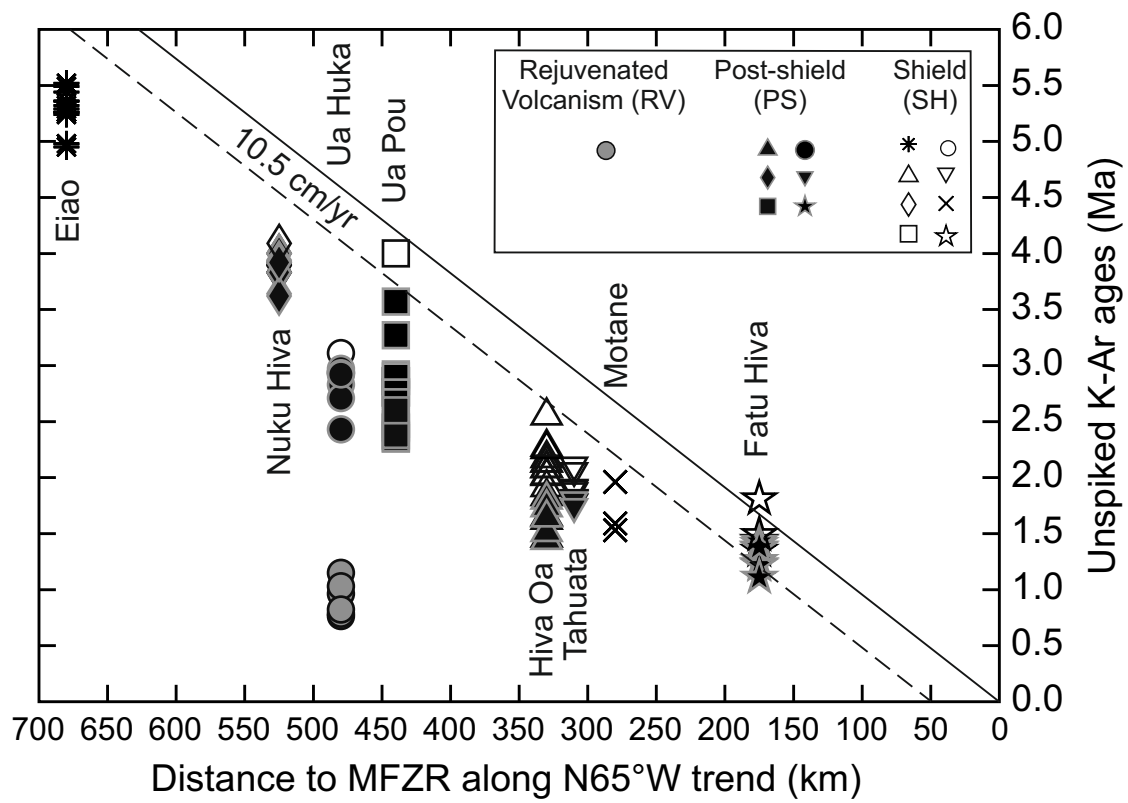
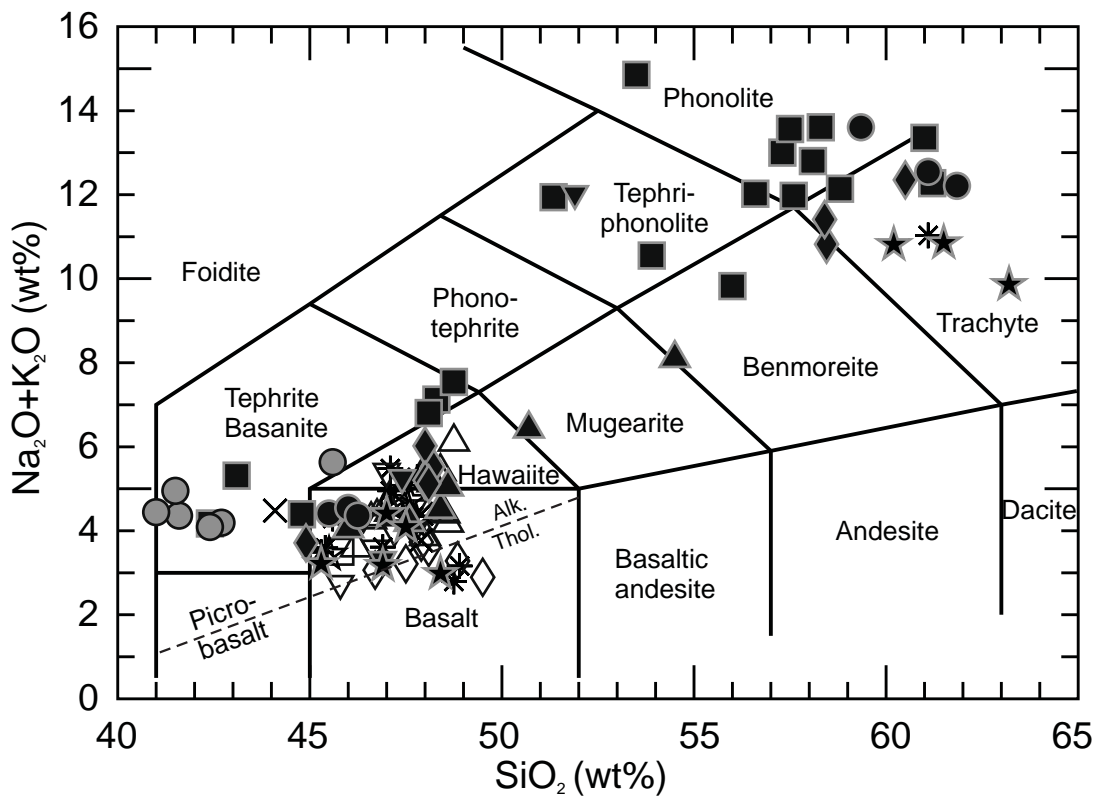


Figure
[Click here to download Figure: Fig2 Guillou et al.pdf](#)



Figure

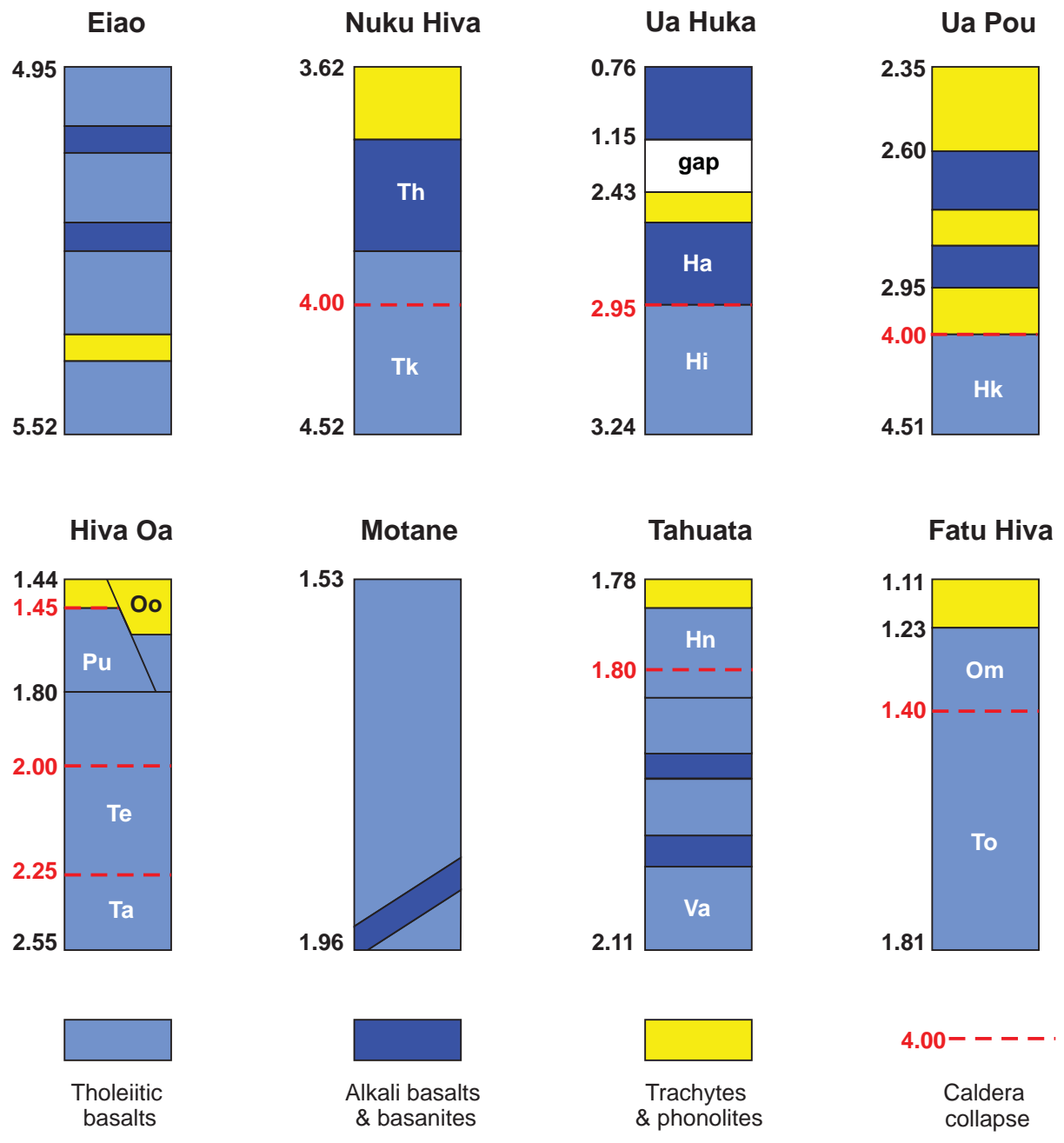
[Click here to download Figure: Fig3 Guillou et al.pdf](#)



	Shield (SH)	Post-shield (PS)	Rejuvenated Volcanism (RV)
Ua Huka	○	●	●
Tahuata	▽	▽	
Motane	×		
Fatu Hiva	☆	★	
Eiao	*		
Hiva Oa	△	▲	
Nuku Hiva	◇	◆	
Ua Pou	□	■	

Figure

[Click here to download Figure: Fig4 Guillou et al.pdf](#)



Figure

[Click here to download Figure Fig5 Guillou et al.pdf](#)

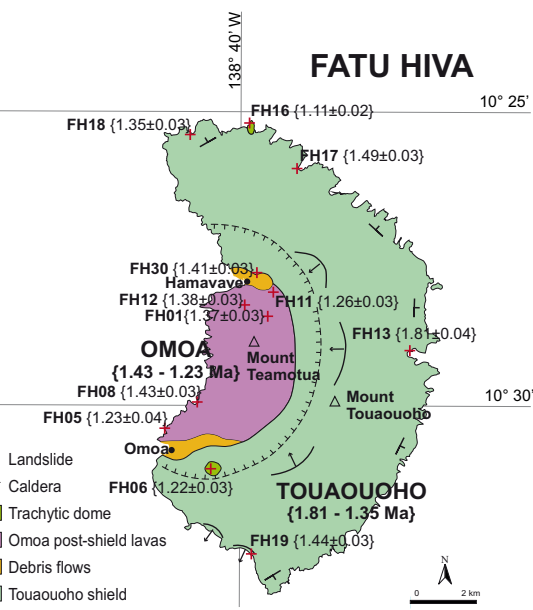
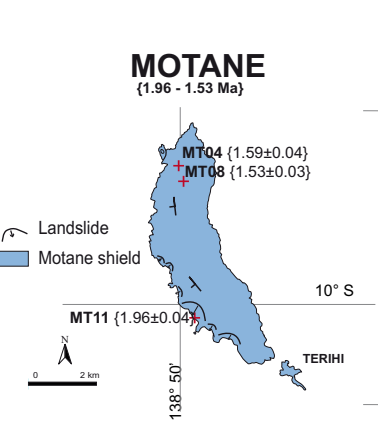
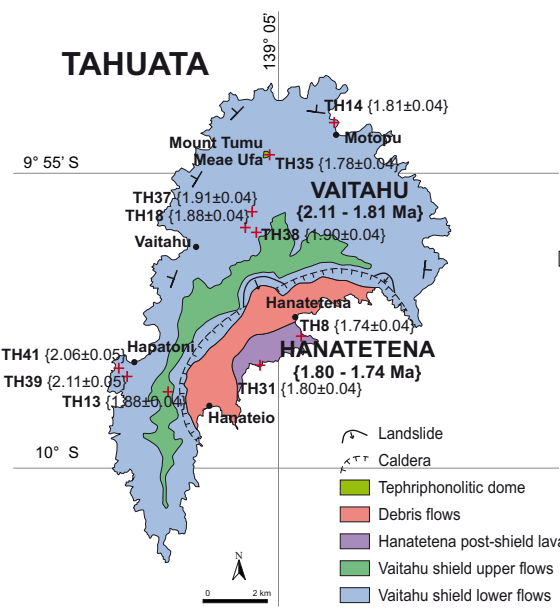
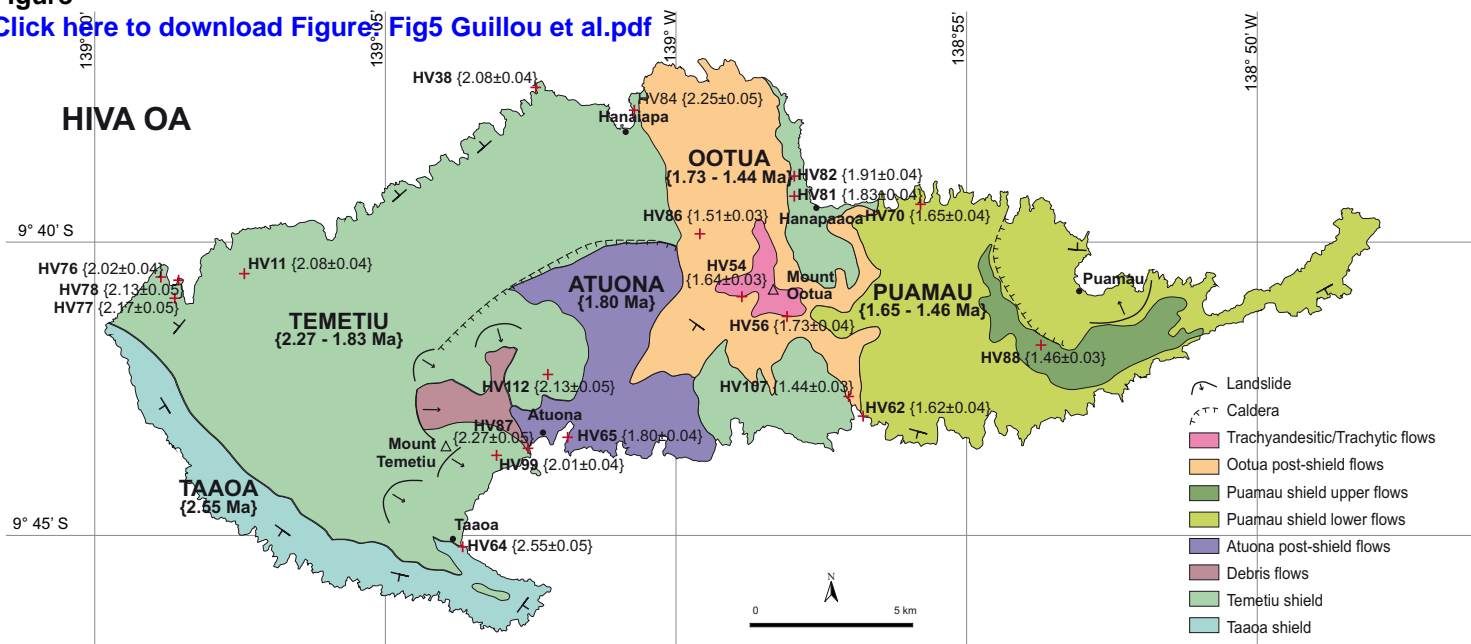


Figure
[Click here to download Figure: Fig6 Guillou et al.pdf](#)

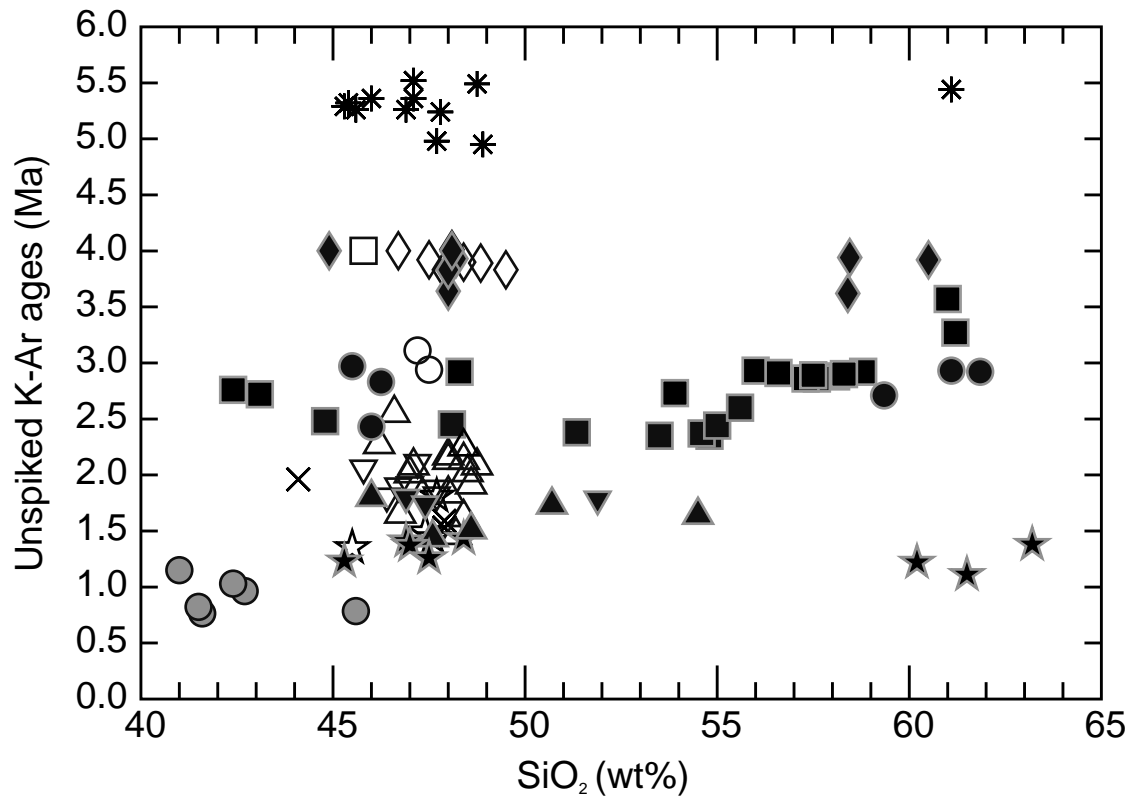


Figure
[Click here to download Figure: Fig7 Guillou et al.pdf](#)

